Report Number 95-04

research

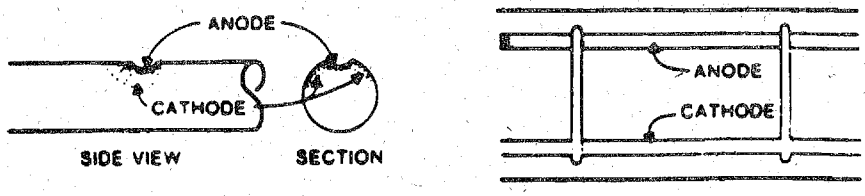

MICROCELL MACROCELL

Effect of Reinforcing Bar Chemical Composition on Corrosion Resistance

UNIVERSITY OF MINNESOTA
CENTER FOR
TRANSPORTATION
STUDIES

Technical Report Documentation Page

1. Report No.	2.	3. Recipient's Accession No.
MN/RC-95/04		

4. Title and Subtitle	5. Report Date
EFFECT OF REINFORCING BAR CHEMICAL COMPOSITION ON CORROSION RESISTANCE	October 1994
	6.

7. Author(s)	8. Performing Organization Report No.
Roberto T. Leon, Moon-Gu Jeon	

9. Performing Organization Name and Address	10. Project/Task/Work Unit No.
Department of Civil Engineering University of Minnesota 122 Civil Engineering Building 500 Pillsbury Drive S.E. Minneapolis, Minnesota 55455	11. Contract (C) or Grant (G) No. (C) 70446 TOC #105 (G)

12. Sponsoring Organization Name and Address	13. Type of Report and Period Covered
Minnesota Department of Transportation 395 John Ireland Boulevard St.Paul Minnesota, 55155	Final Report
	14. Sponsoring Agency Code

15. Supplementary Notes

16. Abstract (Limit: 200 words)

This research report looks at the chemical composition of reinforcing bars, and the sulfur content in particular, and their influences on the corrosion resistance of rebar. The research supports the original hypothesis--which suggests that the reduction in sulfur inclusions would benefit corrosion resistance. The reduction could result in significant savings that would more than offset the higher initial costs for these bars.

To test the hypothesis, the study examined the corrosion resistance of four kinds of steel reinforcing bars; ordinary, low sulfur, copper and tungsten, and nickel. As in other series in the past, this research indicates conflicting results for different measurement techniques used to quantify corrosion rates.

In addition, the mechanism that results in low sulfur bars showing a three-fold increase in corrosion life are not clear and need more study. The report recommends a long-term follow-up study on the use of both small cube and slab specimens in the laboratory, as well as full-scale specimens in the field.

17. Document Analysis/Descriptors		18. Availability Statement
Reinforced concrete Low-sulfur steel Copper-tungsten High nickel Galvanic measurements	Corrosion Cloride ions Thermodynamics Tafel extrapolation	No restrictions. Document available from: National Technical Information Services, Springfield, Virginia 22161

19. Security Class (this report)	20. Security Class (this page)	21. No. of Pages	22. Price
Unclassified	Unclassified	110	

EFFECT OF REINFORCING BAR CHEMICAL COMPOSITION ON CORROSION RESISTANCE

Final Report

Prepared by

Roberto T. Leon
Moon-Gu Jeon
Department of Civil Engineering
University of Minnesota

October 1994

Published by

Minnesota Department of Transportation
Office of Research Administration
200 Ford Building Mail Stop 330
117 University Avenue
St Paul MN 55109

ACKNOWLEDGEMENT

This research could not have been possible without the generous support of the Minnesota Department of Transportation (MNDOT) and the Nippon Steel Corporation. The authors would like to thank in particular Mark Hagen, Research Project Supervisor, and George Cochran, Director of Research - Materials Research and Engineering Laboratory, and all the other members of the MNDOT technical panel for their help and constructive input during the research. The materials were manufactured and provided free of charge by the Nippon Steel Corporation. The cooperation of Shinichi Iguchi, Vice President for Technology R. & D., and Hiroshi Hagiwara, Manager - Technical Services, of Nippon Steel U.S.A., and Shigeki Itoh and Soichi Ito, Steel Research Center, NKK Corporation, Kawasaki, Japan is also gratefully acknowledged. The idea for this research was first proposed by Drs. Iwao Iwasaki and Jiwon Jang and their contributions are also gratefully acknowledged.

TABLE OF CONTENTS

List of Tables

List of Figures

EXECUTIVE SUMMARY

Reinforced concrete is used widely as a structural material because of its economy and versatility. While its strength properties are well understood and seldom present problems, serviceability problems such as cracking and corrosion often result in unacceptably short service life or excessive maintenance costs. From the engineering standpoint there are two approaches to mitigating corrosion problems: one deals with controlling the environment in which the rebars are placed (i.e. permeability, cracking and concrete cover) while the second deals with modifying the chemical and thermodynamics properties of the system (i.e. polymer impregnation, cathodic protection, and rebar chemistry).

Several recent research projects have indicated that the chemical composition of the reinforcing bars, and the sulfur content in particular, have a marked influence on the corrosion resistance of rebar. To test this hypothesis the corrosion resistance of four kinds of steel reinforcing bars (ordinary, low sulfur, copper and tungsten, and nickel) was examined in this study. Small samples of each type of bar were immersed in 3%, 6%, and 20% NaCl solutions with 100g of concrete chips. Galvanic current and potential were measured every three to four days during the experimental period, and polarization resistance and Tafel extrapolation measurements were conducted twice during this period. In the galvanic measurements it was found that:

(a) the 3% NaCl solution is the most corrosive among the three solutions (3%, 6%, and 20%). This is agreement with other published data, but in conflict with those of previous studies conducted by Iwasaki and Jang.

(b) the 3.5% Ni steel is the most corrosion-resistant, and the ordinary steel is most susceptible to corrosion. However, the difference of corrosion rate in the long term is so small that it is very difficult to come to a conclusion based on the limited data available.

(c) the lack of a marked difference in performance between the ordinary and low sulfur bars from these measurements cannot be satisfactorily explained at this time.

The original hypothesis for this research was that the low sulfur reinforcing steel, since it has less of the sulfides which are considered as primary corrosion initiation sites, would perform better. Scanning electron microscope (SEM) studies indicated that in fact the low sulfur bars had less sulfides than ordinary steel. Unfortunately due to logistics problems it was impossible to determine from SEM studies if corrosion actually initiated at the sulfide

inclusions. However, as noted above, the galvanic measurements which were proposed by Iwasaki and Jang did not reflect this potential benefit.

The limited measurements using the polarization resistance and the Tafel extrapolation methods showed that the corrosion resistance of the low sulfur steel was three times that of ordinary steel. From those measurements one can conclude that:

(a) the 3.5% Ni steel is the most corrosion-resistant among the bars tested, and that low sulfur steel shows markedly better performance than ordinary steel.

(b) the polarization resistance method and the Tafel extrapolation appear to be more accurate and consistent with previous research on the same materials than the galvanic measurements.

This research, as many other such series in the past, indicates conflicting results for different measurement techniques used to quantify corrosion rates. This is not unusual in corrosion studies although the controlled laboratory technique used in this case should have minimized the differences. The research indicates that the technique developed by Iwasaki and Jang needs further refinement and calibration against more established techniques.

This research indicates, however, that the original hypothesis by Jang and Iwasaki, i.e. that the reduction in sulfur inclusions would have a beneficial effect on corrosion resistance, is correct. The use of low sulfur bars could potentially result in bridge decks lasting 60 to 70 years as opposed to the current replacement cycle of about 20 years. This would result in significant life cost savings that would more than offset the higher initial costs for these bars. The mechanism that results in low sulfur bars showing a three-fold increase in corrosion life are not clear and should be the subject of a much larger study. This follow up study should concentrate on the use of both small cube and slab specimens in the laboratory as well as full-scale specimens in the field. The study should be long term and should include a variety of steel compositions from U.S. manufacturers as well as epoxy-coated bars. The study should also incorporate a laboratory component similar to the one carried out in this research program in order to evaluate the potential of simple laboratory galvanic, linear polarization and Tafel extrapolation methods to provide a rapid preliminary screening tool for corrosion-resistance materials.

CHAPTER 1

CORROSION OF STEEL REINFORCEMENT

1.1 Introduction

Reinforced concrete is used widely as a structural material because of its economy and versatility. While its strength properties are well understood and seldom present problems, serviceability problems such as cracking and corrosion often result in unacceptably short service life or excessive maintenance costs. The corrosion of reinforced concrete structures is a multimillion dollar problem in the United States and many other countries, especially in environments containing chloride ions from seawater or deicing salts.

There are several factors influencing the service and design life of concrete structures. From the engineering standpoint the amount of cover, the presence of cracks, and the concrete permeability are the most critical parameters in determining the durability of concrete structures. The protection of concrete and reinforcing steel against corrosion basically requires prevention against penetration of moisture, chloride ions, carbon dioxide, and atmospheric pollutants. Generally a large cover to the steel, an absence of cracks, and an impermeable concrete will deter or delay corrosion initiation and propagation as well as carbonation.

Localized corrosion of rebars in concrete is caused by the impurities in the rebar material, defects in the rebar surfaces, differences in concentration of chloride ions near the rebars, and complex interactions of the above factors. Deformations and surface defects of rebars can be the corrosion initiation sites even under very low chloride ion concentrations because of their thermodynamic instabilities. On the other hand no corrosion may be found on deformation-free and defect-free steel surfaces even under relatively high chloride ion concentrations. Galvanic interactions between corroding and non-corroding areas accelerate the localized corrosion at the surfaces of rebars.

Inclusions and other surface defects are usually the corrosion initiation sites because the interface between inclusion and matrix is most unstable thermodynamically. The micro-galvanic cells can be formed between inclusion and matrix and between constituents of microstructures. Previous investigations have showed that pearlite microstructures are attacked preferentially to ferrite structures, and that the corrosion rates of bent and welded rebars were two orders of magnitude higher than those of normal rebar due to the surface defects induced by these processes.

The best corrosion prevention method is elimination of the electrolyte component which

allows the passage of ions. This is practically impossible since concrete is a permeable medium. The permeability can be decreased by changing the microstructure of the concrete, as is the case with the addition of silica fume, or by providing barriers, as is the case with sealants. In the best case in an aggressive environment these measures will only slow down the initiation of corrosion and thus other methods to improve durability have to be explored. As noted above, thermodynamic instabilities give rise to corrosion initiation, and thus the effects of cleanness of the steel, alloying elements, and heat treatment become of interest for improving the corrosion resistance. Among them changing the rebar chemistry, by reducing the sulfur content or adding nickel for example, are very attractive approaches to reducing corrosion. The objective of this report is to describe a research effort aimed at comparing the resistance against corrosion of four different rebar chemistries by utilizing a laboratory technique developed by Iwasaki and Jang [1,2].

1.2 Background

The possibility of corrosion of reinforcement is a problem which has concerned engineers and researchers since the early days of reinforced concrete [3]. Corrosion of unprotected steel occurs in the atmosphere, underwater, underground, by chemical attack and by electrolysis. In most applications of reinforced, prestressed, and post-tensioned concrete corrosion has not been a major problem because of the generally alkaline nature of concrete which maintains the reinforcement in a passive state. Moreover the desire to limit crack widths and provide adequate anchorage has led to cover requirements which tend to maintain the passivity around the rebars. It is only where this passivity is broken down, either locally or more generally, that corrosion becomes possible [4].

In order to properly focus the research to be carried out, a brief review of some of the pertinent issues and research on corrosion will be given in this Chapter.

The alkalinity of the concrete can be lost, and the corrosion process started, due to either:

(1) carbonation (reaction with carbon dioxide) or reactions with similar acidic gases (sulphur dioxide). Carbonation proceeds slowly (1 mm/year) and is linked primarily to the porosity and permeability of the concrete and the exposure conditions; to date it has not been identified as a primary initiator of corrosion in highway structures [5], or

(2) the presence of chloride ions in solution. Chloride ions are present because they were originally introduced as a set-accelerating admixture or because of the presence of deicing salts or salt water in the environment. The latter two, and deicing salts in

particular, are the most common source of corrosion in bridges today. Corrosion damage in bridge decks due to chloride ions is accelerated typically because:

(a) less cover was provided than that normally specified for the particular environment.

(b) the concrete quality was particularly low and therefore the concrete has a high permeability and porosity.

(c) large cracks that allow direct penetration and contact of the chlorides ions with the reinforcement have formed.

(d) excessive amounts of chlorides were present in the mix.

1.3 Principles of Corrosion

1.3.1 Thermodynamics

To understand the corrosion phenomena and to reduce its damage, it is necessary to understand the thermodynamics and electrochemical kinetics involved in this process. A fundamental concept is that thermodynamics, the science of energy and entropy, can give an understanding of the energy changes involved in the electrochemical reactions of corrosion. These energy changes provide the driving force and control the spontaneous direction for a chemical reaction but cannot predict the corrosion rate. The latter is controlled by kinetic laws.

Most chemical reactions are associated with changes of free energy (G) of the system. When the reaction products have a lower energy than the reactants, G is negative in the spontaneous reaction, and its value can be calculated by the fundamental relationship:

$$G = - n F E \qquad (1.1)$$

where,

E = algebraic sum of potentials of involved species,
n = number of electrons exchanged in the reaction, and
F = Faraday's constant (96500 coulombs/equivalent).

The listing of reduction potentials and half cell reactions for several species is given in Table

1.1. One example of a corrosion reaction is the corrosion of iron in a solution of hydrochloric acid in water:

$$Fe + 2HCl \rightarrow FeCl_2 + H_2 \qquad (1.2)$$

The complete reaction can be divided into two half cells:

$$Fe \rightarrow Fe^{2+} + 2e^- \quad (e_a) \qquad (1.3)$$

$$2H^+ + 2e^- \rightarrow H_2 \quad (e_c) \qquad (1.4)$$

where e_a and e_c are half cell potentials of anode and cathode. The total potential involved is the algebraic sum of e_a and e_c which can be found in Table 1.1. Thus:

$$E = e_a + e_c = 0.440 + 0 = 0.440 \text{ V}$$

Thus from Equation (1.1) the free energy change (G) for this reaction is:

$$G = -2 \ \ 96500 \ 0.440 = - 84920 \text{ Joules}$$

The negative free energy change or positive cell potential means that the products (Fe^{2+}) of the reaction shown in Equation (1.2) are more stable than the reactants (Fe), and thus the reaction proceeds in the direction of arrow.

Generally, an electrode reaction can be written

$$Ox + ne^- = Red$$

where Ox is the concentration of oxidant and Red is the concentration of reductant.

According to the thermodynamics of chemical equilibria, the free energy change in the general state (G) and in the standard state (G°) are related by equation:

$$\Delta G = \Delta G^\circ + RT \log\left(\frac{Red}{Ox}\right) \qquad (1.5)$$

where R is the gas constant and T is absolute temperature.

Table 1.1 - Standard electromotive force potentials (reduction potentials) [13].

Electrode Reaction	Standard Potential ϕ°(in volts) at 25°C
$Au^{3+} + 3e^- = Au$	1.50
$Pt^{2+} + 2e^- = Pt$	ca. 1.2
$Pd^{2+} + 2e^- = Pd$	0.987
$Hg^{2+} + 2e^- = Hg$	0.854
$Ag^{+} + e^- = Ag$	0.800
$Hg_2^{2+} + 2e^- = 2Hg$	0.789
$Cu^{+} + e^- = Cu$	0.521
$Cu^{2+} + 2e^- = Cu$	0.337
$2H^{+} + 2e^- = H_2$	0.000
$Pb^{2+} + 2e^- = Pb$	−0.126
$Sn^{2+} + 2e^- = Sn$	−0.136
$Mo^{3+} + 3e^- = Mo$	ca. −0.2
$Ni^{2+} + 2e^- = Ni$	−0.250
$Co^{2+} + 2e^- = Co$	−0.277
$Tl^{+} + e^- = Tl$	−0.336
$In^{3+} + 3e^- = In$	−0.342
$Cd^{2+} + 2e^- = Cd$	−0.403
$Fe^{2+} + 2e^- = Fe$	−0.440
$Ga^{3+} + 3e^- = Ga$	−0.53
$Cr^{3+} + 3e^- = Cr$	−0.74
$Cr^{2+} + 2e^- = Cr$	−0.91
$Zn^{2+} + 2e^- = Zn$	−0.763
$Nb^{3+} + 3e^- = Nb$	ca. −1.1
$Mn^{2+} + 2e^- = Mn$	−1.18
$Zr^{4+} + 4e^- = Zr$	−1.53
$Ti^{2+} + 2e^- = Ti$	−1.63
$Al^{3+} + 3e^- = Al$	−1.66
$Hf^{4+} + 4e^- = Hf$	−1.70
$U^{3+} + 3e^- = U$	−1.80
$Be^{2+} + 2e^- = Be$	−1.85
$Mg^{2+} + 2e^- = Mg$	−2.37
$Na^{+} + e^- = Na$	−2.71
$Ca^{2+} + 2e^- = Ca$	−2.87
$K^{+} + e^- = K$	−2.93
$Li^{+} + e^- = Li$	−3.05

For the corresponding electrode potentials, division by -nF gives the equation:

$$E = E^\circ + \left(\frac{RT}{nF}\right) \log\left(\frac{Ox}{Red}\right) \qquad (1.6)$$

$$E = E^\circ + \left(\frac{0.059}{n}\right) \log\left(\frac{Ox}{Red}\right) \qquad (1.7)$$

The above equation is called the Nernst equation and shows how the electrode potential varies with the concentrations (activities) of participating substances.

Measurements of cell potential, E, are necessary to determine the driving force in an electrochemical cell which consists of two half-cells. By making one of the half-cells a known (reference) half-cell, one can measure the potential of the second one. Several reference electrodes are commonly used, and their potential values with respect to SHE are listed on Table 1.2. Among them the saturated calomel electrode (SCE) is the most popular in the laboratory because in its saturated state the cell potential is almost constant, and because due to the small and similar mobilities of K^+ and Cl^- ions the liquid junction potential is minimized [6].

The potential/Ph diagram (Poubaix diagram) may be thought of as a map showing conditions of solution oxidizing power (potential) and Ph for the various possible phases that are stable in an aqueous electrochemical system. Of special interest are conditions in which corrosion is thermodynamically impossible. While potential and/or Ph can be adjusted to prevent corrosion thermodynamically and provide a strong thermodynamic basis for understanding corrosion, they do not give any information on corrosion rate [7]. Figure 1.1 shows the simplified Poubaix diagram for iron. It indicates that iron can be passive at a relatively high alkalinity and high negative potential, and that when a certain potential is supplied to the system, the system can be immune to the corrosion regardless of Ph. The technology known as cathodic protection, which is utilized in bridge decks, is based on this principle.

1.3.2 Electrochemical kinetics

Chemical kinetics is the study of rates of chemical reactions. Because corrosion is thermodynamically possible for most environmental conditions, it is specially important to know how the rate of corrosion is affected by environmental factors. An understanding of the fundamental laws of electrochemical kinetics is essential to develop more corrosion-resistant alloys and to improve methods of protection against corrosion.

Table 1.2 - Potential values for several reference electrodes.

Electrode System	Half-Cell Reaction	Potential vs. SHE
Mercury-Mercurous Sulfate	$HgSO_4 + 2e^- = 2Hg + SO_4^{2-}$	+0.615
Copper-Copper Sulfate	$CuSO_4 + 2e^- = Cu + SO_4^{2-}$	+0.318
Saturated Calomel	$Hg_2Cl_2 + 2e^- = 2Hg + 2Cl^-$	+0.241
Silver-Silver Chloride(saturated)	$AgCl + e^- = Ag + Cl^-$	+0.222
Standard Hydrogen	$2H^+ + 2e^- = H_2$	0.000

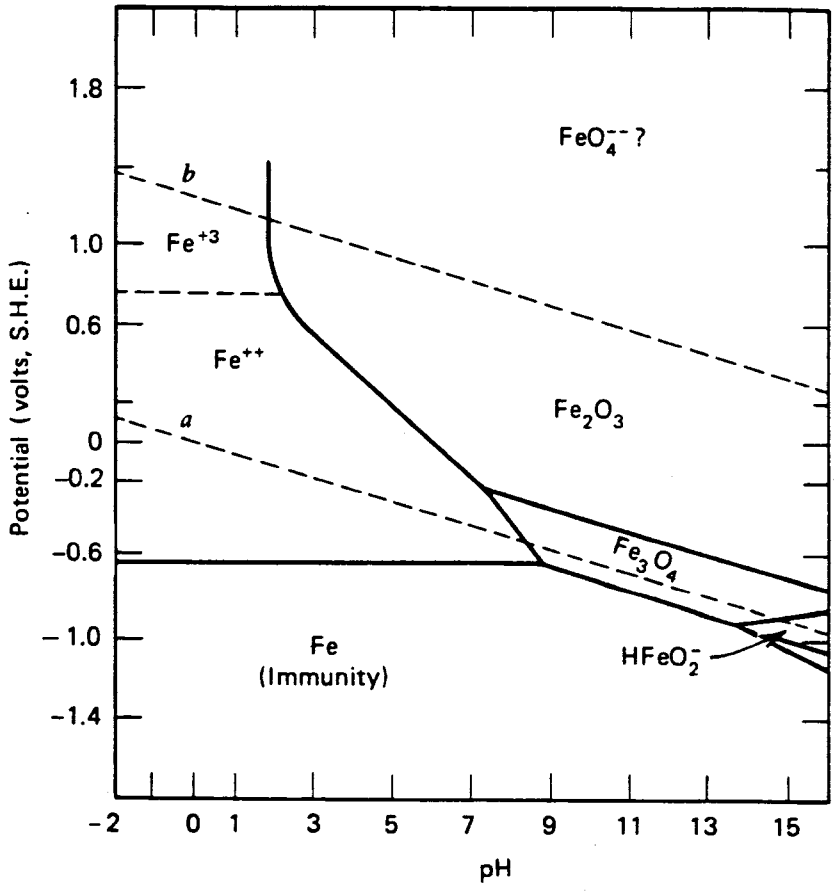

Figure 1.1 - Poubaix diagram for iron [13].

Faraday found that the products of an electrochemical reaction were proportional to the applied current. Thus, the rate of electron flow to or from a reaction interface can be a measure of the reaction rate:

$$m = \frac{I\ t\ a}{n\ F} \tag{1.8}$$

where, I is the applied current, t is the time, a is the atomic weight, n is the number of equivalents exchanged, and m is mass reacted.

Dividing both sides by the time t and the area A, gives the corrosion rate, r:

$$r = \frac{m}{t\ A} = \frac{i\ a}{n\ f} \tag{1.9}$$

where i is the current density and is given by I/A.

Polarization is the potential change from the equilibrium half-cell electrode potential, caused by a net surface reaction rate for the half-cell reaction. Typically there are two kinds of polarization. One is activation polarization (η_{act}) which is caused by a certain slow step in the electrode process requiring an activation energy for overcoming the reaction hinderance, and is given by:

$$\eta_{act} = \beta \log\left(\frac{i}{i_o}\right) \tag{1.10}$$

The other type is concentration polarization (η_{con}) caused by a deviation of the concentration on the electrode surface from that of the bulk solution. For corrosion processes only the cathodic part is important since the concentration polarization for anodic oxidation can be ignored because an unlimited supply of metal atoms is available at the interface. The concentration polarization is given by:

$$\eta_{con} = \left(\frac{2.3\ R\ T}{n\ F}\right) \log\left(1-\frac{i_c}{i_L}\right) \tag{1.11}$$

where η_{con} is the concentration polarization at the cathode, i_c is the current density at the cathode, and i_L is the limiting current density.

The total cathodic polarization ($\eta_{T,con}$) is the sum of activation and concentration polarization:

$$\eta_{T,con} = \eta_{act,c} + \eta_{con,c} \tag{1.12}$$

$$\eta_{T,con} = \beta_c \log\frac{i_c}{i_o} + \frac{2.3\,R\,T}{n\,F}\log\left(1-\frac{i_c}{i_L}\right) \tag{1.13}$$

When a metal is corroding in an acid solution, both the anodic and the cathodic half-cell reactions occur simultaneously on the surface. Each has its own half-cell electrode potential and exchange current density. However, the two half-cell electrode potentials cannot coexist separately on an electrically conductive surface. Each must polarize or change potential to a common intermediate value (E_{corr}) which is called the corrosion potential. At E_{corr} the rates of the anodic and cathodic reactions are equal, and also are identical to the corrosion rate(i_{corr}).

Passivity is defined as a state where a metal is stable in a corrosive solution. This corrosion resistance arises due to the formation of thin surface films under an oxidizing condition with high anodic polarization. Figure 1.2 shows a typical anodic active-passive polarization behavior.

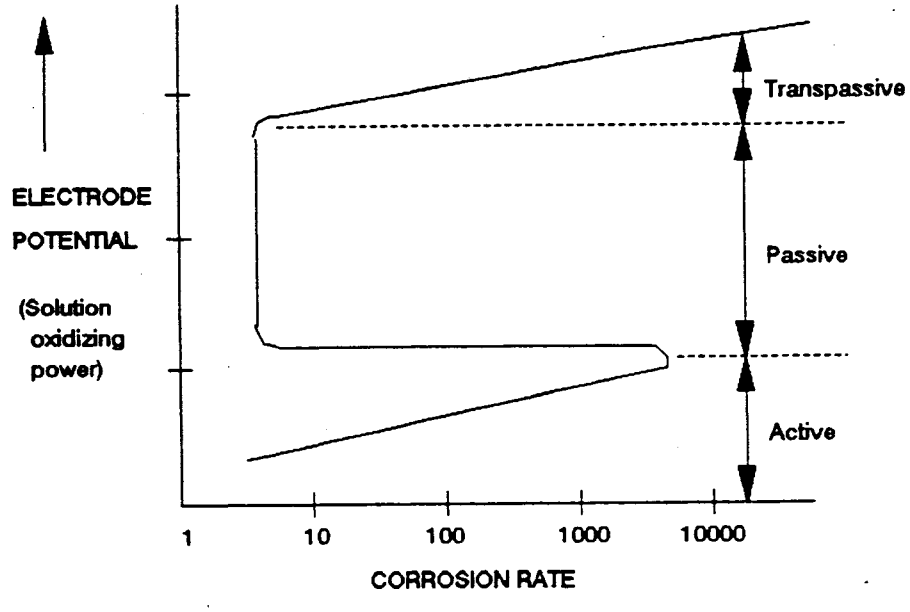

Figure 1.2 - Typical anodic active-passive polarization behavior.

The corrosion state is divided into three parts: active, passive, and transpassive. Below E_{pp} there is an active state which is a low potential state and where corrosion rate increases with potential. Above E_{pp} the passive film becomes stable, and the corrosion rate falls dramatically

(passive state). If an active-passive state is maintained in the passive region, its corrosion rate will be very low. This method is called anodic protection and is another possible corrosion protection method. At still higher potential, the passive films break down and the corrosion rate increases in the transpassive state.

1.3.3 Types of corrosion

Several types of corrosion can be identified based on generalized characteristics:

(a) Uniform corrosion is a uniform, regular removal of metal from the surface when corrosion has the same access to all parts of the metal surface. The metal itself must be metallurgically and compositionally uniform for this to occur. Atmospheric corrosion is probably the most typical example of uniform corrosion at a visually apparent rate. The other frequently cited example is uniform corrosion of steel in an acid solution.

(b) Galvanic corrosion occurs when two dissimilar alloys are coupled in the presence of a corrosive electrolyte. One of them is preferentially corroded while the other is protected from corrosion. This means that one should be very cautious in selecting metals for joints or connections since materials with very different potentials will lead to rapid corrosion of one of the metals. This also means that one can utilize galvanic corrosion to prevent corrosion of important parts of a structure by sacrificial corrosion. For example, in zinc-coated rebar, the steel reinforcement is protected by the sacrificial galvanic corrosion of zinc (in the galvanic series zinc is more active than steel).

(c) Crevice corrosion refers to the fact that corrosion of an alloy is often greater in the small sheltered volume of a crevice created by contact with another material. The second material may be part of a fastener (bolt, rivet, washer) of the same or a different alloy, a deposit of mud, sand, or other insoluble solid, or a nonmetallic gasket or packing. Corrosion within a crevice may be caused in atmospheric exposures by retention of water, while the outer surfaces can drain and dry.

(d) Pitting corrosion is produced by localized attack in an otherwise resistant surface. A number of investigations have shown that localized corrosion attacks are initiated at sulfide inclusions in carbon steels as well as in stainless steels. In stainless steel, the sulfide inclusions are usually less noble than the surrounding passive surface and they are therefore selectively dissolved, which results in a micropit containing a solution rich in H_2S. In carbon steel, and nickel, on the other hand, the sulfide inclusions are usually more noble than the surrounding matrix which is therefore attacked preferentially [8].

(e) Environmentally Induced Cracking(EIC) is a general term for brittle mechanical failures that result from a synergism between tensile stress and a corrosive environment. EIC includes stress corrosion cracking (SCC), corrosion fatigue cracking (CFC), and hydrogen induced corrosion (HIC) [6].

(1) SCC is the brittle failure at relatively low constant tensile stress of an alloy exposed to a corrosive environment. Historically, it has been thought that three conditions must be present simultaneously to produce SCC: a critical environment, a susceptible alloy, and some component of tensile stress (normally static tensile stress). Although the three factors are not usually present together, time and service conditions may conspire to produce the necessary combinations that result in surprising and expensive failures. Electrochemical potential has a critical effect on SCC. Figure 1.2 shows the schematic potentiodynamic anodic polarization curve for a typical active-passive corrosion-resistant alloy, with crosshatched zones where SCC occurs in susceptible alloy-solution combinations. The passive film is an apparent prerequisite for SCC.

(2) CFC is a brittle failure of an alloy caused by a fluctuating stress in a corrosive environment. Steel in bridge decks contaminated by chloride ions may be an example of CFC. The frequency of cyclic stress is important. Lower frequency leads to greater crack propagation per cycle, but very high frequencies eliminate the effects of the corrosive environment. CFC is similar to SCC inasmuch as a corrosive solution induces brittle fracture in an alloy that is normally ductile in a noncorrosive environment. However, in contrast to SCC, CFC requires neither a specific corrodent nor a very low corrosion rate. A minimum required corrosion rate of about 1 mmpy has been observed for steel. Exposure to any type of corrosive solution will accelerate fatigue failures of both pure metals and alloys.

(3) HIC is a brittle mechanical fracture caused by the penetration and diffusion of atomic hydrogen into the crystal structure of an alloy. Hydrogen may be present from the reduction of water or acids in neutral and acidic solutions, respectively. Aqueous hydrogen sulfide, H_2S, dramatically accelerates hydrogen entry and hydrogen damage in most alloys. HIC is generally limited to steels having a hardness of 22 or greater on the Rockwell C scale. The FCC (face centered cube) stainless steel and FCC alloys of copper, aluminum, and nickel are more resistant because of their inherent high ductility and lower diffusivity for hydrogen, but all can become susceptible if highly cold worked. HIC is similar to SCC inasmuch as brittle fracture occurs in a corrosive environment under constant tensile stress. However, cathodic polarization initiates or enhances HIC but suppresses or stops

SCC. Cathodic polarization occurs in service during cathodic protection, metal plating, and on galvanized steel at breaks in the coating.

(f) Atmospheric corrosion in air is confined to temperatures and conditions resulting from exposure to the natural ambient environment, which contains variable amounts of water from rain and splashing [6]. Dissolved oxygen is more readily transported through a thin layer of surface water than through bulk water during complete immersion. Thus, corrosion in the splash zone above the water line is higher than in full immersion. Periodic washing by rainwater or tidal fluctuation creates conditions less severe than those of continuous splashing. There are three important atmospheric parameters affecting corrosion: humidity, presence of pollutants and temperature. As mentioned above humidity is necessary for atmospheric corrosion. Pollutants increase atmospheric corrosion. Among them sulfur dioxide, SO_2, is most important. In atmospheres containing 0.01% SO_2, the corrosion rate of carbon steel increased rapidly above a critical humidity of 60%. Corrosion will remain low without SO_2, even near 100% relative humidity. Ambient atmospheric temperatures keep corrosion rates relatively low but may enhance the condensation of an aqueous surface film to increase corrosion. Exposure to sunlight raises surface temperature, which does not necessarily accelerate corrosion. Higher temperatures may dry the surface and reduce corrosion. As a result, shaded surfaces often corrode more rapidly than those exposed to direct sunlight. Thus the maximum atmospheric corrosion occurs in marine tropical or semitropical environments.

1.4 Corrosion Cells in Concrete

When a concrete structure is first built, the alkalinity of the concrete is sufficient to ensure that the steel is in a passive state and corrosion will not occur. Contrary to what was previously believed this alkalinity is the result of the concentration in the pore solution of potassium and sodium hydroxides and is not due to calcium hydroxide released during curing [9]. These compounds, with a Ph of 13-14, result in a passive film that will protect the steel if not attacked by certain ions. Chloride ions have been shown to replace hydroxyl ions in this film, leading to localized pitting and the beginning of the corrosion process. As seen in Figures 1.3 and 1.4, the corrosion of steel in concrete initiates due to an ingress of chloride or similar ions along with the presence of oxygen and water. Oxidation of Fe produces Fe^{++} and free electrons which move to the cathode through electric conductance.

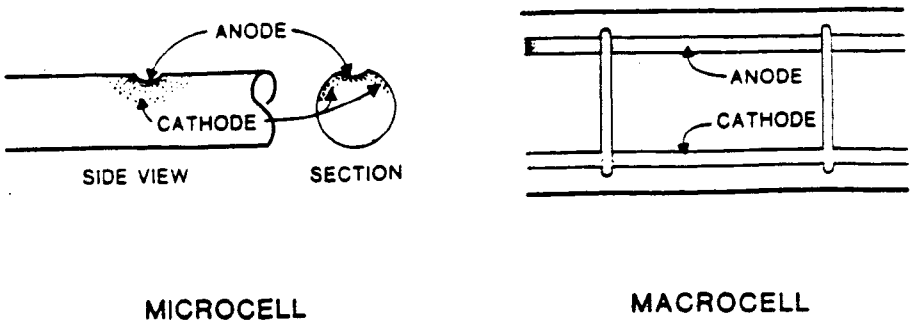

Figure 1.3 - The corrosion process.

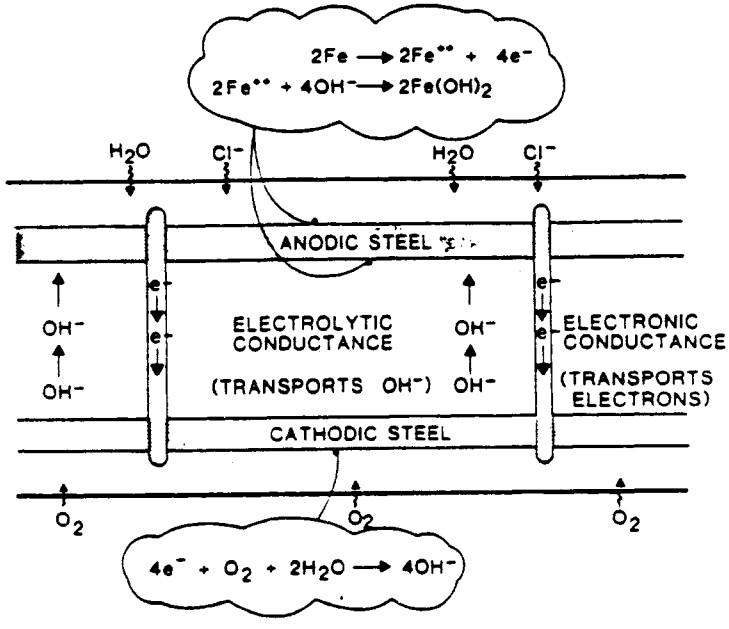

Figure 1.4 - The corrosion process.

The free electrons are then consumed at the cathode by a reduction reaction. Hydroxyl ions resulting from the reduction reaction go to the anode to react with ferrous irons. This produces corrosion products which have several times the volume of the original steel. The stresses produced by this additional volume cause the concrete to crack. This eventually results in delamination and spalling, and thus the integrity of the concrete structure is lost.

The consensus among researchers is that the rate of corrosion in concrete is affected by many factors, including heterogeneities in the steel, amount of oxygen present, moisture conditions, degree of carbonation, concrete quality (permeability and porosity), and amount of cover.

A very controversial issue, on the other hand, is the effect of cracking on corrosion initiation and corrosion rate. The issue revolves around whether a crack, by providing an easy path to the reinforcement, results in faster and more corrosion than would be observable in uncracked concrete. To some degree the different points of view can be explained by the origin, width, and orientation of the cracks. For cracks that are perpendicular to the reinforcement, the corroded length is not likely to exceed three bar diameters [3]. In contrast, cracks which follow the line of reinforcement are probably more damaging since the corroded length is greater, and consequently, the concrete's resistance to spalling and delamination is reduced.

Schiessl [10] has shown that the rate of penetration down a crack is a function of crack width. On reaching a bar, depassivation can be expected to spread along the bar for some distance due to the tendency of the concrete to separate from the bar surface in the region of a crack. In uncracked concrete, or between cracks in cracked concrete, the movement of the depassivating front will be much slower and, where adequate cover is provided, it may well not reach the bar at all. Thus, in cracked concrete corrosion will start at the cracks and will start sooner at larger cracks than at smaller ones.

Once corrosion has started, the rate of corrosion will not depend upon crack width; it will depend upon the ability of oxygen to reach the cathode of the corrosion cell. This is situated on parts of the surface of the bar in the sound concrete away from the crack while those areas which have become depassivated near the crack form the anode. The rate of corrosion will also depend upon the electrical resistance of the path through the concrete between the cathode and the anode. This path will depend upon the moisture content and also on the concentration of salts dissolved in this water. The water content is a critical factor in determining corrosion rate. If the concrete is completely saturated, then the resistance is low but the rate at which oxygen can diffuse through saturated concrete is also very low and this inhibits corrosion. If the concrete is dry, but oxygen supply is adequate, the resistance is high so corrosion is inhibited. As a result of this, corrosion is most commonly a problem in areas subjected to alternate wetting and drying as this is likely to lead to the optimum moisture content being present at least occasionally. Significant corrosion is unlikely to occur in situations where the concrete is either always saturated or always dry [11].

The corrosion of steel in concrete and the mechanisms governing it are not well understood because of the complex nature of the physical and electrochemical factors involved. Carbonation, cracking, defects of reinforcing steel due to rolling, bending and welding, and

the concentration of chloride or similar ions are widely known as important factors of corrosion initiation of reinforcing steel. A short description of each follows:

(1) Carbonation - Reinforcing steel in uncarbonated concrete is initially passive as a result of the high alkalinity of cement pastes. In the presence of carbon dioxide, calcium carbonate, which is insoluble, precipitates out of solution:

$$CO_2 + Ca(OH)_2 \rightarrow CaCO_3 + H_2O$$

This reaction stops unless some free CO_2 exists in the water. If some free CO_2 exists:

$$CACO_3 + CO_2 \rightarrow Ca(HCO_3)_2$$

The free carbon dioxide transforms calcium carbonate into soluble bicarbonate, a soft and soluble compound, which makes the concrete weak and degradable. The carbonation reaction requires moisture, and occurs most rapidly at humidity in the range 50 to 70% [12]. The rate of penetration of carbonation depends on a number of factors including the atmospheric humidity, the concrete permeability, and the partial pressure of the carbon dioxide. Some experiments have shown that the penetration of carbonation is approximately proportional to the square root of the time.

(2) Chloride ions - The breakdown in the protective passivity of steel in concrete occurs most commonly because of the presence of chloride ions. They come either from calcium chloride, which is frequently used in cement as an accelerator or antifreeze agent, or from sodium chloride or similar compounds which are often used in deicing agent. Chloride ions can disrupt the passivating reactions that occur on the steel surface in the highly alkaline conditions even in uncarbonated concrete. In carbonated concrete a smaller amount of chloride ion can activate the steel, and the corrosion processes are accelerated. The corrosion of steel in a NaCl solution increases up to about 3% initially because of enhanced solution conductivity [13]. However, still higher concentrations of dissolved salt decrease the solubility of oxygen, and the corrosion rate steadily decreases (Figure 1.5). The effect of chloride ions on rebar corrosion was investigated in a previous project [1] where it was found that corrosion of reinforcing steel increased with increasing chloride ion concentration up to a 6% concentration and decreased afterwards.

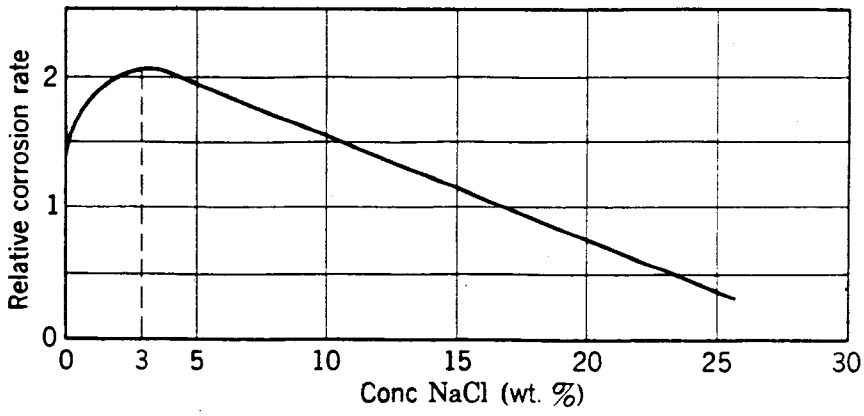

Figure 1.5 - Effect of NaCl concentration on corrosion [13].

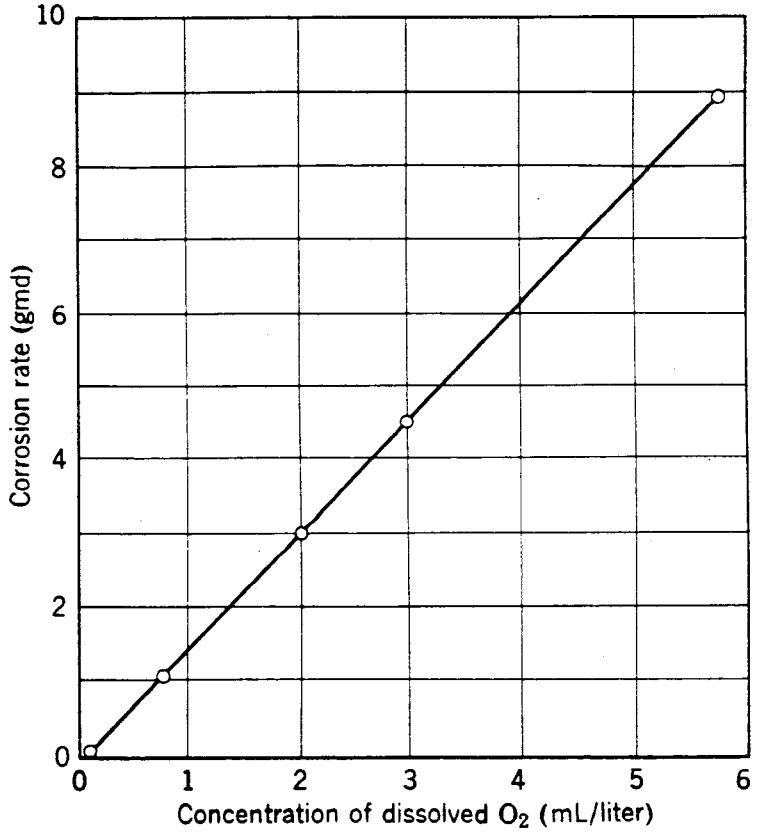

Figure 1.6 - Effect of dissolved oxygen on corrosion[13].

(3) Two other important factors in the development of a corrosion cell are the presence of dissolved oxygen and inclusions. A protective magnetite film is stable in the absence of dissolved oxygen. Thus, appreciable corrosion of steel requires dissolved oxygen in neutral and alkaline solutions, and is directly proportional to it (Figure 1.6). Differences in dissolved oxygen transport readily create differential aeration cells, which result in localized corrosion on steel surfaces at ambient temperature.

Inclusions normally constitute a part of the microstructure of steels. The type and properties of these inclusions depend on the chemistry of the steel and manufacturing practice. The main elements present in the inclusions are S (sulfur), Mn (manganese), and Si (silicon). Sulfur tends to bond to the manganese and become MnS which is the most pronounced sulfide. There are several principal types of sulfide inclusions [14]:

(a) Type I inclusions, which are globular and randomly dispersed, are common to steels with high oxygen contents, often have multiplex structures, and may contain silicates and/or oxides.

(b) Type II inclusions form in deoxidized steels (silicon and aluminum killed), and their morphology can be described as thin, chain-like, and often with a fan-like structure, although some can be rod-shaped or oval.

(c) Type III inclusions are usually angular, equiaxed, and dispersed randomly. They are not associated with oxides or silicates.

Active sulfides can be detected by a micro-corrosion test which was developed by Norel-Brandel. In this test active and inactive sulfides are differentiated by whether, after an unetched specimen surfaces are exposed to a 3% NaCl solution for 30 seconds, the sulfide inclusions causes an attack of the metallic matrix immediately surrounding the sulfide inclusion. It is known that localized corrosion initiates at inclusions. The electrochemical potentials of the inclusions are more noble than those of the surrounding steel matrix. Thus the inclusions act as a cathode and the matrix as an anode. Pitting is initiated by dissolution of the inclusion, by corrosion of surrounding metal, or from disbondment along the interface between the inclusions and the metal matrix. The mechanisms of dissolution will depend on both the type of inclusions and the solubility of the inclusions in the electrolyte. Corrosion around active sulfides is particularly rapid. Due to the large area of contact between the inclusions and matrix, the anode activity in the matrix close to active sulfides is very high due to microgalvanic couples, and as a result of hydrolysis of metal ions, anode areas tend to become acid increasing the dissolution of sulfides. Within the pit rapid

dissolution of metal tends to produce an excess of positive charge in this area, resulting in the migration of chloride ions to maintain electroneutrality. High concentrations of hydrogen and chloride ions resulting from hydrolysis of $FeCl_2$ stimulate the dissolution of metal. Outside the pit iron hydroxide forms due to interaction between the OH^- produced by the cathode reaction and the pit corrosion products. This hydroxide is further oxidized by the dissolved oxygen in the solution into $Fe(OH)_3$, Fe_3O_4, Fe_2O_3 and other oxides.

1.5 Strategies to Minimize Corrosion

It is very difficult to prevent steel corrosion completely because moisture and oxygen can not be removed from concrete. Deterioration processes involve several phenomena: chloride penetration, chloride accumulation, start of steel corrosion, crack initiation, crack propagation. Strategies to minimize corrosion of rebar in concrete can be roughly divided into two categories: the first attempts to modify the surface or chemistry of the rebars while the second attempts to prevent the ingress of chlorides by rendering the concrete more impervious. The former includes epoxy coated rebar, galvanized rebar, corrosion resistant rebar, and cathode protection. The latter includes polymer impregnated concrete, concrete surface coating, and the use of low water/cement ratio.

(a) Epoxy Coated Rebar - Epoxy coatings provide the rebar with excellent chemical resistance, and have been found to be essentially impervious to chloride ions. The specified coating thickness requires a minimum of five mils to obtain sufficient corrosion protection, and a maximum of twelve mils to maintain the mechanical bond in concrete formed by the deformations on the reinforcing bars [15,16]. In utilizing this method care should be taken to minimize the defect areas of the coating as the bar can be more rapidly corroded due to the unfavorable effect of a large cathode and a small anode.

(b) Galvanized Rebar - A galvanized rebar contains a galvanized coating made of a metal which is more active (such as zinc) than the metal (iron in this case) in a galvanic series. This coating sacrifices itself to provide the base metal with cathodic protection. Swamy [17] has demonstrated the excellent corrosion resistance of galvanized and chromated bars in cracked concretes exposed to sea water. In both accelerated laboratory cyclic wetting and drying tests and natural exposure tests in a tidal zone less than 10% of the bar surface was affected by pitting corrosion. Plain uncoated bars showed extensive corrosion and much deeper pitting. Chloride ion penetration into concrete decreased towards the interior from the surface. However, at a given depth the

chloride concentration increased as the depth of cover decreased. The Ph of the concrete at all cover depths remained between 12.6 and 12.8 near the bar surface. The corrosion products of the sacrificial material (typically zinc) also act as a passifying layer, depending on their stability in the concrete environment (Ph of 12-13 plus chlorides).

(c) Corrosion-Resistant Steels - The use of a corrosion resistant steel, which tends towards the composition of a stainless steel, may be an effective method to reduce the corrosion problem. Sulfur, manganese and silicon, as mentioned above, are the most influential elements on inclusions in the steel, and alloying elements such as copper, molybdenum, tungsten, and nickel are believed to act as corrosion inhibitive elements. Some elements, such as copper, are only effective if alternate cycles of wet/dry conditions are present; they do not work under constant saturation.

(d) Cathodic Protection - The basic concept of cathodic protection is that a direct electric current is intentionally introduced to the metal-electrolyte system of interest to reduce or eliminate naturally occurring electric currents which cause corrosion. Cathodic protection has been widely used to prevent corrosion in such applications as pipelines, chemical plants, and underground storage tanks. However, its application to steel embedded in concrete presents several particular problems [5]:

(1) Concrete has a high resistivity.

(2) Concrete is attacked by acid which may be generated at the anode.

(3) The potential of the steel must be maintained within a narrow range. If it is too positive, corrosion can occur; if it is too negative, the concrete around the reinforcing steel may deteriorate, anode life is shortened, and hydrogen may be evolved at the cathode.

The most important property in a concrete system utilizing cathodic protection is to maintain a uniform potential distribution on the steel with a minimum of applied current. That means that the resistance between the external anodes and the reinforcement must be uniform and low, and that the anodes should be as large as possible. Cathodic protection is the only commonly recognized technique which can successfully halt existing rebar corrosion in chloride contaminated concrete, but there are some technical and economical difficulties in implementing this solution.

(e) Polymer-impregnated concrete - This is one of many techniques that intend to provide

a thick barrier to chloride penetration by reducing the permeability of the concrete. In this case the polymer impregnation of concrete with a synthetic monomer forms a water interception layer. According to most tests a 3 cm impregnated layer thick is sufficient for controlling corrosion of rebar. In general these techniques require a "thick" barrier as opposed to some of the "thinner" ones utilized in surface treatments (see (f)). This is a rapidly evolving field and many new compounds, not all polymers, have been suggested for possible use.

(f) Concrete surface coatings - The effective application of impervious surface coatings may stop or improve ongoing corrosion of steel in the presence of chloride either by reducing the oxygen content of the concrete substantially, which will reduce the rate of cathodic reaction or by reducing the moisture content of the concrete, which will result in an increase in electrical resistance and a consequent reduction in corrosion current. Coating materials generally consist of binder, pigments, fillers, and a carrier. A large number of polymer types such as chlorinated rubber, urethanes, epoxies, and acrylics have been used in coatings. In this experiment [18] five materials were tested for effectiveness, but none of them succeeded in stopping the corrosion of embedded steels that were already corroding when the surface treatments were applied. However, none of the materials made the corrosion worse and they all prevented further ingress of chloride ions. The alkyl alkoxy silane was the only material to produce a significant reduction in the rate of corrosion.

(g) Low water/cement ratio - Low water/cement ratios tend to reduce the permeability of the concrete, especially when combined with additives such as silica fume. Reducing the permeability will generally result, all other variables being equal, in a lower potential for corrosion.

1.6 Objectives of this Research

The main objectives of this research are to determine from laboratory experiments on small samples (1) whether the rate of corrosion is significantly affected by the rebar material chemistry, (2) whether a galvanic corrosion measurement is adequate for determining corrosion resistance of steels in concrete contaminated by chloride ions, and (3) what percentage of NaCl solution is the most corrosive in the reinforced concrete system. Thus this research falls within category (c) of the corrosion minimization methodologies described above (Section 1.5).

To compare the effect of rebar chemistry, four types of bars will be tested. One is an

ordinary bar (O bar) with a relatively high sulfur content. The other three are bars manufactured in Japan by Nippon Steel and will be labelled "low sulfur" (Low-S), "copper-tungsten" (Cu-W), and "high nickel" (Ni) to reflect their chemical composition. The main interest is in the low-sulfur bars, since it is believed that they will show good corrosion resistance because of lower sulfides content (for example, manganese sulfides) which are considered as corrosion initiation sites. The Cu-W bars are assumed to accomplish the same purpose by copper and tungsten to bind to the undesirable sulfides. Similarly, nickel alloys are an excellent corrosion resistant material and it is expected that rebars with high nickel content will perform well. The expected performance of these bars ranges from poor for the ordinary bars, to very good for the low-sulfur and copper-tungsten ones, to excellent for the nickel ones.

The rebar samples were immersed in three different concentrations of NaCl solutions: 3%, 6% and 20%. Previous research [1,2] indicated that the 6% solution was the most corrosive. Other established literature indicates that the 3% solution should be the most corrosive. By testing a wide range of concentrations it is expected that these differences can be reconciled.

The bars were subjected to three types of measurements: galvanic corrosion-potential and current density, polarization resistance, and Tafel extrapolation. The intent is to determine whether the different techniques provide consistent results.

The experiments are described in Chapter 2. The results will be presented in Chapter 3, and conclusions and recommendations given in Chapter 4.

CHAPTER 2

EXPERIMENTAL PROGRAM

2.1 Background to Corrosion Experiments

Research into the origin and development of corrosion in steel embedded in concrete presents significant practical problems whether it is conducted on full-scale structures in the field or on small-scale laboratory specimens. The problems with field studies relate primarily to the time, size constraints, and the type of measurement to be carried out. The main problems with laboratory specimens relate to the simulation of the alkaline environment of the concrete and the scale effects involved.

A real structure will normally be expected to provide a useful life of at least 30-50 years without the occurrence of serious corrosion damage. A research project, to be useful, must produce results over a much shorter time scale, ideally 2 or 3 years. This has led corrosion researchers to take one of two possible courses of action: either the corrosion process has to be accelerated or short term results have to be extrapolated. Both of these procedures give dubious and inconsistent results.

Insofar as field studies are concerned, "realistic" specimens tend to be large, difficult to load and handle, and expensive. Few organizations can afford to set up a useful sized series of tests using such members and therefore smaller units usually containing small bars are used. Nevertheless, covers and crack widths have to be maintained at 'practical' levels. This has led to distortions of the corrosion process in most test series. A more complex problem arises on the type of measurement to be made. Most of the long-term studies on corrosion in structural members have sought to utilize some visual scale to classify performance. Since access to the corroded areas is not possible, the validity of such measurements is questionable.

More recently two basic types of methods have been proposed for use in measuring rates of corrosion in actual structures. One entails the use of polarization techniques (sometimes labelled incorrectly as "linear polarization techniques"), while the other relies on a electrical resistance rate-of-corrosion probe. Field results from these techniques are conflicting primarily because of the inability to correct for the environmental conditions [19]. Appendix A contains a detailed description of some of the most comprehensive long-term field and short-term laboratory studies of corrosion. A complete bibliography on corrosion is included

in Appendix B.

When laboratory specimens are used, the test series can be divided into two types. One type utilizes small specimens on which saline solutions are ponded, while the other utilizes small steel specimens in aqueous solutions. The former are considered more realistic, since cracks and macrocell phenomena can be modelled, but control of environmental factors is always problematic. This type of study is useful when extensive use of control specimens is made [20].

On the other hand, tests in aqueous solutions, where a saturated solution of $Ca(OH)_2$ or cement extracts are used, do not model the correct chemical composition of the pore liquid solution since the latter contains mostly NaOH and KOH. Moreover, these studies cannot model the electrical resistivity, pore geometry, precipitates, and constant evolution of chemical composition of the pore solution. They are useful, however, to assess the effect of various compositions of the pore liquid and to conduct fundamental studies. Tests of this type are the subject of this research and are based on extensive work conducted previously by Jang and Iwasaki [1,2].

2.2. Corrosion Monitoring Methods in a Concrete System

There are a number of corrosion measurement methods currently used to study the corrosion of reinforcing steel in concrete. Some of these methods are limited to laboratory research projects, but others can and have been used in actual field tests of reinforced concrete structures. Corrosion monitoring methods also can be divided into qualitative and quantitative methods. Some methods can be used to estimate the amount of corrosion for a quantitative analysis, while other methods are limited to detecting the (probable) presence of corrosion or the relative strength of the corrosion cell.

2.2.1 Polarization Methods

Electrochemical polarization methods may be classified as galvanostatic (controlled current) and potentiostatic (controlled potential). Galvanostatic procedures are relatively simple instrumentally, and were the first used historically. However, these are not popular because galvanostatic procedures are inadequate to define the active-passive curve properly. The potentiostatic procedures which are predominantly used today do not have such a problem, but still have a problem of E_{corr} drift.

Two methods are available for measurement of corrosion by electrochemical polarization: Tafel extrapolation and polarization resistance. The Tafel extrapolation method for

determining corrosion rate uses data obtained from cathodic or anodic polarization measurements. Polarization potentials are generally time dependent, and considerable care is necessary to achieve a steady-state polarization curve truly representative of the pertinent corrosion reactions. In this respect, cathodic polarization is preferred, since it is generally more rapid and reversible than anodic polarization. Although the polarization resistance technique is even faster than the Tafel technique, the Tafel technique provides an extremely rapid means of determining the corrosion rate when compared with weight-loss measurement, and can be very advantageous for such studies as inhibitor evaluations, oxidizer effects, and alloy comparison.

Figure 2.1 shows a simplified plot of anodic and cathodic polarization curves of a typical corrosion cell. If the potential of the working electrode is plotted against the log of the corrosion current, at relatively high values of current both the anodic and cathodic polarization curves behave as linear functions. These linear segments of the polarization curve are referred to as the "Tafel regions." As shown in Figure 2.1, the intersection of the Tafel slopes can be used to calculate the instantaneous corrosion intensity, i_{corr} [21,22].

The other commonly used method for making corrosion measurements in the laboratory and field is the polarization resistance method. Early research observed experimentally that the degree of polarization at a given applied current was greater for a lower corrosion rate, an apparent linearity was observed at the origin of the polarization curve for overvoltages up to a few millivolts. Thus, the slope of this linear curve is inversely proportional to the corrosion rate. Stern and Geary [23] have provided a firm theoretical background for polarization resistance measurements, and derived the equation:

$$\frac{\Delta E}{\Delta i_{app}} = \frac{\beta_a \beta_c}{2.3\, i_{corr} (\beta_a + \beta_c)} \qquad (2.1)$$

where $\Delta E/\Delta i_{app}$ is the slope of the polarization curve, β_a is the anodic Tafel slope, β_c is the cathodic Tafel slope, and i_{corr} is the corrosion current in amperes.

The values β_a and β_c refer to the Tafel slopes of the anodic and cathodic reactions respectively. These values can be approximated for the steel/concrete system from previous studies. By determining the slope of the linear portion of the polarization curve ($\Delta E/\Delta i_{app}$), one can determine the corrosion rate of the system by expressing the i_{corr} value in terms of current density (current/electrode surface area) [16].

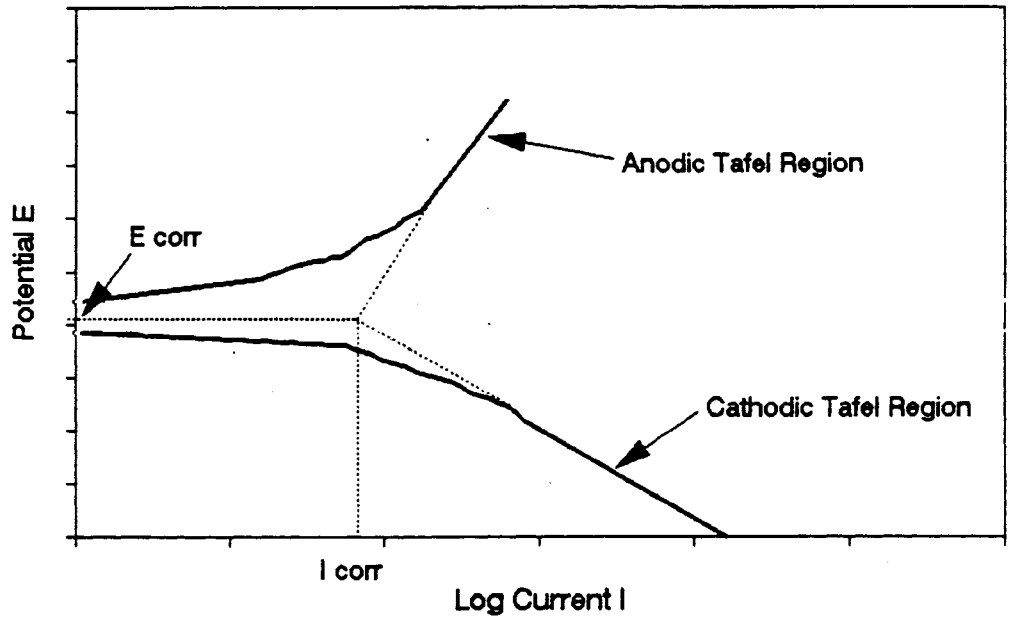

Figure 2.1 - Anodic and cathodic polarization [20].

Polarization resistance measurements have been shown to provide very good results on systems in which macrocell corrosion is not taking place [24]. In macrocell corrosion systems the steel is polarized away from its normal free-corrosion potential, and the results have been less reliable. Two or three electrode probes are used to measure the polarization resistance (Fig. 2.2). In the three-electrode apparatus the corrosion rate of only the test electrode (WE) is measured.

The polarization curve is assumed linear up to a 10-mV overvoltage, and the current is adjusted automatically to obtain a 10-Mv change in the potential of WE. The current required to obtain the 10-Mv change is proportional to the corrosion rate:

$$R_p = \frac{\Delta E}{\Delta i_{corr}} = \frac{\beta}{i_{corr}} \qquad (2.2)$$

The current meter may then be calibrated to read the corrosion rate directly. The two-electrode probe uses two identical corroding electrodes and eliminates the third reference electrode. In the two-electrode method the potential between the two electrodes is measured directly.

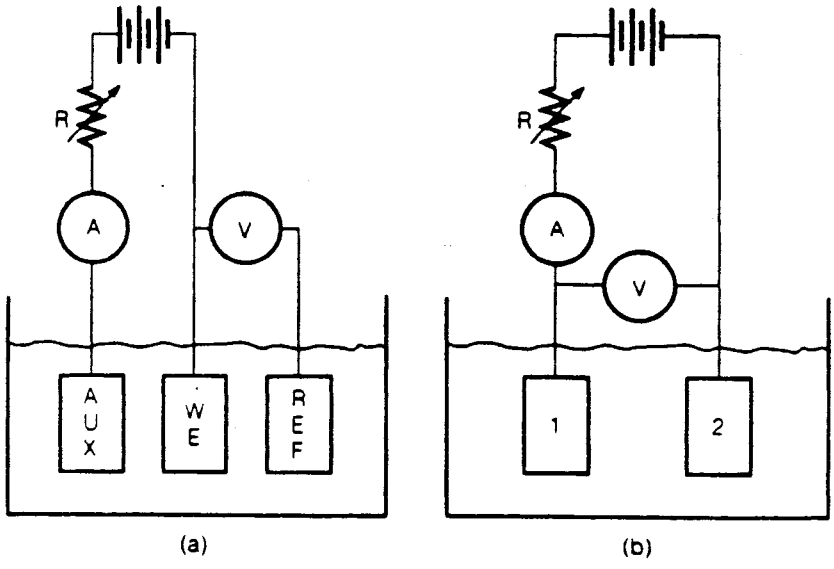

(a) Three-electrode (b) Two-electrode system

Figure 2.2 - Polarization measurements setups [13].

2.2.2 Potential Mapping

In the United States potential mapping of steel reinforced concrete bridge decks is a common technique for estimating corrosion damage to a structure. Based on a large amount of experience with corrosion of steel in concrete, ASTM has determined the probability of corrosion for a given system based on the potential measurements. ASTM states [19] that a -.350 V vs. CSE (copper sulfate electrode) is the potential for the identification and location of active corrosion of steel in concrete. It has been shown that the potential is a good indicator of probability of corrosion in concrete, but it is not related to corrosion rate. In this measurement method, the most commonly used reference cells are copper-copper sulfate, silver-silver chloride, and saturated calomel. Laboratory studies have found that the silver-silver chloride or saturated calomel reference electrodes are both stable and accurate. However, for field testing of actual structures, the durable and relatively inexpensive copper-copper sulfate half cell is generally used. The potential mapping technique is an early warning system that can assess the magnitude of the problem of corrosion and follow the extent of the anodic area as it changes with time. In conjunction with data from other tests such as resistivity or chloride ion content, the technique can be used effectively to assess the corrosion status of a structure.

2.2.3 Other Corrosion Monitoring Methods

Electrochemical noise monitoring is the measurement and analysis of the random or stochastic events occurring naturally during a corrosion process [25]. For on-site measurement it is feasible to monitor potential noise using the potential mapping instrumentation. Perhaps a more useful indicator from potential noise measurements is the identification of pitting corrosion, where transients showing a rapid drop followed by an exponential type recovery indicate film breakdown and repassivation processes. The biggest problem with potential noise analysis, for reinforced concrete structures, is the time required to obtain data and subsequent analysis.

A number of researchers have, over the past ten years, used electrochemical impedance to provide information on the concrete interface and corrosion rate. A small amplitude voltage sine wave is applied and the current response is obtained as the modulus of impedance and phase shift, the data being plotted in the complex plane (resistive vs. capacitive with frequency as a parameter) or as frequency spectra [26].

The visual examination of concrete may indicate the presence of corrosion, but it is not always a reliable indicator. For field investigations, delamination, and rust staining of a concrete surface are two possible indications that reinforcing steel corrosion is occurring. Unfortunately, when these symptoms are observable at the concrete surface, significant damage to the structure may have already occurred.

2.3 Effect of Metal Composition

As noted in Section 1.5, one of the most promising ways of reducing corrosion is by altering the reinforcing bar chemistry. The extreme application of this concept, of course, is the use of stainless steel rebars. These are very costly but have been used successfully in facades and other applications where the aesthetic consideration required them. Over the years a number of alternates have been suggested. In 1986 Nippon Steel [27] produced two types of rebars, one with high Ni and one with Cu-W, that showed in electrochemical measurements tests that these bars were far superior to ordinary reinforcing bars. Similar results, although not of the same magnitude, were found when the tests were conducted in actual concrete specimens. Nippon Steel produced these bars commercially but found few customers because of their high costs. The high Ni bars have also been promoted within the U.S. as an attractive alternative to stainless steel [28].

In 1990, Nippon Steel in cooperation with Tata Iron and Steel of India, produced several new types of bars that showed similar performance to those produced in 1986. The chemical

composition of these bars has not been made public, except to note that they have carbon equivalent contents between 0.30% and 0.45% and contain Cu, Cr and P [29].

Wallwork and Harris [30] thought that localized corrosion might affect the performance of many metals in the variety of environments but the pitting of stainless steel, aluminum and mild steel particularly in chloride environments, is a significant practical problem. Using metallographic and electrochemical methods they showed that pitting corrosion initiated at manganese sulfides. Jang believes that reducing the manganese sulfides gives a great improvement of corrosion resistance of steel in concrete-chloride environments [1,2]. It was primarily to test Jang's hypothesis that this research project was started.

2.4 Materials

For this research four types of rebars were utilized. The first type was an ordinary steel reinforcing bar which has a relatively high percentage of sulfur. The three other rebars were provided by Nippon Steel and consisted of a low sulfur rebar, a copper-tungsten rebar, and a high nickel rebar. The chemical composition of these bars is given in Table 2.1

2.5 Experimental Setup

As noted before, these experiments are based on the work of Iwasaki and Jang [1] and utilize a replica of their experimental setup (Figures 2.3 and 2.4). The corrosion cell consists of two rebar specimens embedded in an epoxy matrix acting as electrodes, two different electrolytes, and salt bridge. The rebar electrode was made by attaching an electrical wire to 0.25" long and 0.5" diameter steel section with a silver conductive epoxy, and by mounting them in an epoxy (Figure 2.5). After the epoxy hardened, the bottom face of the mounted rebar was ground using silicon carbide abrasives, polished using 1 micron diamond compound, and finally polished using 0.05 micron aluminum oxide. The intent was to reduce the surface defects to something less than 0.000005 in. to minimize or eliminate their effect.

The salt bridge for ionic passage was made from a glass tube, whose inside was filled with saturated potassium chloride and both ends were blocked by porous vycor.

Two kinds of electrolyte were used in both half cells. One type of electrolyte was made from just deionized water containing 100 grams of concrete pieces (Series 1). This electrolyte showed 11.5 - 12.5 Ph a day after immersion of concrete. However, the Ph decreased continuously even without any visual corrosion developing. With this electrolyte 3%, 6% and

20% NaCl solutions were used in the anode cells to examine the effect of the concentration of chloride on corrosion of steel in concrete. Each different concentration solution group had 6 samples. Thus a total of 72 corrosion cells (4 rebar samples times 6 samples per bar times 3 concentrations) were prepared.

Table 2.1 - Chemical Composition

	Ordinary Steel	Nippon Steel Low Sulfur	Nippon Steel 3.5 Ni	Nippon Steel CuW
C	0.47	0.216	0.104	0.27
Si	0.243	0.293	0.634	0.097
Mn	0.738	1.079	0.592	0.437
P	0.018	0.014	-	-
S	0.035	0.006	0.004	0.004
Cu	0.349	0.004	0.016	0.24
Ni	0.111	0.034	3.446	0.018
Al	0.002	0.001	0.044	0.038
W	0.002	-	0.005	0.120

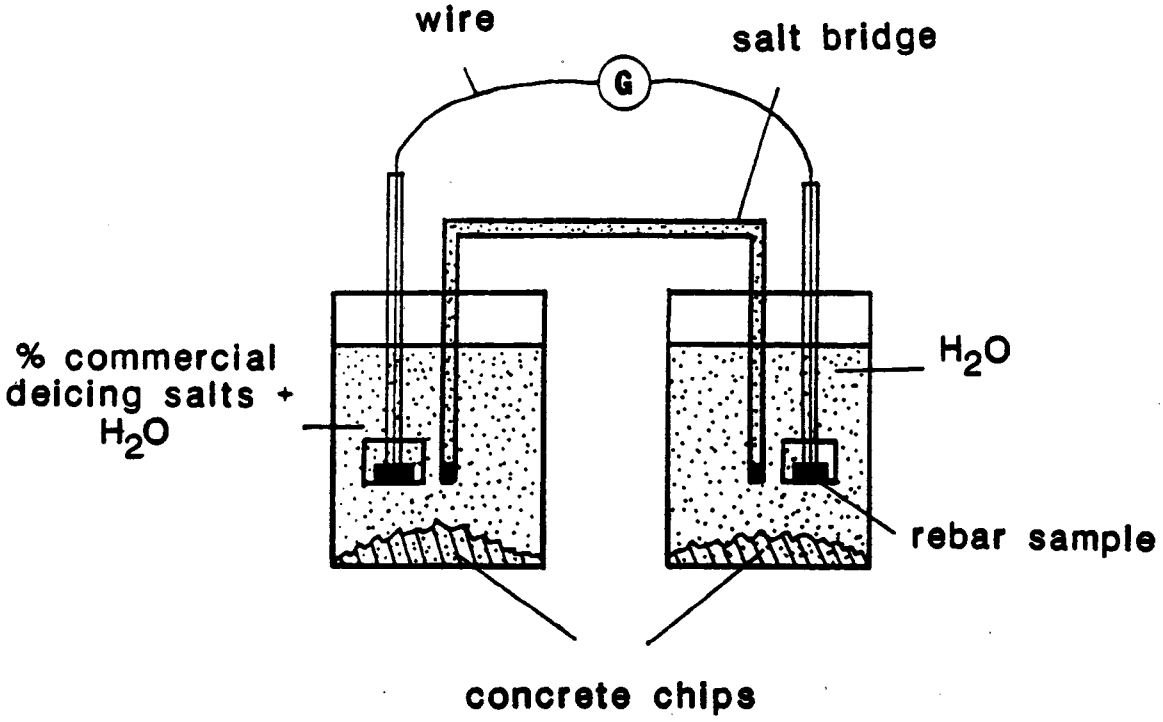

Figure 2.3 - Corrosion cell setup.

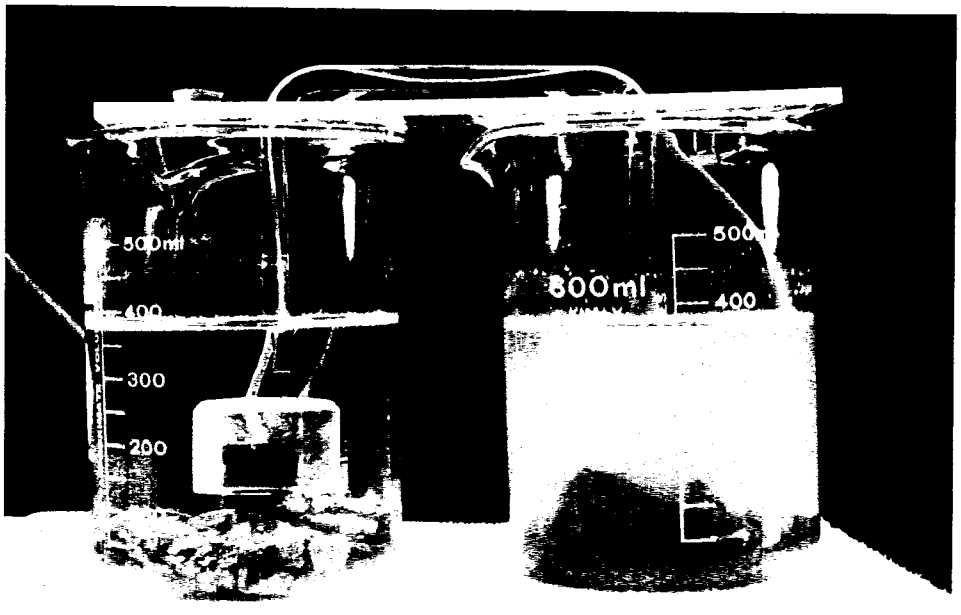

Figure 2.4 - View of typical setup.

The other type of electrolyte was made by adding calcium hydroxide to the former electrolyte (series 1) to maintain the constant Ph (Series 2). By comparing the performance between Series 1 and 2 one can see the effect of changing Ph. For this electrolyte a total of 16 galvanic cells with only one concentration (3% NaCl solution) were made for the four different kinds of bars.

The laboratory corrosion cell was completed by dipping two separate electrodes into two separate beakers and connecting them electronically and ionically by an electrical wire and a salt bridge, respectively.

In this experiment galvanic corrosion current density, corrosion potential, and polarization techniques were examined to find out the effect of chloride ion and chemical composition of steel, and to see if the galvanic method is as efficient as the well-known polarization resistance methods or Tafel extrapolation.

These measurements were made with an EG&G Model 350A corrosion measurement console, a microprocessor-driven device capable of doing potentiodynamic, potentiostatic, Tafel, polarization resistance, pitting, and galvanic measurements. The saturated calomel electrode (SCE) was used as the reference electrode in measuring current and potential.

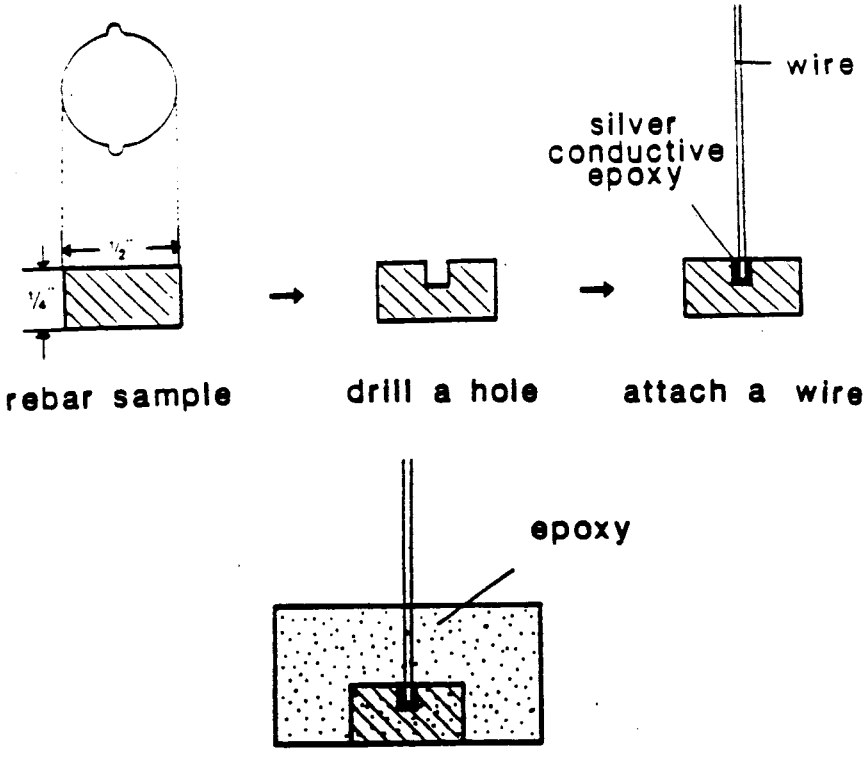

Figure 2.5 - Reinforcing steel electrode

CHAPTER 3

RESULTS AND DISCUSSION

This chapter is organized in four sections. Section 3.1 contains a brief description of the visual observations made during the tests. Section 3.2 presents the results obtained from the galvanic corrosion-potential measurements and their analysis. Section 3.3 discusses the galvanic corrosion-current densities measurements made with the corrosion cells. Sections 3.4 and 3.5 present the polarization resistance measurements and Tafel measurements respectively.

3.1 Visual Observations

In the original tests (Series 1), visual evidence of corrosion was detectable within a week after immersion for several anodes of the corrosion cells. These corrosion spots were probably caused by the surface defects and also by the imperfect boundary between the steel and the epoxy. In the original research plan it had been decided to try to keep track of the corrosion initiation by using high definition microscopes and electron microscopes. Figure 3.1 shows some of the electron microscopy results for the original specimens; the differences in the size and number of the inclusions is clear.

After about two weeks most of the corrosion cells in Series 1 showed light brown corrosion products at their anodes and the electrolytes were becoming turbid. Initially the corrosion products, in general a thin brown film, seemed to be uniformly distributed but as time went by they seemed to concentrate in a specific portion of the sample. At this early stage it seemed that there was some visual difference between the corrosion products in the four types of specimens. The ordinary rebar and the low-sulfur bars seemed to have the largest concentration of corrosion products. However, by the time four weeks had elapsed it was impossible to tell the difference in performance visually. At this stage the electrolytes had also become very turbid and their Ph decreased substantially, ranging from 10.8 to 11.5. Figure 3.2 shows the results for the 3% NaCl solution, while Figures 3.3 and 3.4 show the results for the 6% and 20% solutions respectively. Note that the specimens for the low sulfur tests at 20% are missing since problems were encountered with excessive initial corrosion at the epoxy interface. These pictures were taken after 90 days of immersion and 90 days in air. Most of the corrosion in the cathodes took place after the specimens were removed from the corrosion cells. Figure 3.5 shows a comparison of selected anodes for the three concentrations and four different types of bars.

(a) Ordinary rebar (1500x mag.).

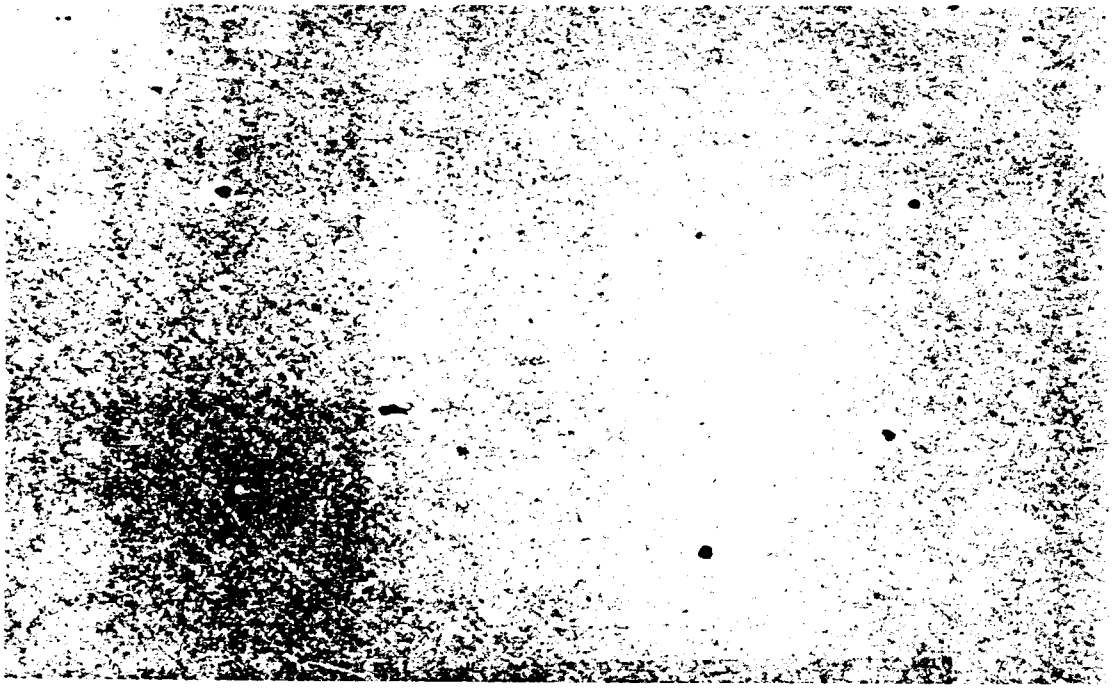

(b) Low-sulfur bar (1500X mag.).

Figure 3.1 - Electron microscope scans.

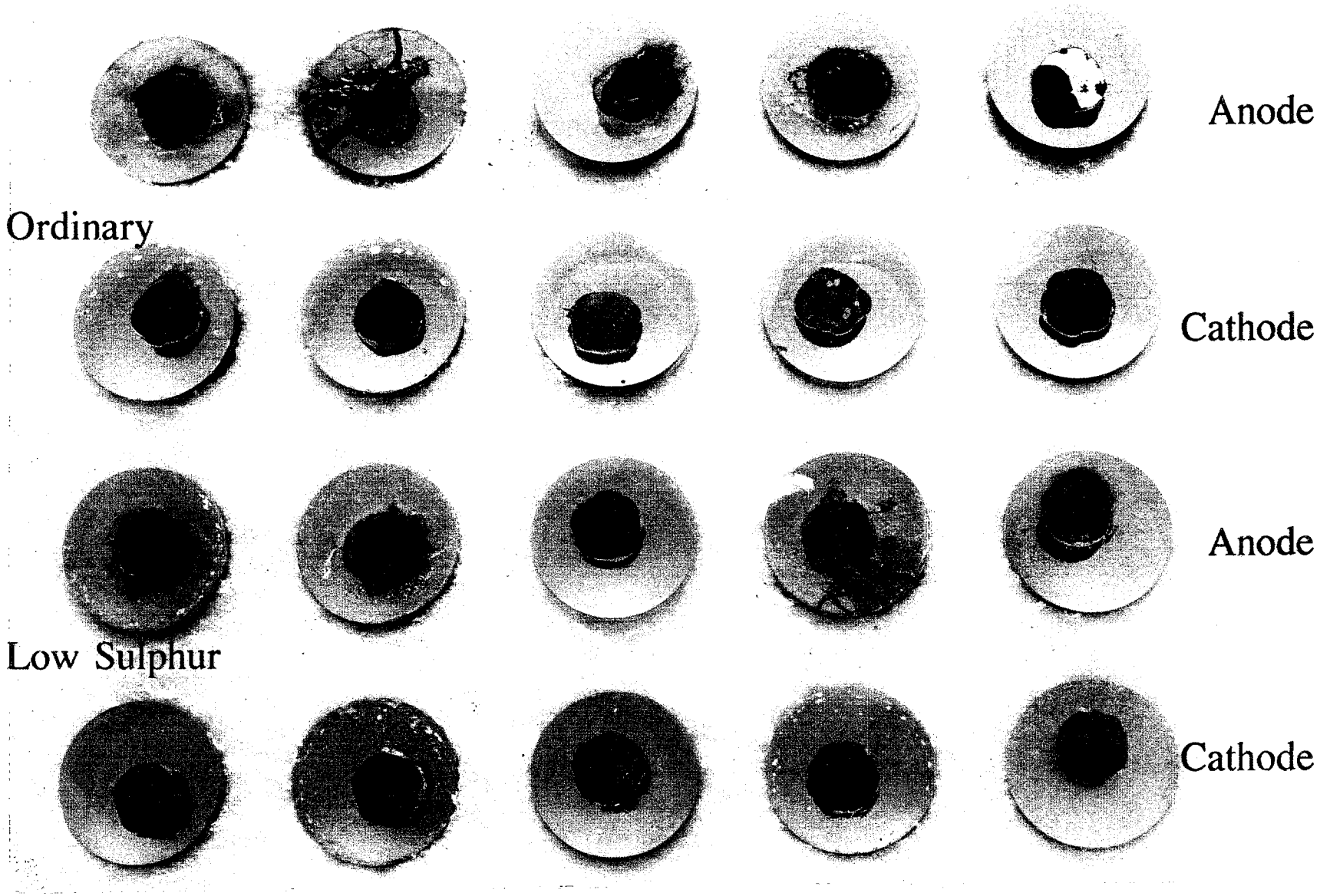

Figure 3.2 - View of ordinary and low sulphur specimens - 3% Solution (Series 1)

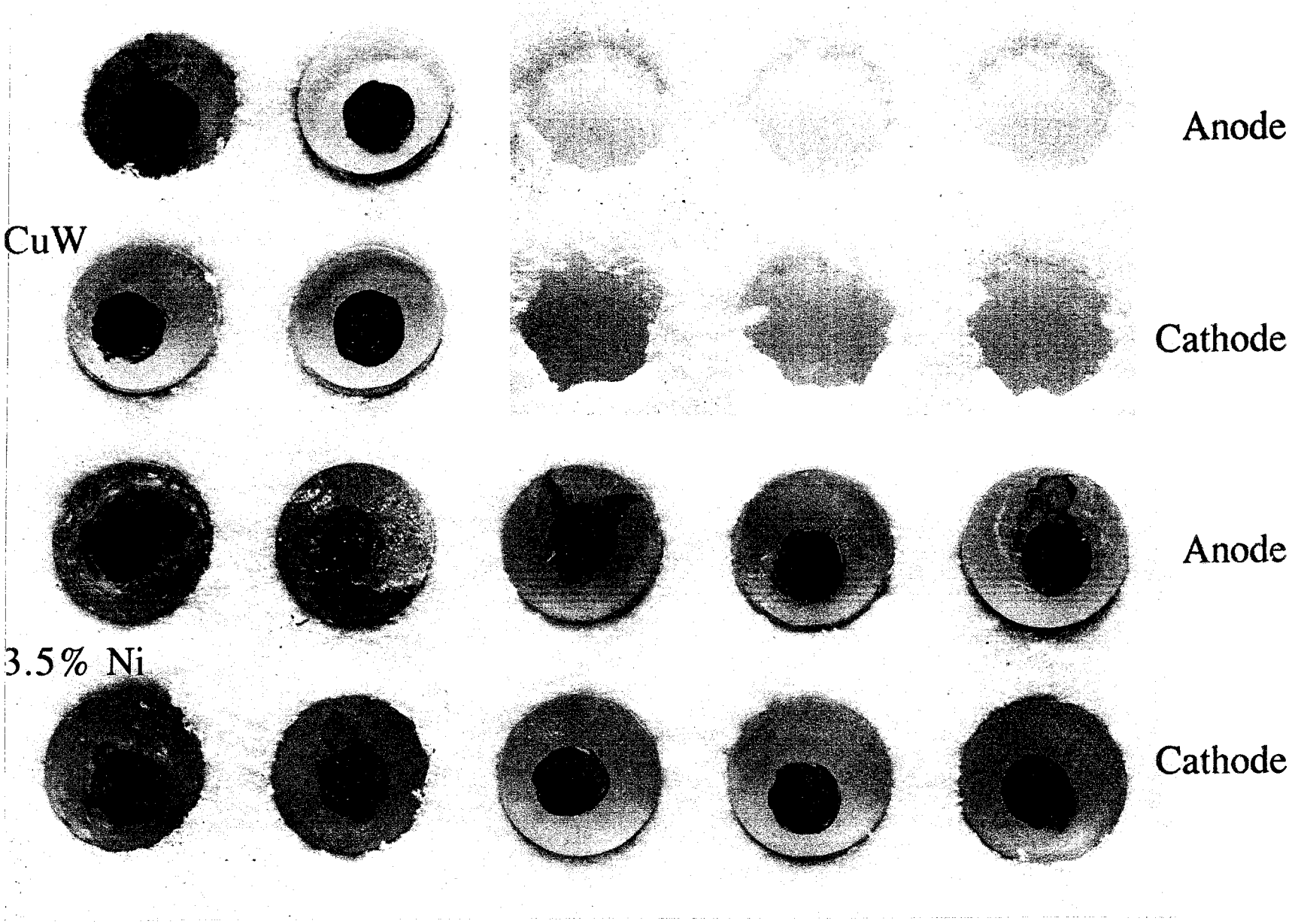

Figure 3.2 - View of copper-tungsten and nickel specimens - 3% Solution (Series 1)

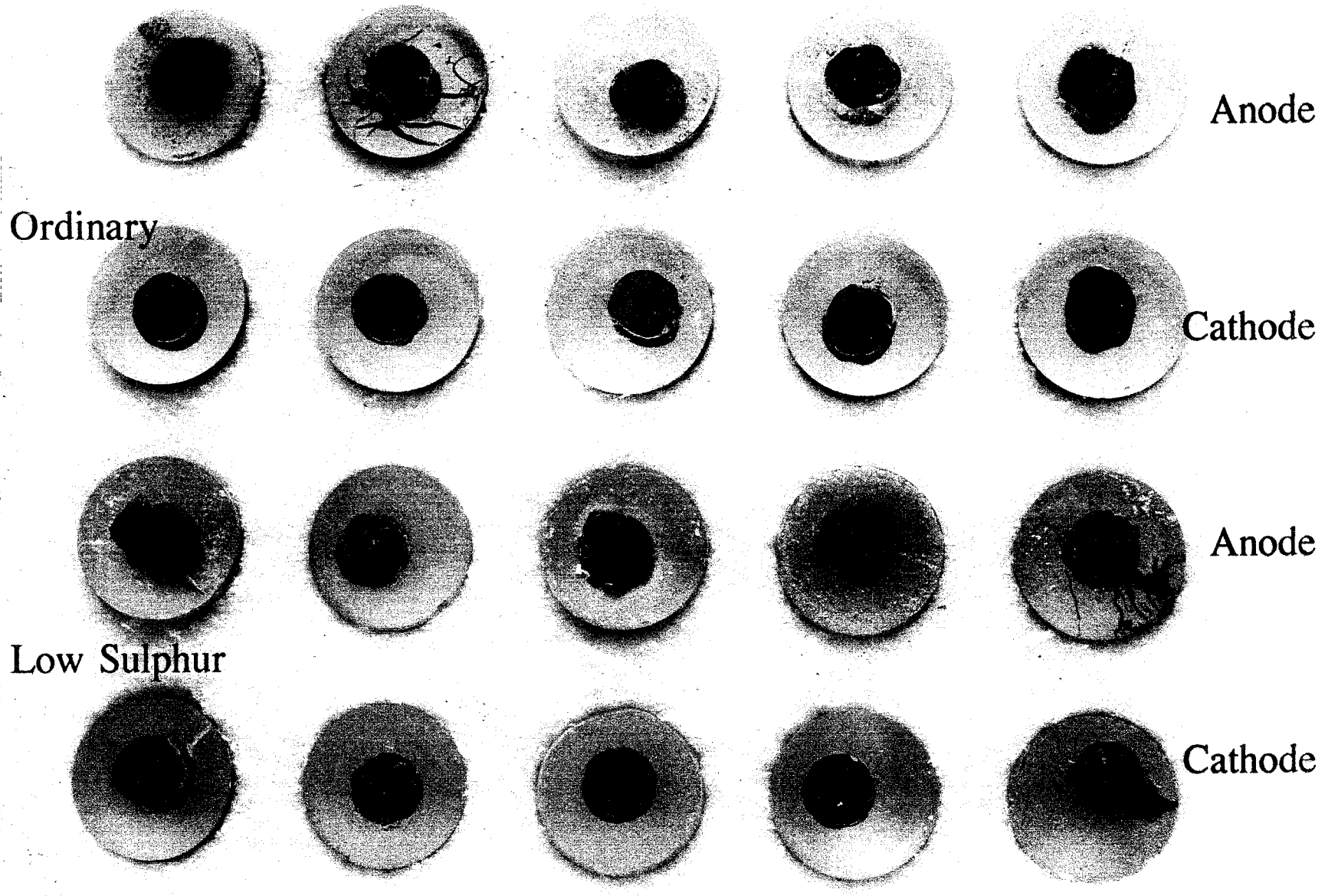

Figure 3.3 - View of ordinary and low sulphur specimens - 6% Solution (Series 1)

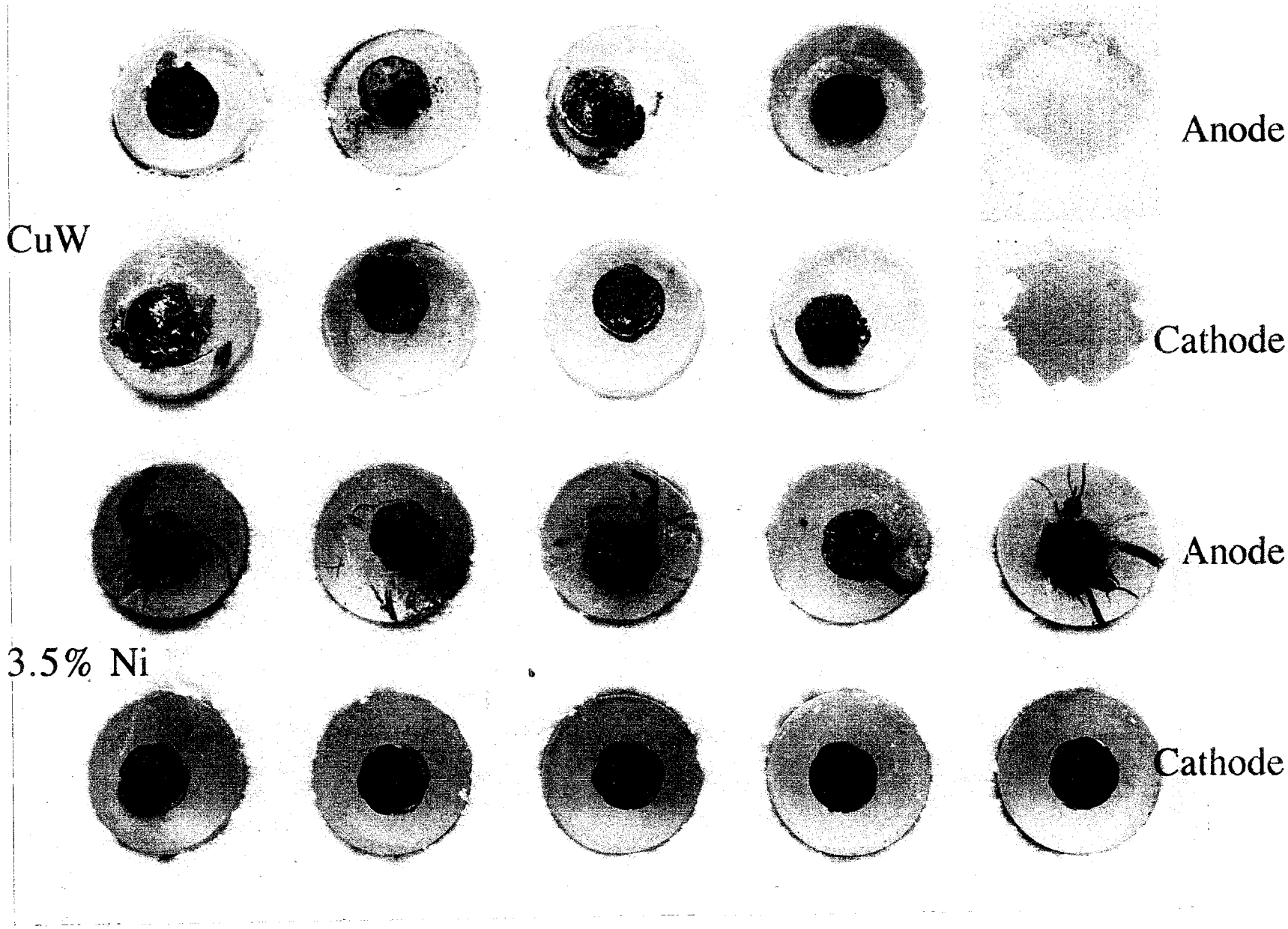

Figure 3.3 - View of copper-tungsten and nickel specimens - 6% Solution (Series 1)

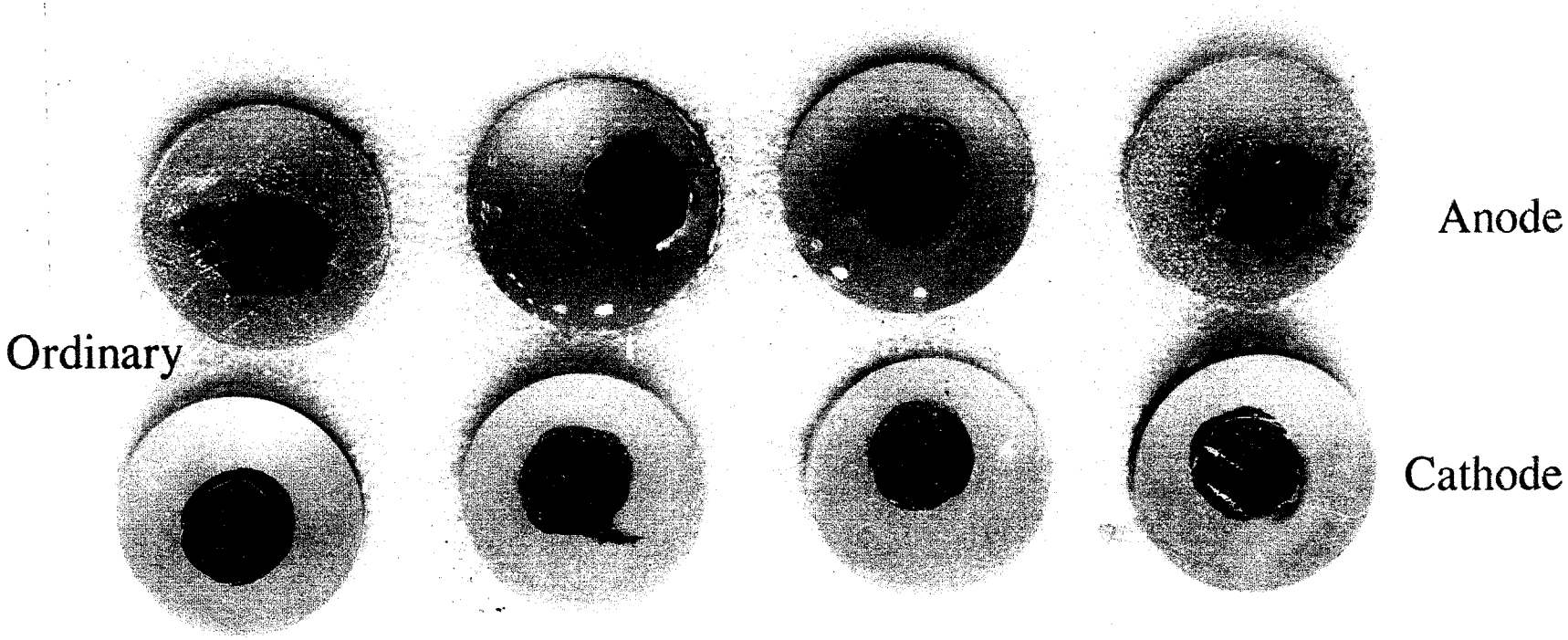

Figure 3.4 - View of ordinary specimens - 20% Solution (Series 1)

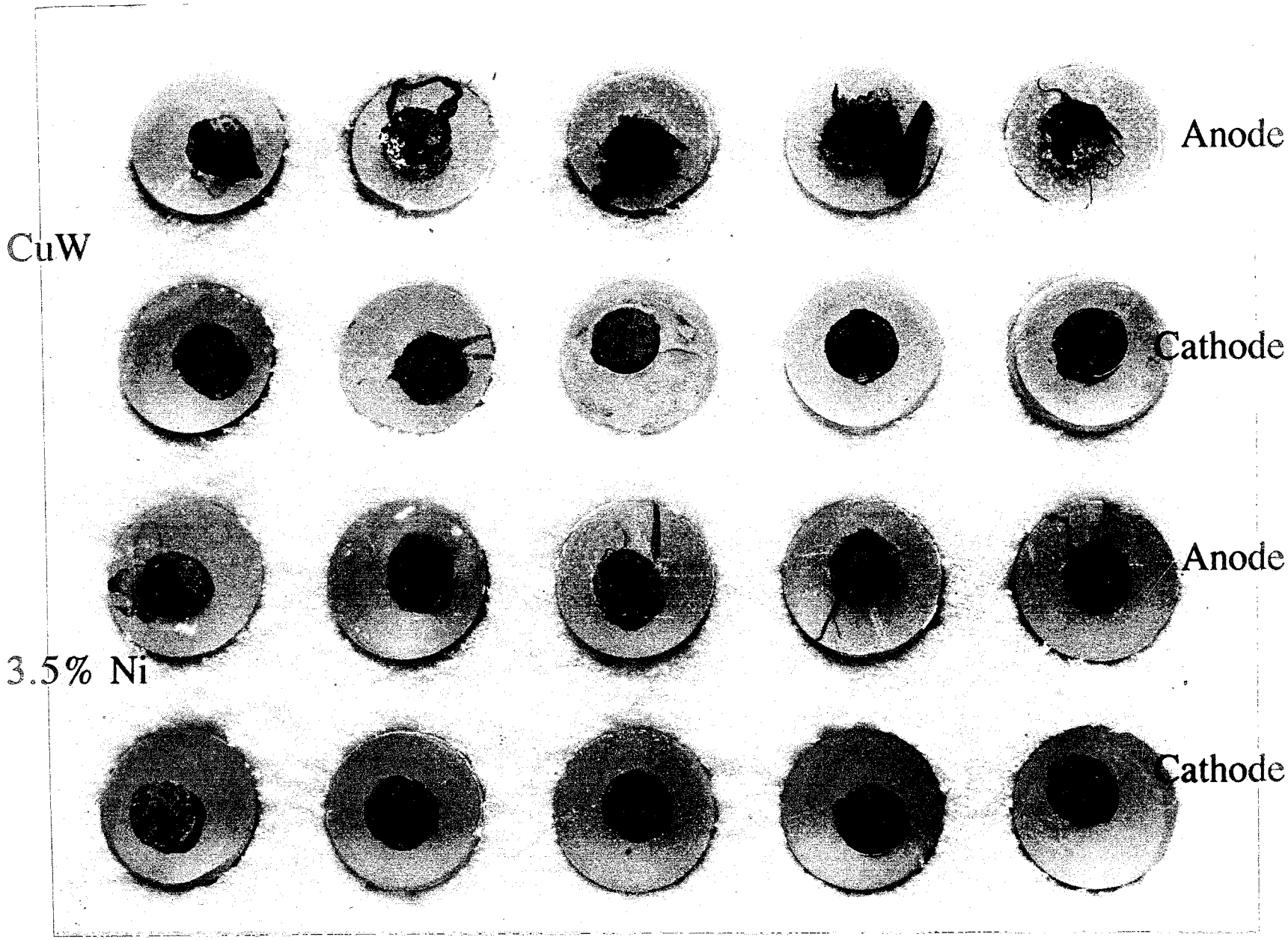

Figure 3.4 - View of copper-tungsten and nickel specimens - 20% Solution (Series 1)

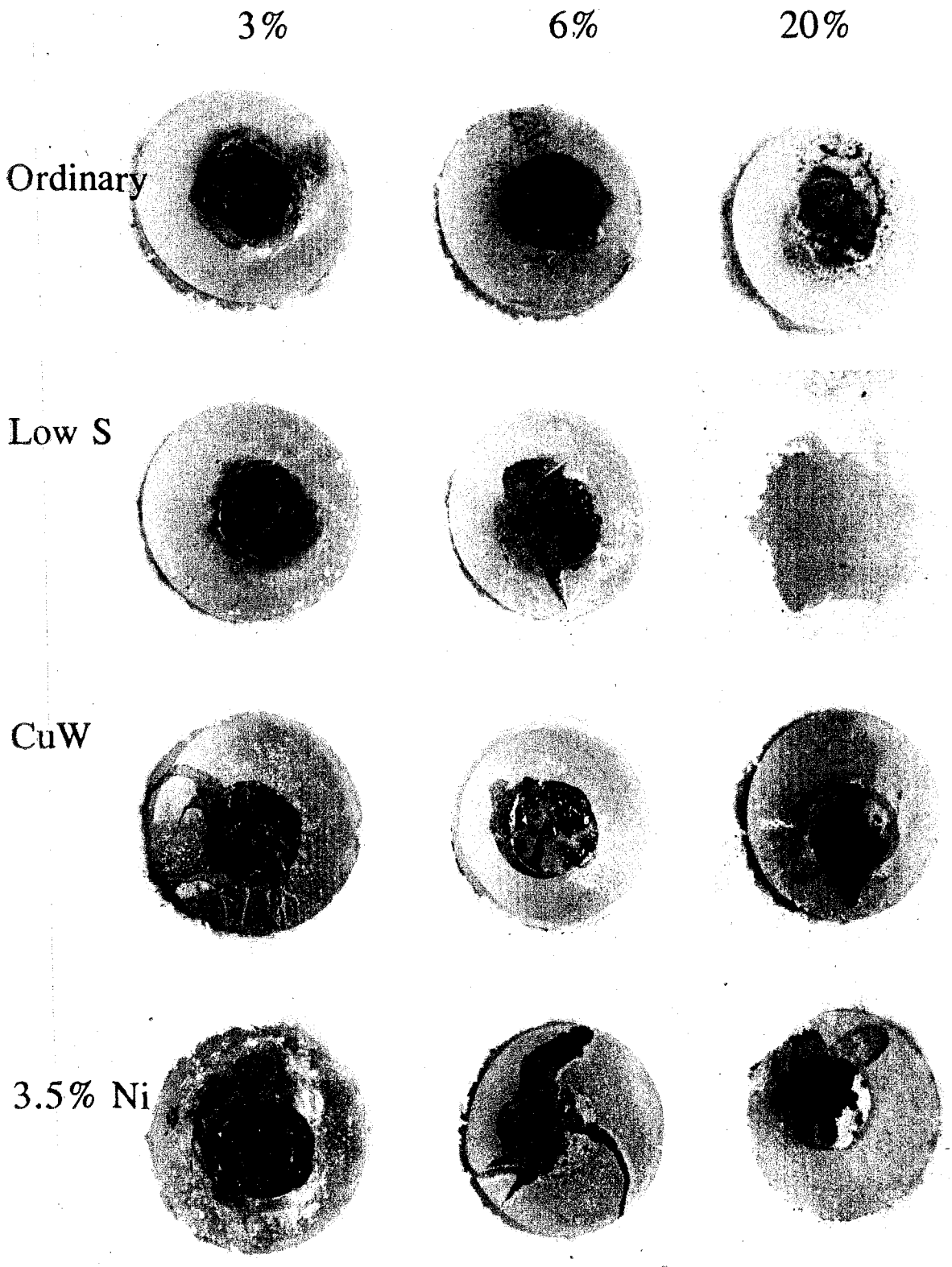

Figure 3.5 - Comparison of cathodes for Series 1.

For Series 2, in which the Ph of the electrolyte was carefully controlled and kept at 12.5, the performance was qualitatively similar (Figure 3.7). However, it appeared that the amount of corrosion product generated was somewhat smaller (see Figure 3.6).

Unfortunately it was impossible, due to scheduling conflicts with the electron microscope in particular, to properly track the development of the corrosion products visually. Thus it is impossible to state that the corrosion initiated at the sulfur inclusions as Iwaskai and Jang speculated [1,2].

The weight loss measurements made, which typically are another method of quantifying the corrosion products, gave very unreliable results and could not be used to quantify the performance. Many of the specimens indicated weight gains rather than weight losses probably because of water that appeared to be trapped in the epoxy and at the epoxy-steel interface. Even the results that showed the proper trend had a tremendous scatter and did not conform to visual observations.

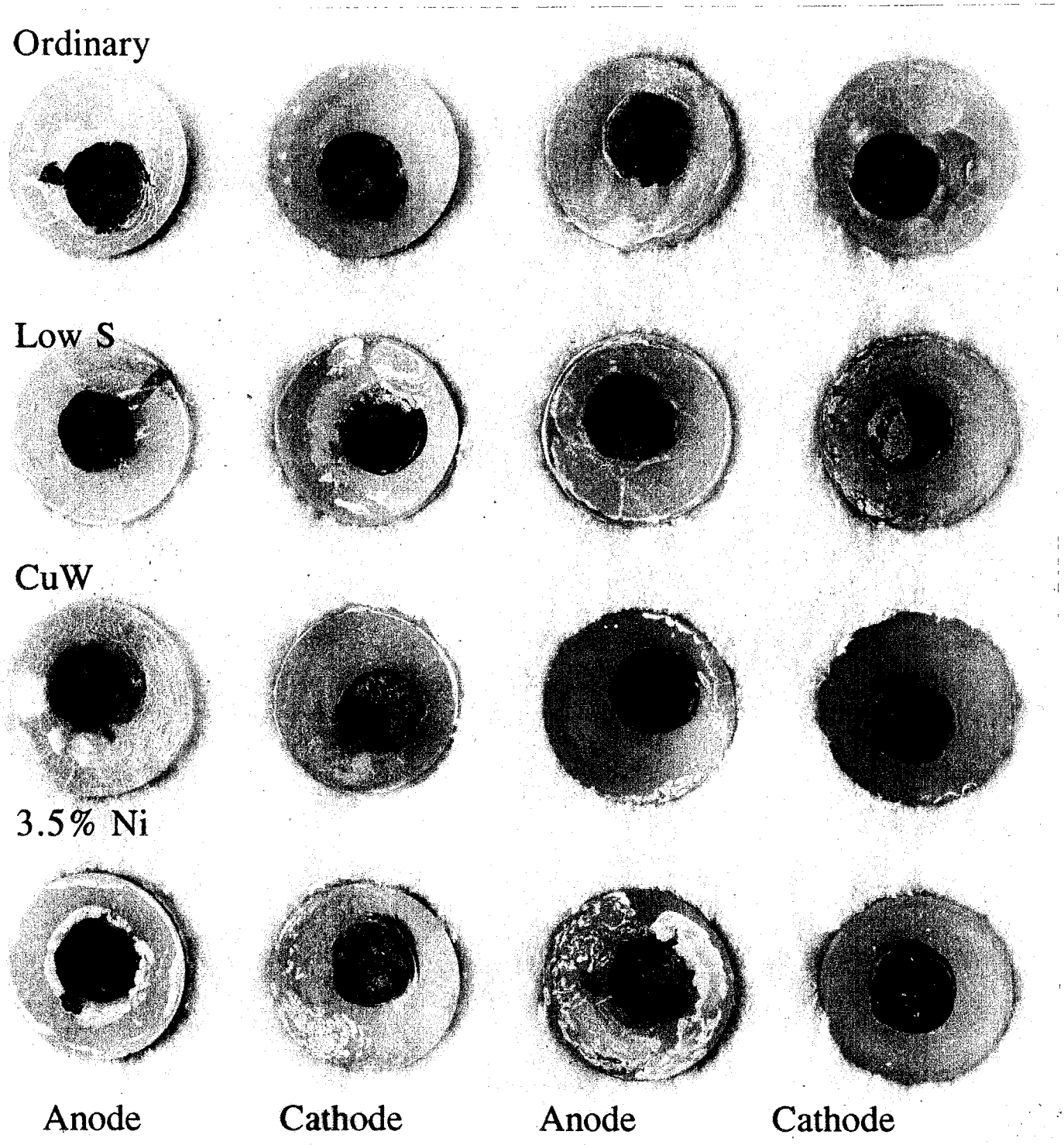

Figure 3.6 - Corrosion in the specimens for Series 2.

3.2 Potential Measurements

Because of technical problems encountered with the EG&G 350A corrosion measurement system described in Chapter 2, the potential and current density measurements carried out on the original specimens (Series 1) during the first 30 days were deemed not to be reliable. Thus the results shown here are divided into two sets. The first consists of the data from Series 2, where the Ph of the electrolyte was adjusted to 12.5, and from the last few weeks of Series 1 where the Ph of the electrolyte was not adjusted.

Figures 3.7 through 3.14(a) show these results. In these plots the vertical axis is the potential (in volts) reference to the saturated calomel electrode (SCE). In general potentials greater than -0.20 volts vs. CSE(-0.193 volts vs. SCE) indicate 90% probability of no corrosion, while potentials lower than -0.35 volts vs. CSE(-0.273 volts vs. SCE) indicate 90% probability of corrosion activity. As mentioned before, potential measurements are only an indicator of the likelihood of corrosion, and they can not be used to determine the corrosion rate. Figure 3.14 also includes a typical scatter plot to show the dispersion of the data. This scatter plot is similar to those for all the other cases, and indicates that the average measurements plotted in Fig. 7 through 3.14(a) are a reasonable representation of the data.

In the results of Series 2 (Figure 3.7) one can see a continuously decreasing trend in the potential with time. All values given in the figures are the averages of all the measurements. The ordinary and low-sulfur bars, labelled Ord and 296B in these graphs respectively, reached the -0.20 volt threshold with four to six days, and the -0.35 volt limit at about 44 to 47 days. The CuW and Ni bars reached these same limits in 25 to 28 days and 53 days respectively. The fact that corrosion was visible within the first two weeks in most specimens indicate that the voltage thresholds developed for the ASTM test on bars embedded in concrete may not be the same as for small rebar specimens in an electrolyte. The most surprising result was that the low-sulfur bars performed marginally worse than the ordinary rebars. Based on the hypothesis that sulfide inclusions play an important role in corrosion initiation one would have expected a much better performance from them.

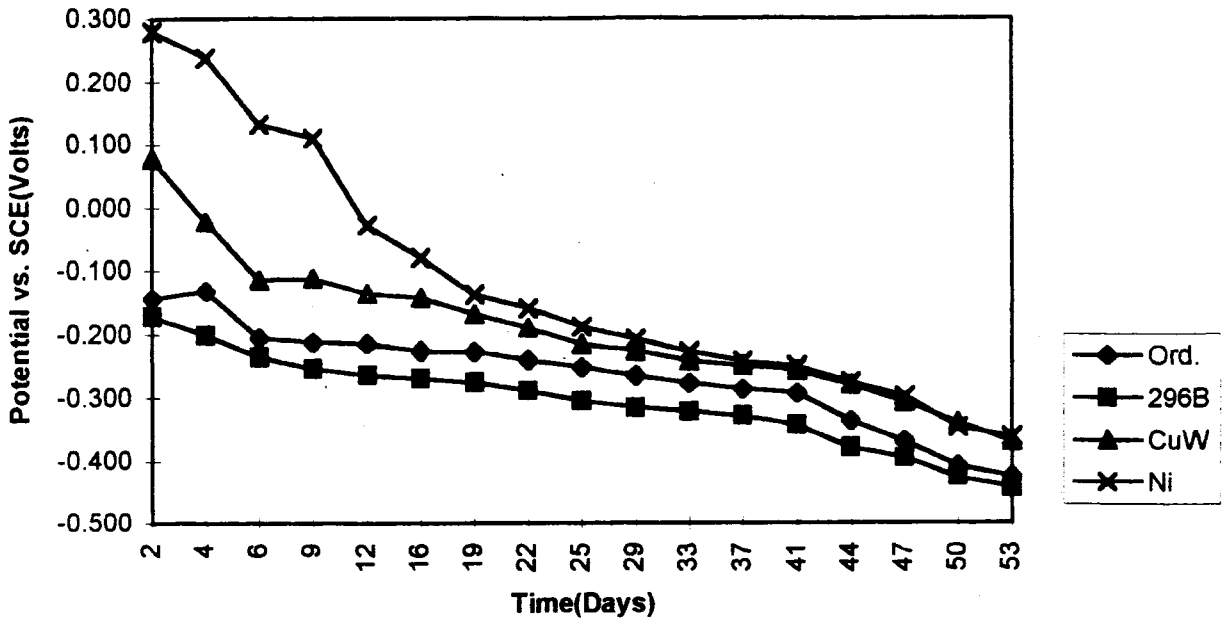

Figure 3.7 - Potential curves in the 3% NaCl solution (Series 2).

From the valid data available for Series 1 it is clear that the trends were similar to those of Series 2. Figures 3.8 through 3.10 show the potential curves of the four different types of rebars in 3%, 6%, and 20% NaCl solutions respectively. Figures 3.11 through 3.14 show the same data but plotted by individual type of bars. The potentials decreased continuously, with the specimens in the 3% solution showing the worst performance. The potential curves in the 3% NaCl solution show that the 3.5% Ni bars were the noblest, followed by the CuW bars, the ordinary bars, and most active were the low-sulfur bars. However, the differences between the noblest and the most active is only 0.1 Volts. Surprisingly, this type of measurement indicates, just as for Series 1, that the low sulfur bars are less efficient in resisting corrosion than the ordinary rebars. In 6% NaCl solution the trends are same as those in the 3% NaCl solution. In 20% NaCl solution CuW bar seems to be nobler than 3.5% Ni bar.

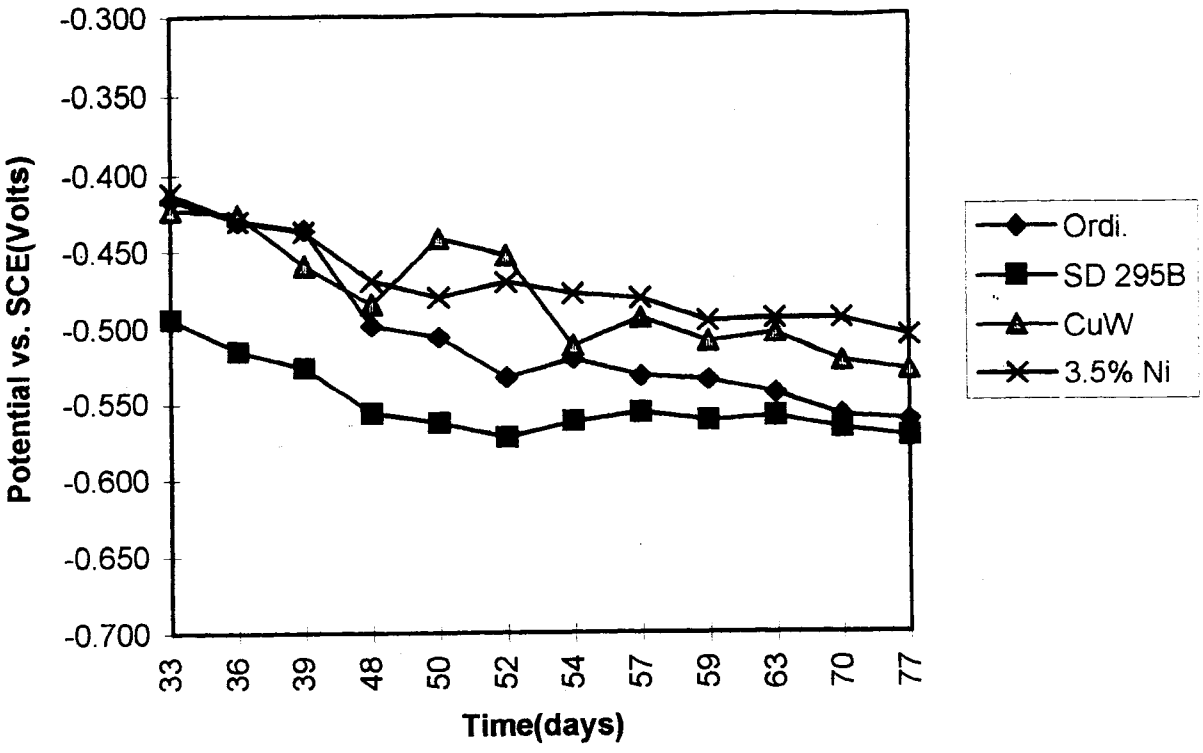

Figure 3.8 - Potential curves in the 3% NaCl solution (Series 1).

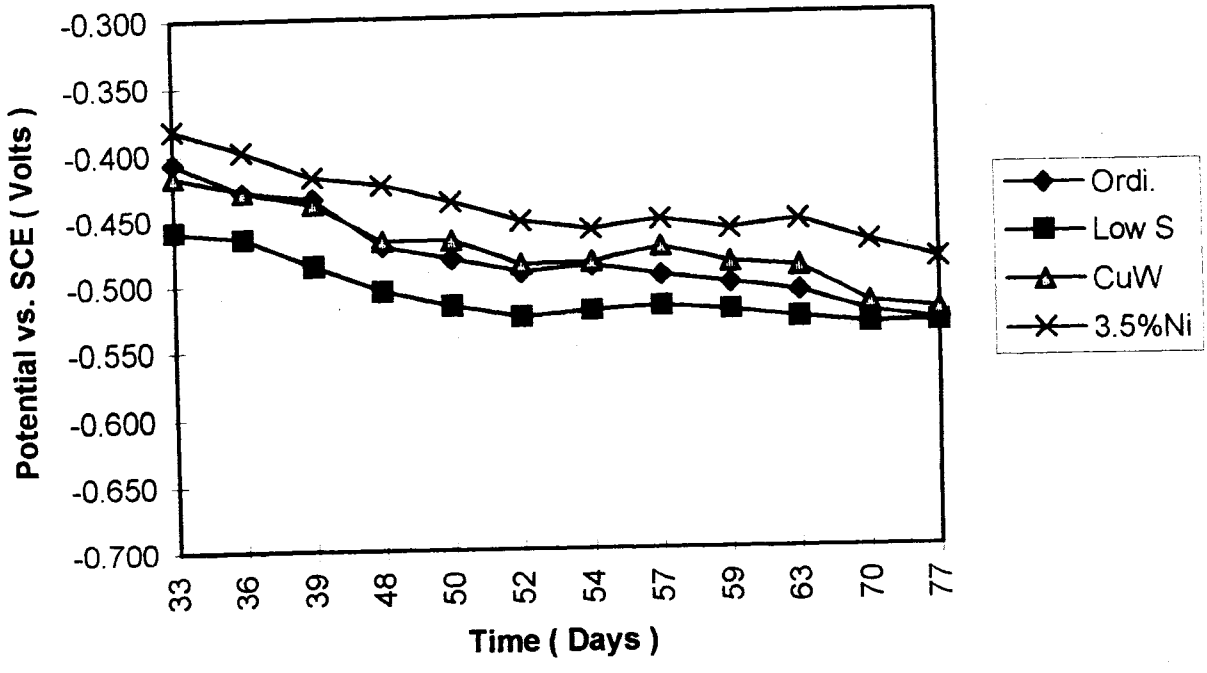

Figure 3.9 - Potential curves in the 6% NaCl solution (Series 1)

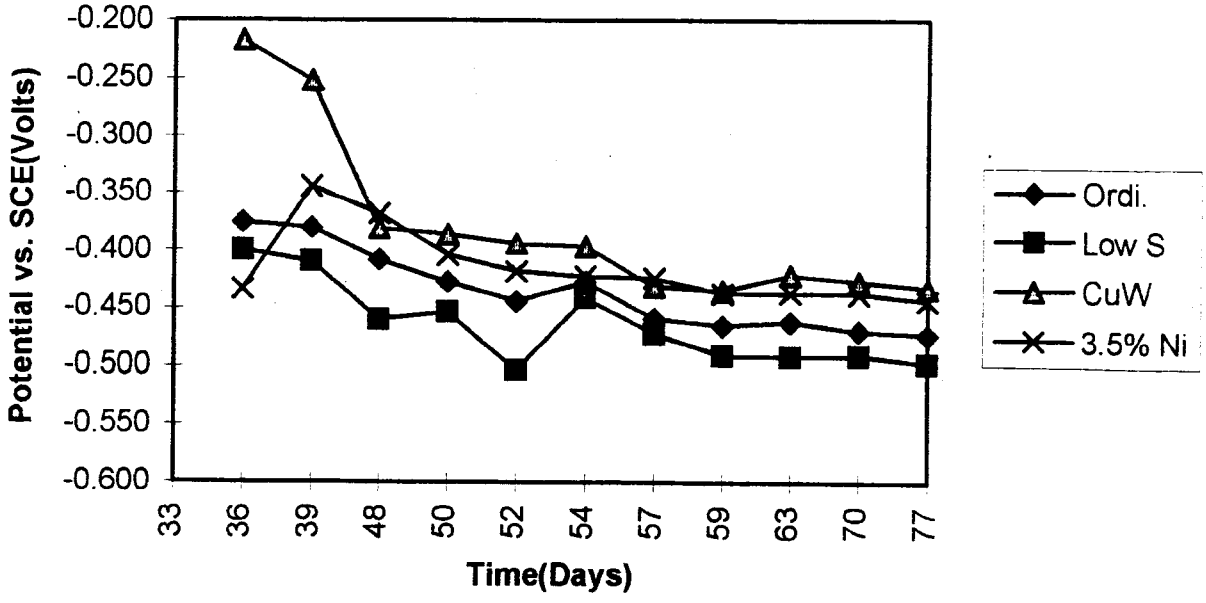

Figure 3.10 - Potential curves in the 20% NaCl solution (Series 1)

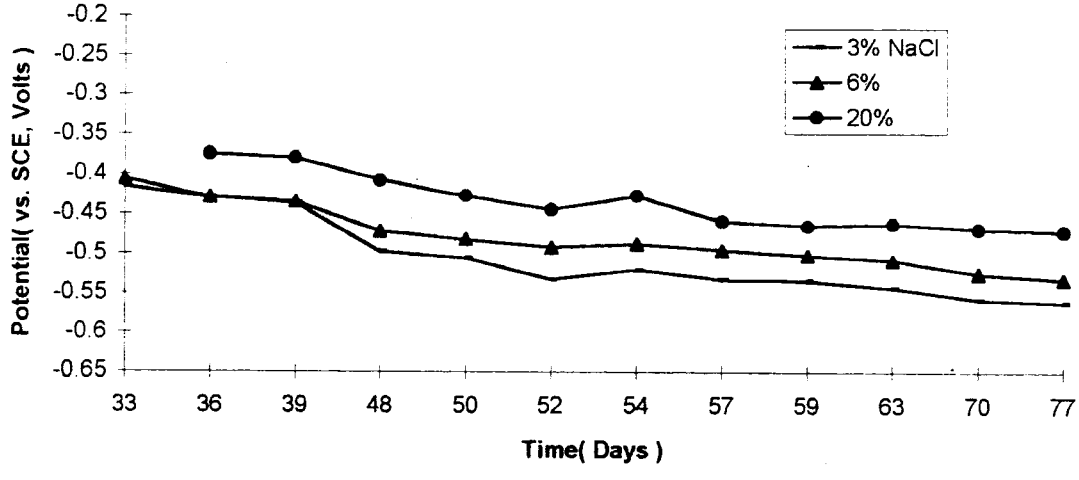

Figure 3.11 - Potential curves of ordinary bars in NaCl solutions (Series 1).

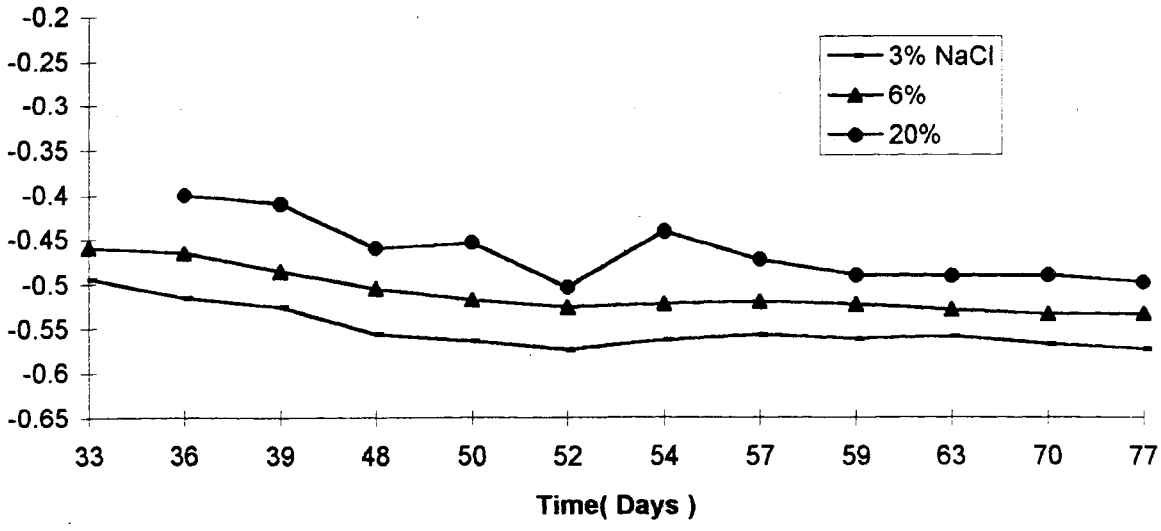

Figure 3.12 - Potential curves of low sulfur bars in NaCl solutions (Series 1).

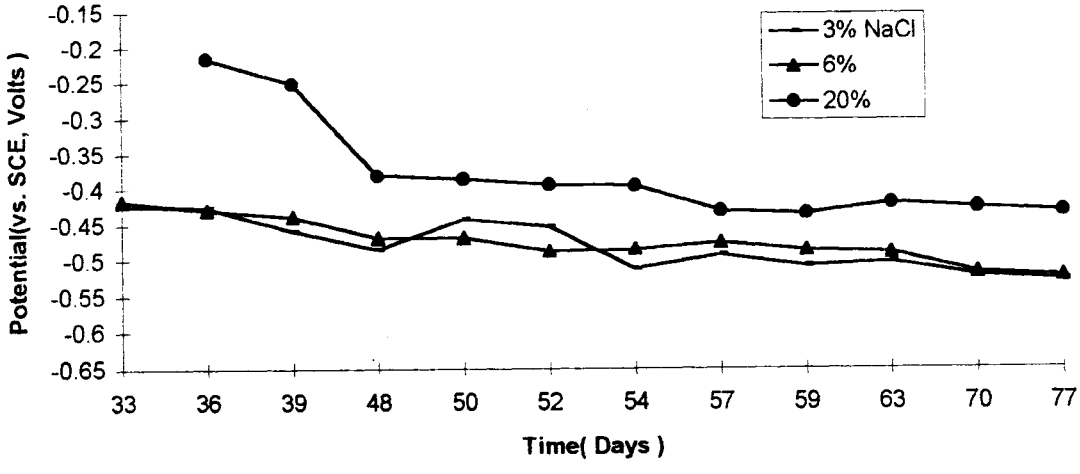

Figure 3.13 - Potential curves of CuW bars in NaCl solutions (Series 1).

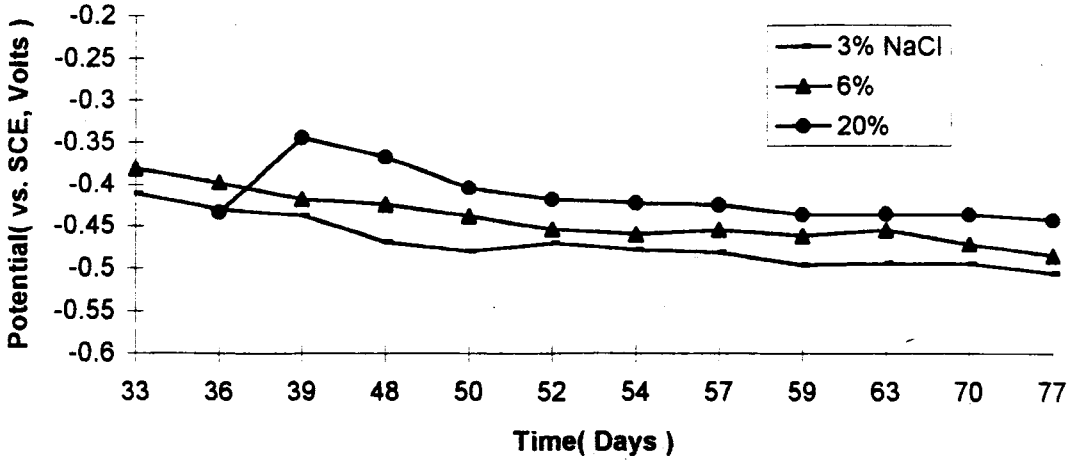

(a) Potential curves of 3.5% Ni bars in NaCl solutions (Series 1).

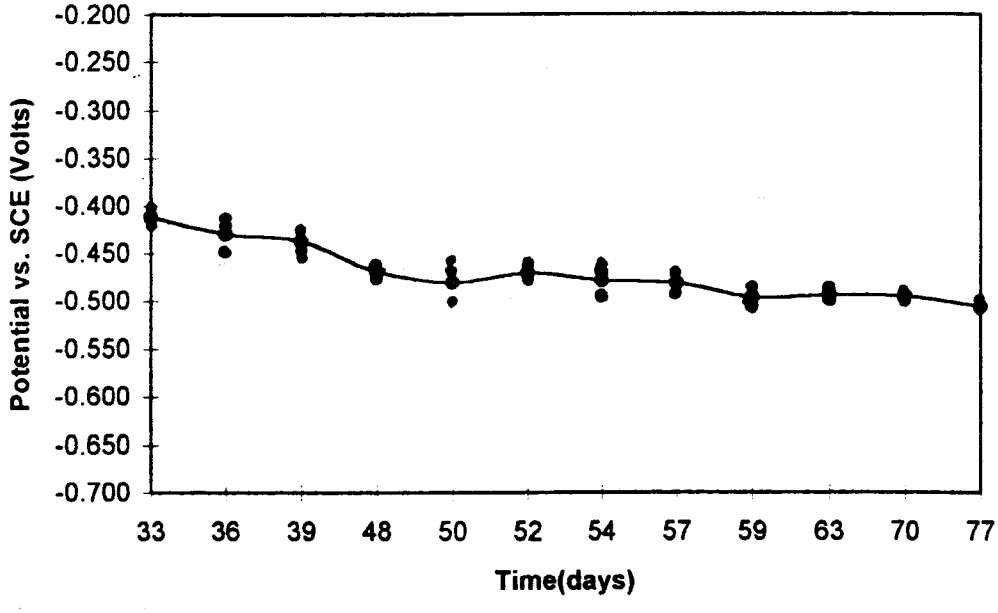

(b) Scatter plot of the measurements for 5.3% Ni bars.

Figure 3.14 - Data for 3.5 Ni bars.

3.3 Current Density Measurements

Figures 3.15 through 3.22 show the current density curves in the same order as for the potential measurements. The units on the vertical axis are nanoAmperes per square centimeter times 10,000. From the beginning of the tests the current density increased until about the 16th day, and decreased from that point until the end of the tests. The reason for the reversal in the trend is that the current density increases before the oxide film or corrosion product forms on the surface of steel. Once the protective film or corrosion product has formed, it will reduce the corrosion reaction rate. Visual examination of the samples at 15 days after immersion showed that most anodic sides of corrosion cells had begun to actively corrode as evidenced by the presence of some sparse red/brown corrosion products.

As anodic dissolution of iron by following anodic reaction continues in the anode cell, the Ph decreases. Fe^{2+} cations hydrolyze to form a soluble weak base, $Fe(OH)_2$, leaving behind excess H^+:

$$FE \rightarrow Fe^{2+} + 2e^-$$

$$Fe^{2+} + 2H_2O \rightarrow Fe(OH)_2 + 2H^+$$

At the same time, as reduction of dissolved oxygen continues in the cathodic cell, the Ph is observed to increase due to the liberation of OH^-:

$$O_2 + 2H_2O + 4e^- \rightarrow 4OH^-$$

The increased alkalinity passivates the cathode, but the increased acidity increases the anodic activity of the anode.

In the second series of tests (Series 2), the cathodic steel was corrosion-free or corroded very little, and the Ph of its electrolyte was maintained around 12.5, very close to the original value. The anodic steel, on the other hand, corroded very severely, and the Ph of its electrolyte dropped from 12.5 to 11.6.

Usually the corrosion rate is proportional to temperature, oxidizer concentration, and solution velocity. Figures 3.16 through 3.22 show the increased current density after agitation of solution (day 54, marked by an arrow in the figures).

Figure 3.15 shows the results from the Ph-controlled electrolyte samples of 3% NaCl solution. The figure shows that the current density increases up to day 16, and then decreases

gradually. The maximum value is about 3.5 x 10^4 Na/cm^2 for the ordinary bar, but after day 41 the corrosion rates for all the bars were almost identical.

Figures 3.16 through 3.18 present the current densities curves for four types of rebars in 3%, 6%, and 20% NaCl solutions respectively (Series 1). All figures show that at the early age there are differences in the corrosion rate, but from about day 48 on it is difficult to detect differences in the corrosion rates.

Figures 3.19 through 3.22 show the effect of NaCl concentration on the corrosion of the steel samples. Although the differences in corrosion activity are not large, the 3% NaCl solution is the most corrosive for all the steel samples.

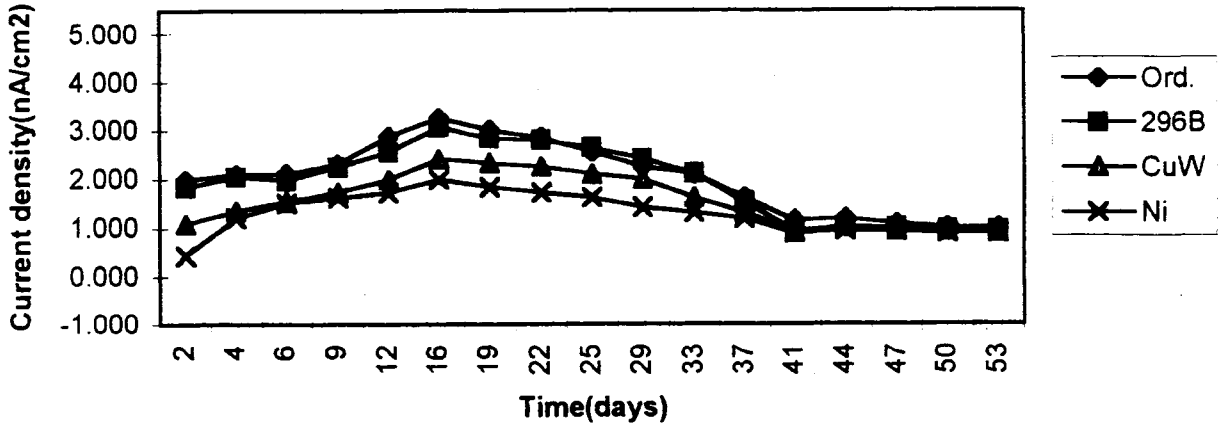

Figure 3.15 - Current density curves for 3% NaCl solution (Series 2).

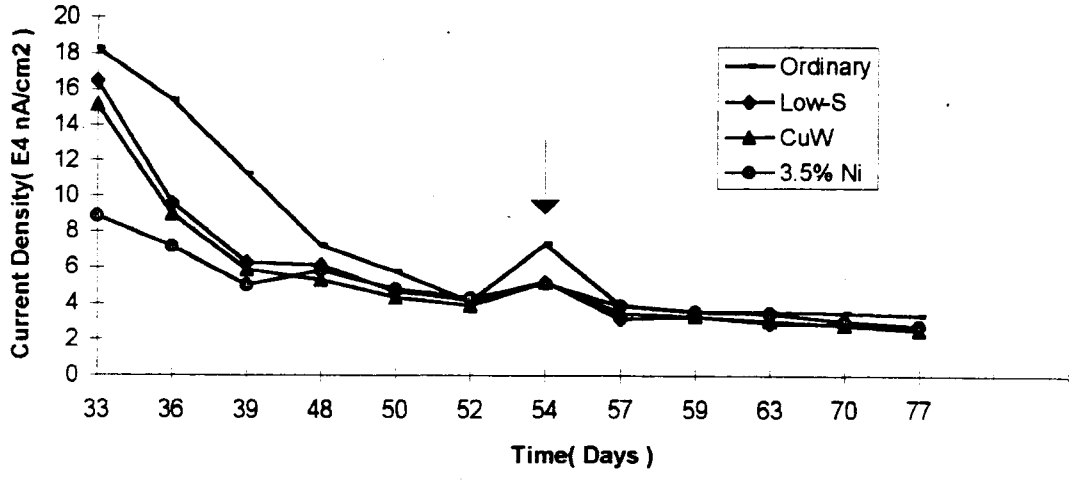

Figure 3.16 - Current density curves in the 3% NaCl solution (Series 1).

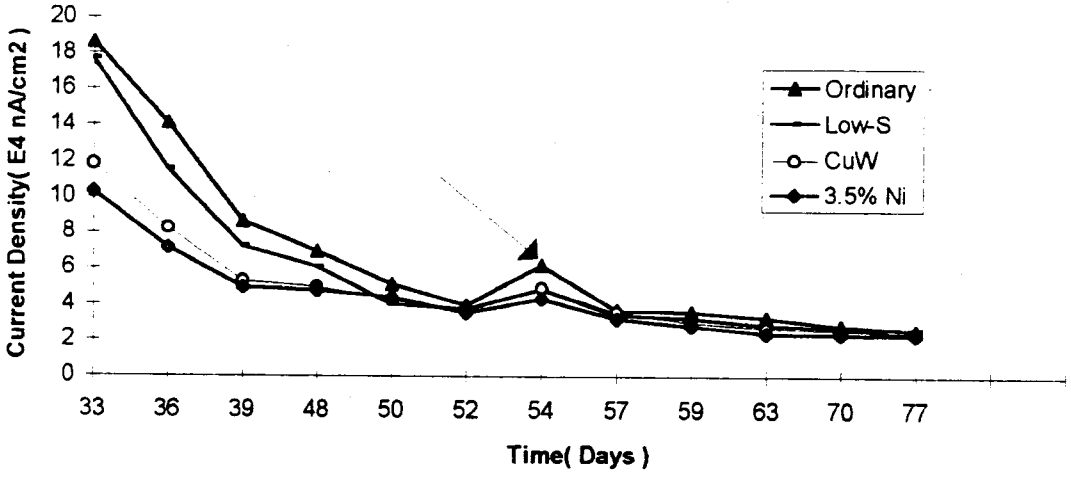

Figure 3.17 - Current density curves in the 6% NaCl solution (Series 1).

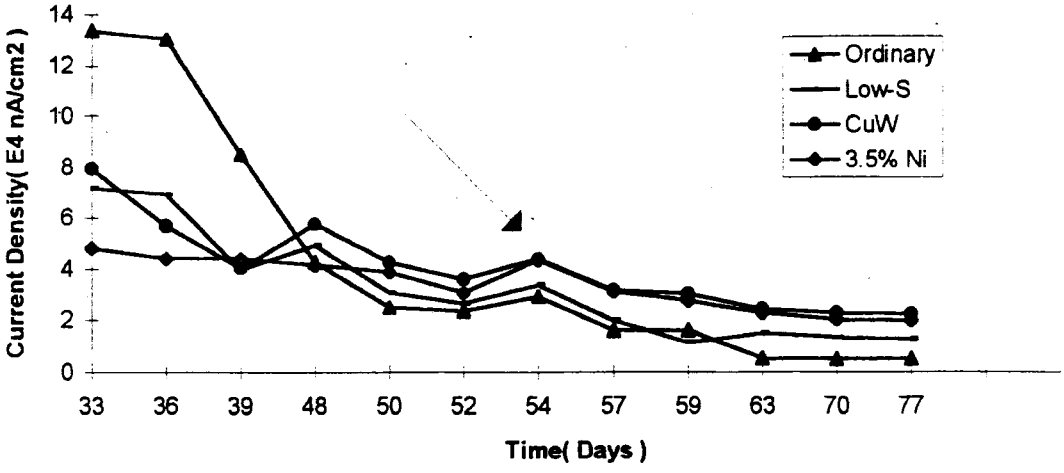

Figure 3.18 - Current density curves in the 20% NaCl solution (Series 1).

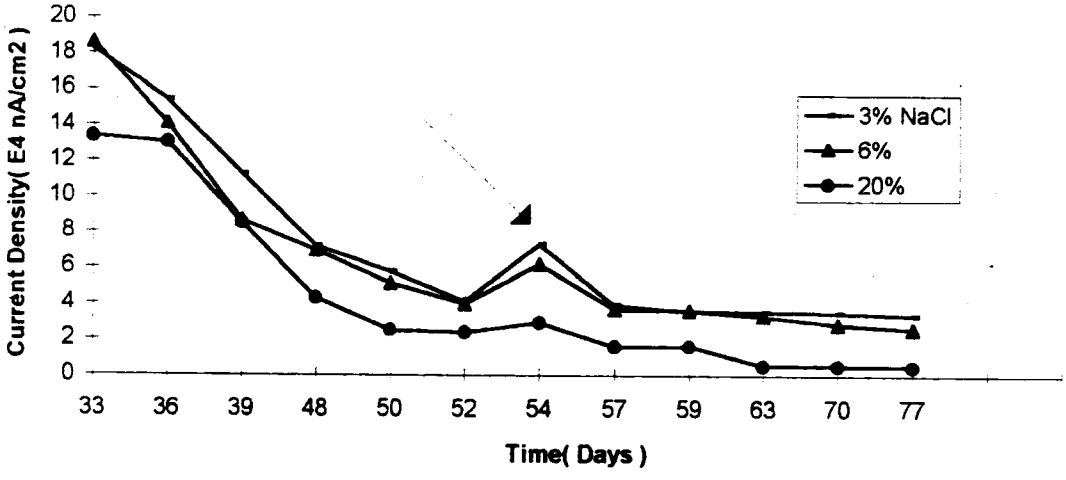

Figure 3.19 - Current density curves of the ordinary bars (Series 1).

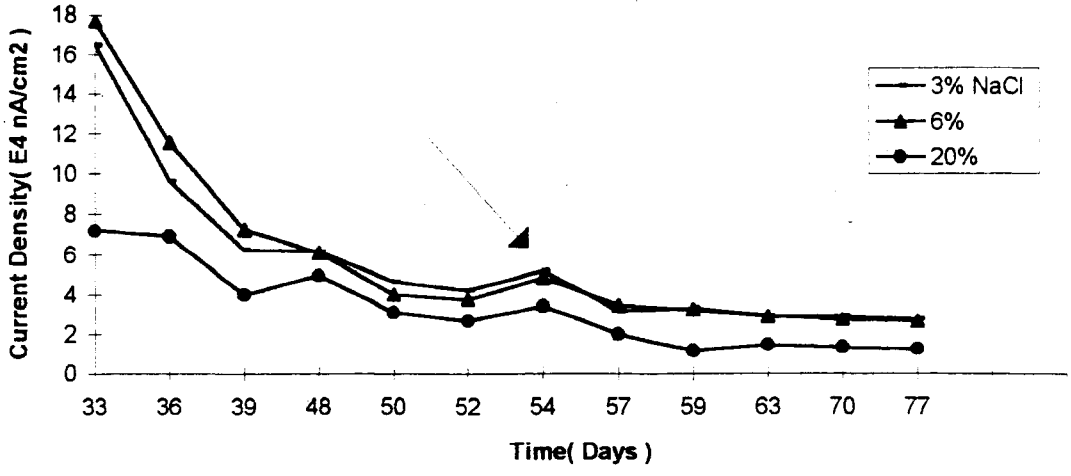

Figure 3.20 - Current density curves of the low sulfur bars (Series 1).

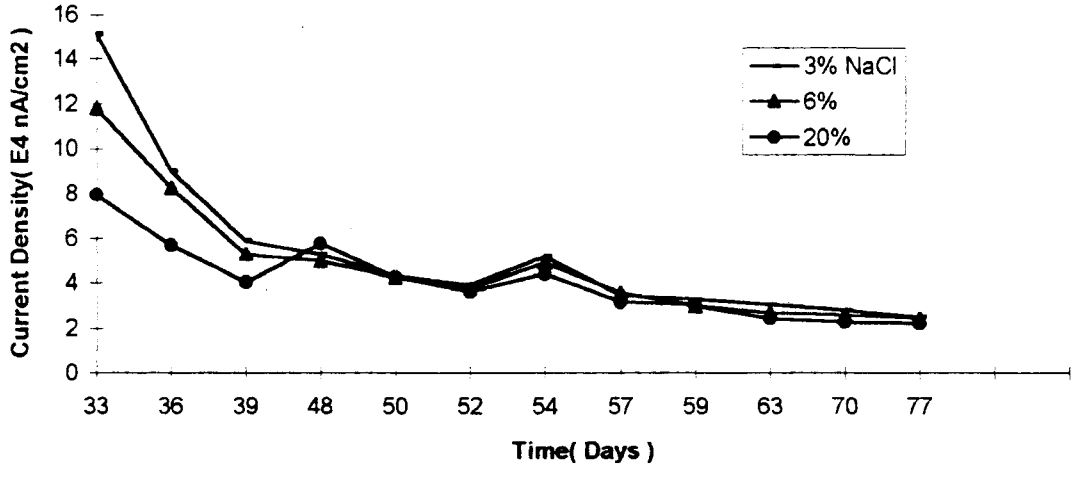

Figure 3.21 - Current density curves of the CuW bars (Series 1).

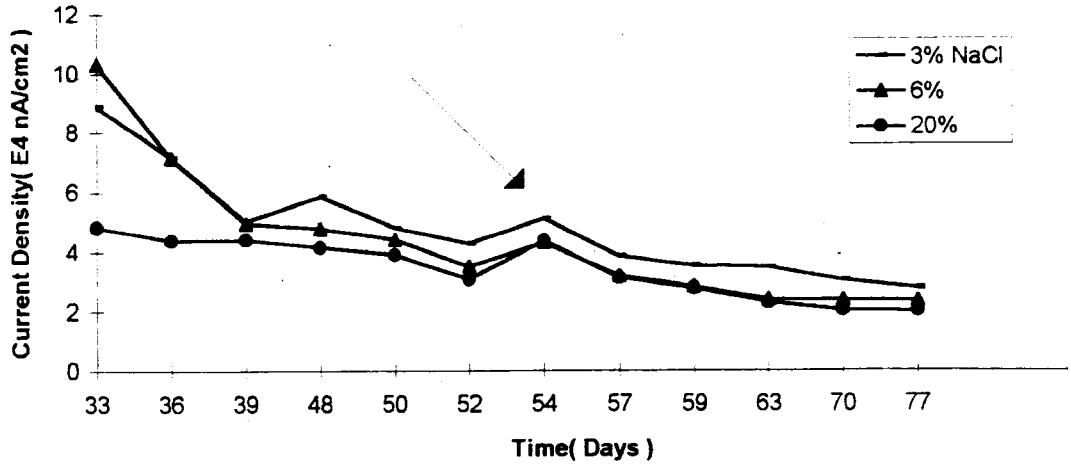

(a) Current density curves of the 3.5% Ni bars (Series 1).

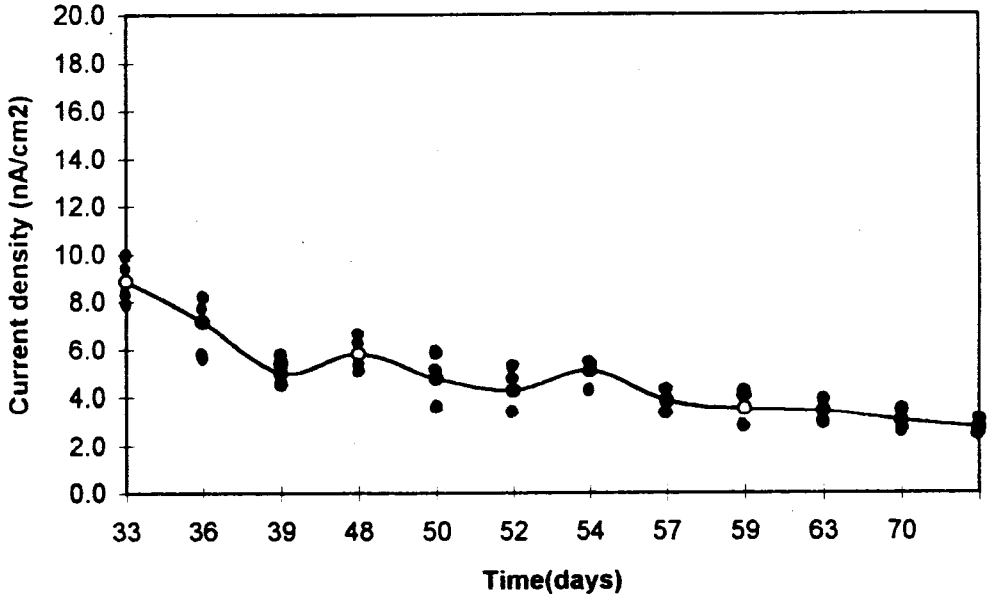

(b) Scatter plot of the data for the 3.5 Ni bars (Series 1).

Figure 3.22 - Data for the 3.5 Ni bars (Series 1).

3.4 Polarization Resistance Method

As mentioned before, the polarization resistance method is a nondestructive method of determining the corrosion rate and is applicable to both field and laboratory concrete systems. The technique uses a potentiostat to supply the current necessary to vary the potential between a reference electrode and the working (test) electrode away from the corrosion potential. The voltage versus current curve is plotted on a linear scale. The polarization resistance (R_p) is the slope ($\Delta E/\Delta i_{app}$) at the origin of the polarization curve. The polarization resistance values are related to the corrosion rate by:

$$I_{corr} = \frac{\beta}{R_p}$$

where

$$\beta = \frac{\beta_a \beta_c}{2.3 (\beta_a + \beta_c)}$$

For the typical assumption of $\beta_a = \beta_c = 100$ Mv, β is 22 Mv.

The polarization resistance was measured several times for the anodic electrodes of the galvanic cells with the EG&G 350A corrosion measurement system. For the sake of convenience only one set of results is shown in Figures 3.23 through 3.26. The tests correspond to 14 days after immersion for the second set of samples (series 2), and the corresponding numerical data obtained is summarized in Table 3.1.

As was expected the corrosion rate of the ordinary bars is the highest and that of Ni bars is lowest. Unlike the galvanic measurement, however, the polarization resistance measurements give a relatively large difference in corrosion rate between the different samples. This data are based on assumed Tafel constants of 100 Mv. When the Tafel constants are taken from Tafel measurements (see next section), one would expect even better results.

Table 3.1 - Results of Polarization Resistance Measurements
(MPY = mils of penetration per year, 1 mil = 0.001 in.)

Sample	R_p	i_{corr}.	MPY
Ordinary	4.752 E2	4.569 E4	21.07
Low S	1.175 E3	1.848 E4	8.523
CuW	2.693 E3	8.062 E3	3.715
3.5% Ni	4.037 E3	5.379 E3	2.479

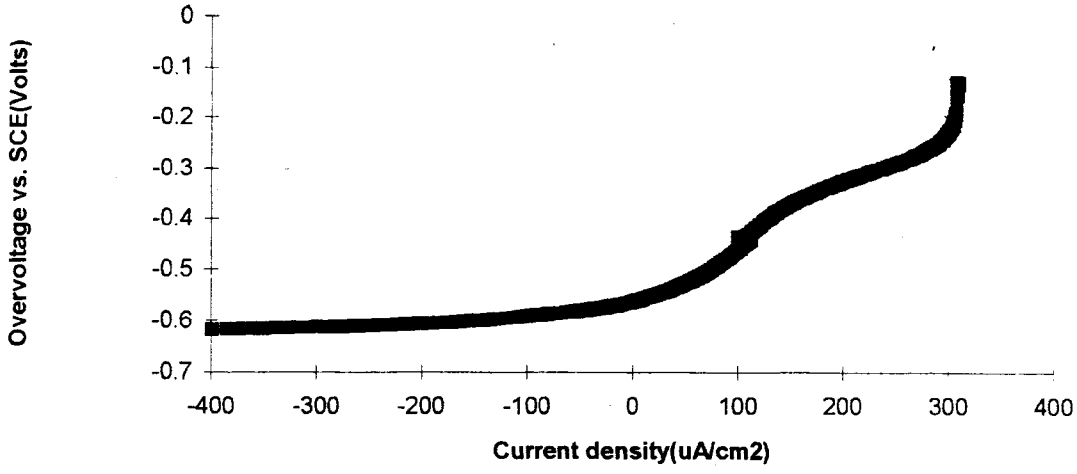

Figure 3.23 - Polarization curve of the ordinary bar.

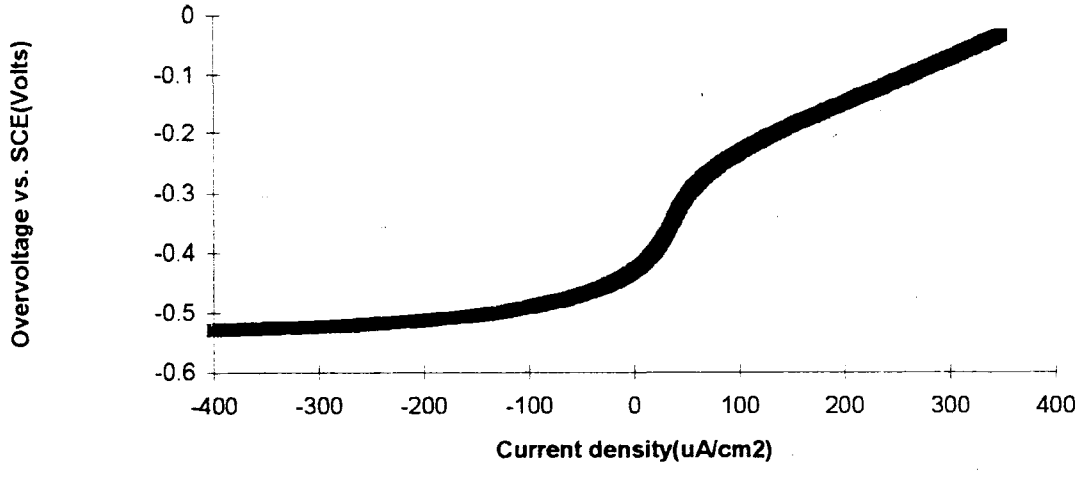

Figure 3.24 - Polarization curve of the low sulfur bar.

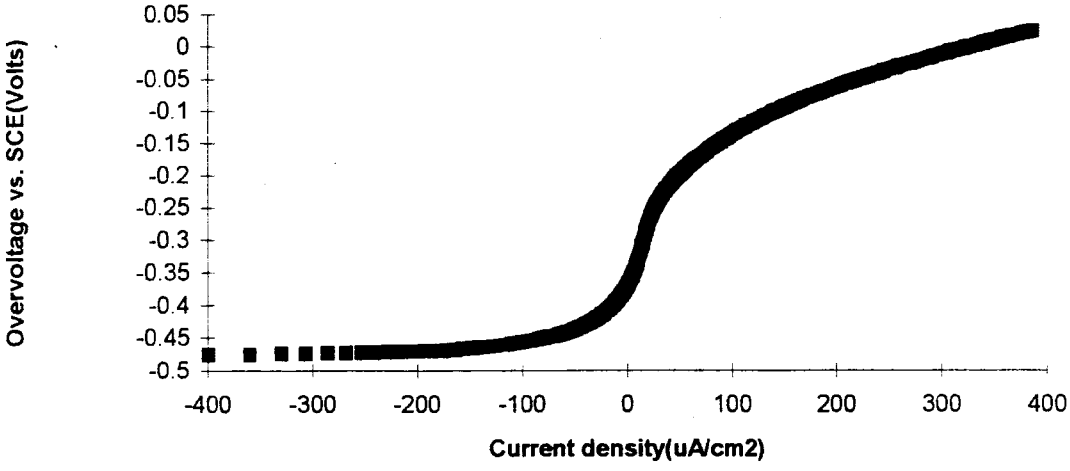

Figure 3.25 - Polarization curve of the CuW bar.

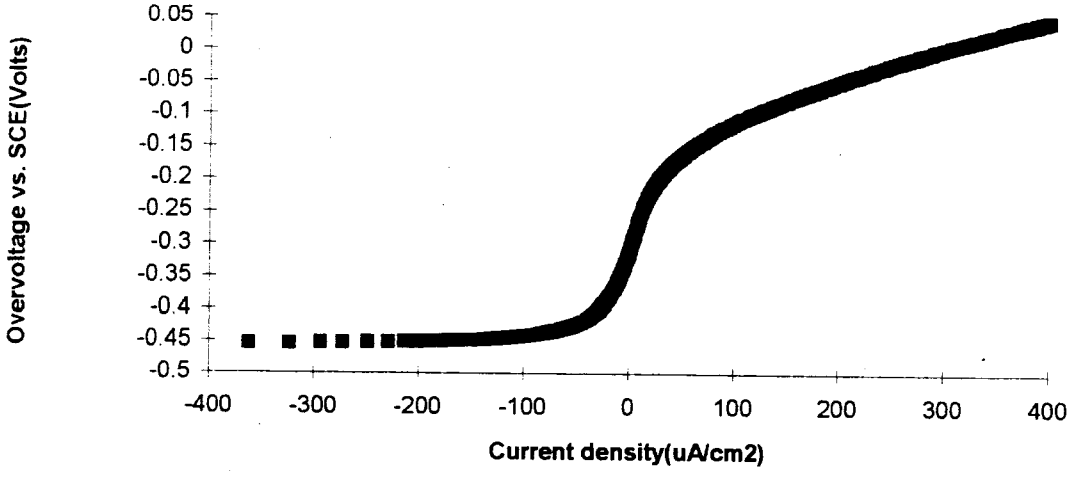

Figure 3.26 - Polarization curve of the 3.5% Ni bar.

3.5 Tafel Extrapolation

In this technique, a controlled potential is applied to a working electrode, starting at E_{corr}. The potential is extended in either the anodic or the cathodic direction for a few hundred millivolts. When the resultant potential-current function is plotted on a semi-log scale, it typically exhibits a linear region. The slope of the linear region is called the Tafel constant. A projection of the linear region defines $i_{corr.}$ at the intersection with E_{corr}. For more exact calculation of corrosion rates, the Tafel constants calculated from these methods should be used in polarization resistance methods.

Figures 3.27 through 3.30 represent Tafel plots made on the same day and on the same electrodes as those of polarization resistance measurements shown in the previous section. The values of corrosion rate extrapolated from the Tafel plots agree very well with those from the polarization resistance methods (Table 3.2). Thus, it seems that the assumed Tafel constants in the polarization resistance methods are very close to the true values.

Table 3.2 - Comparison between Tafel extrapolation and polarization resistance measurements (PRM = Polarization Resistance, TE = Tafel Extrapolation).

	$i_{corr.}$(Na/cm^2) (PRM)	$i_{corr.}$(Na/cm^2) (TE)
Ordinary	4.569E4	5.012E4
Low S	1.848E4	1.778E4
CuW	8.062E3	8.318E3
3.5% Ni	5.379E3	3.802E3

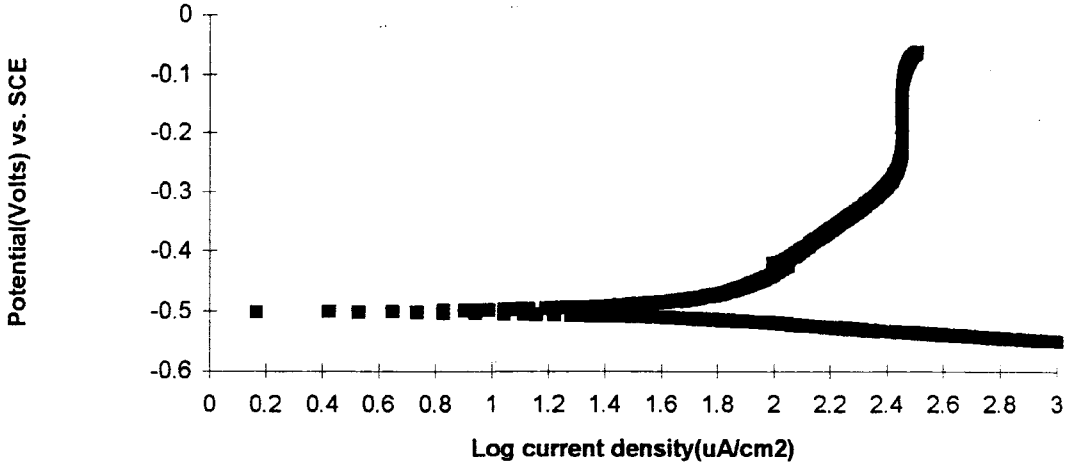

Figure 3.27 - Polarization curve for the ordinary bars by Tafel extrapolation (i_{corr} = 5.012 x 10^4 nA/cm^2).

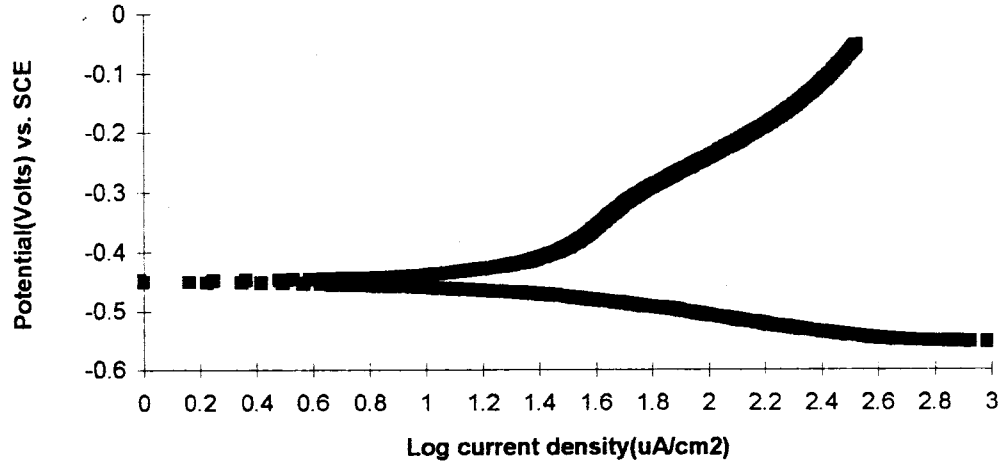

Figure 3.28 - Polarization curve for the low sulfur bars by Tafel extrapolation (i_{corr} = 1.778 x 10^4 nA/cm^2).

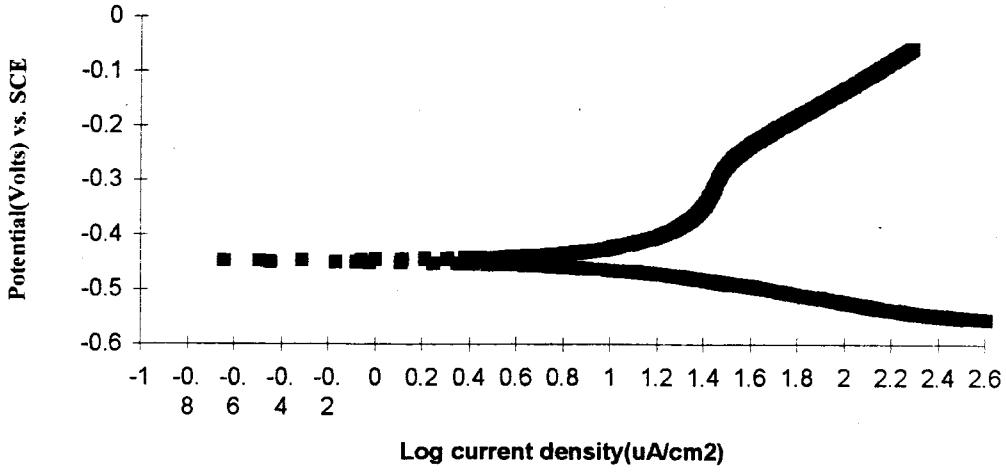

Figure 3.29 - Polarization curve for the CuW bars by Tafel extrapolation (i_{corr} = 8.318 x 10^3 nA/cm^2).

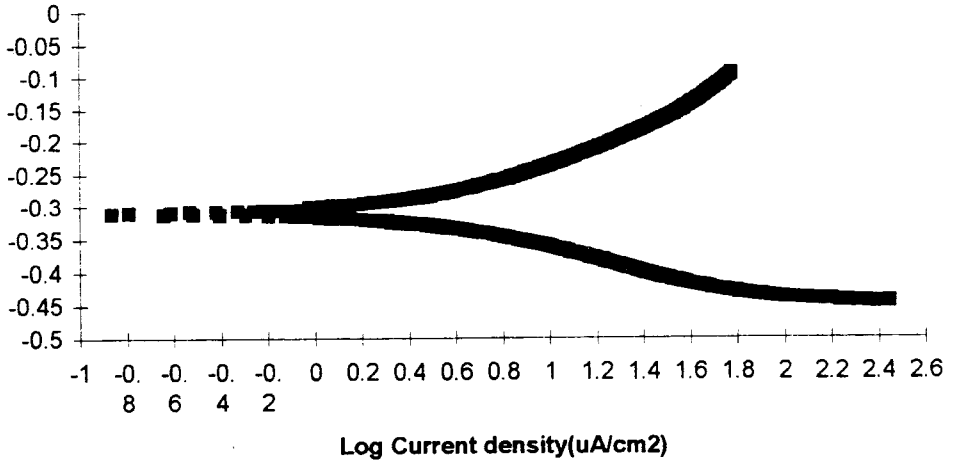

Figure 3.30 - Polarization curve for the Ni bars by Tafel extrapolation (i_{corr} = 3.802 x 10^3 nA/cm^2).

CHAPTER 4

CONCLUSION AND RECOMMENDATIONS

4.1 Conclusions

The corrosion resistance of four kinds of steel reinforcing bars (ordinary, low sulfur, copper and tungsten, and nickel) was examined in this study. Small samples of each type of bar were immersed in 3%, 6%, and 20% NaCl solutions with 100g of concrete chips. Galvanic current and potential were measured every three to four days during the experimental period, and polarization resistance and Tafel extrapolation measurements were conducted twice during this period.

In the galvanic measurements it was found that:

(a) the 3% NaCl solution is the most corrosive among the three solutions(3%, 6%, and 20%). This is agreement with other published data [13] but in conflict with those of previous studies conducted by Iwasaki and Jang [1].

(b) the 3.5% Ni steel is the most corrosion-resistant, and the ordinary steel is most susceptible to corrosion. However, the difference of corrosion rate is so small that it is very difficult to come to a conclusion based on the limited data available.

(c) the lack of a marked difference in performance between the ordinary and low sulfur bars from these measurements cannot be satisfactorily explained at this time.

The original hypothesis for this research was that the low sulfur reinforcing steel, since it has less of the sulfides which are considered as primary corrosion initiation sites, would perform better. Scanning electron microscope (SEM) studies indicated that in fact the low sulfur bars had less sulfides than ordinary steel. However, as noted above, the galvanic measurements which were proposed by Iwasaki and Jang [1] did not reflect this potential benefit.

The limited measurements using the polarization resistance and the Tafel extrapolation methods showed that the corrosion resistance of the low sulfur steel was three times that of ordinary steel. From those measurements one can conclude that:

(a) the 3.5% Ni steel is the most corrosion-resistant among the bars tested, and that low sulfur steel shows markedly better performance than ordinary steel.

(b) the polarization resistance method and the Tafel extrapolation appear to be more accurate and consistent with previous research on the same materials than the galvanic measurements.

4.2 Recommendations

This research, as many other such series in the past, indicates conflicting results for different measurement techniques used to quantify corrosion rates. This is not unusual in corrosion studies although the controlled laboratory technique used in this case should have minimized the differences. The research indicates that the technique developed by Iwasaki and Jang needs further refinement and calibration against more established techniques.

This research indicates, however, that the original hypothesis by Jang and Iwasaki, i.e. that the reduction in sulfur inclusions would have a beneficial effect on corrosion resistance, is correct. The use of low sulfur bars could potentially result in bridge decks lasting 60 to 70 years as opposed to the current replacement cycle of about 20 years. This would result in significant life cost savings that would more than offset the higher initial costs for these bars. The mechanism that results in low sulfur bars showing a three-fold increase in corrosion life are not clear and should be the subject of a much larger study. This follow up study should concentrate on the use of both small cube and slab specimens in the laboratory as well as full-scale specimens in the field. The study should be long term and should include a variety of steel compositions from U.S. manufacturers as well as epoxy-coated bars. The study should also incorporate a laboratory component similar to the one carried out in this research program in order to evaluate the potential of simple laboratory galvanic, linear polarization and Tafel extrapolation methods to provide a rapid preliminary screening tool for corrosion-resistance materials.

REFERENCES

[1] Jang, J. and Iwasaki, I., 1991, "Rebar Corrosion under Simulated Concrete Conditions Using Galvanic Current Measurements," Corrosion, Vol. 47, No. 11.

[2] Jang, J. and Iwasaki, I., 1992, "Effect of Salt Additives on Rebar Corrosion," MN/DOT Report.

[3] Beeby, A.W., 1978, "Corrosion of Reinforcing Steel in Concrete and its Relation to Cracking," The Structural Engineer, Vol. 56A, No. 3.

[4] Treadaway, K.W.J., 1979, "Durability of Steel in Concrete," in Corrosion of Steel Reinforcements in Concrete Construction, Society of Chemical Industry, London.

[5] Manning, D.G., 1990, "Cathodic Protection of Concrete Highway bridges," in Corrosion of Reinforcement in Concrete (edited by Page, Treadaway and Banforth), Society of Chemical Industry, London and New York.

[6] Jones, D.A., 1992, Principles and Prevention of Corrosion, Macmillan, New York.

[7] Scully, J.C., 1990, The Fundamentals of Corrosion, Pergamon Press, New York.

[8] Wranglen, G., 1971, "Active Sulfides and the Pitting Corrosion of Carbon Steels," U.R. Evans Conference on Localized Corrosion, Williamsburg, Va, Dec. 1971.

[9] Locke, C.E., 1983, "Mechanism of Corrosion of Steel in Concrete," in Solving Rebar Corrosion Problems in Concrete, National Association of Corrosion Engineers, Houston.

[10] Schiessl, P., 1975, "Admissible Crack Widths in R.C. Structures," Inter-Association Colloquium on the Behavior in Service of Concrete Structures, Preliminary Reports, Vol. II, N. 3-17, Liege, Belgium.

[11] Espelid, B. and Nilson, N., 1988, "A Filed Study of the Corrosion Behavior on Dynamically Loaded Marine Concrete structures," in Concrete in Marine Environments (edited by V.M. Malhotra), SP 109, ACI, Detroit.

[12] Mehta, P.K. & Monteiro, P.J.M, 1993, Concrete, Prentice Hall, Englewood Cliffs, New Jersey.

[13] Uhlig, H. and Revie, R.W., 1985, Corrosion and Corrosion Control, 3rd. Ed., John Wiley and Sons, New York.

[14] White, W. E., 1988, "Inclusions and their Influence on Corrosion and Corrosion-Assisted Fracture," Proceedings of a Symposium held in conjunction with the 1988 World Materials Congress, Chicago, 24-30 Sept., 1988.

[15] Baldwin, W.R., 1983, "Update on Epoxy Coated Reinforcing Steel," in Solving Rebar Corrosion Problems in Concrete, National Association of Corrosion Engineers, Houston.

[16] Clear, K.C., and Virmani, Y.P., 1983, "Solving Rebar Corrosion Problems in Concrete - Methods and Materials," in Solving Rebar Corrosion Problems in Concrete, National Association of Corrosion Engineers, Houston.

[17] Swamy, R.N., 1990, "Resistance to Chlorine of Galvanized Rebars," in Corrosion of Reinforcement in Concrete (edited by Page, Treadaway and Banforth), SCI, London and New York.

[18] Vassie, P.R., 1990, "Concrete Coatings," in Corrosion of Reinforcement in Concrete (edited by Page, Treadaway and Banforth), SCI, London and New York.

[19] ASTM 222

[20] Lorentz, T., French, C. and Leon, R.T., 1992, "Corrosion of Coated and Uncoated Reinforcing steel in Concrete," Report submitted to the University of Minnesota, Center of Transpotation Studies, and National Science Foundation, May 1992.

[21] Fontana, M., 1986, Corrosion Engineering, McGraw-Hill, New York.

[22] Wranglen, G., 1985, An Introduction to Corrosion and Protection of Metals, Chapman and Hall, New York, N.Y..

[23] Stern, M. and Geary, A.L., 1957, " ... ", Journal of Electrochemical Society, Vol. 104.

[24] Slater, J.E., 1983, "Corrosion of Metals in Association with Concrete," ASTM STP 818, American Society for Testing and Materials, Philadelphia.

[25] Bertocci, U., 1979, "Detection and Analysis of Electrochemical Noise for Corrosion Studies," Proceedings, 7th International Congress Metallic Corrosion.

[26] Andrade, C., Castelo, V., Alonso, C. and Gonzalez, J.A., 1986, "The Determination of the Corrosion Rate of Steel Embedded in Concrete by the Polarization Resistance and AC Impedance Methods," ASTM STP 906,

[27] Nippon Steel Corporation, 1986, "Salt Corrosion-Resistant Rebars," Technical Material (in Japanese).

[28] Pearce, M.O, 1992, "Nickel-Containing Alloys Today and Tomorrow," MP, April, pp. 73-74.

[29] Jha, R., Singh, S.K. and Chatterjee, A., 1992, "Development of New Corrosion Resistant SteelReinforcing Bars", MP, April, p. 68-74

[30] Wall, G.R. and Harris, B., 1971, "Localized Corrosion in Mild Steel," U.R. Evans Conference on Localized Corrosion, Williamsburg, Dec. 1971, pp. 292-304.

APPENDIX A

FIELD STUDIES OF CORROSION

Appendix A - Field Studies of Corrosion

This appendix gives a brief summary of some of the exposure tests that have been carried out and the conclusions obtained. The survey is not exhaustive and is limited to tests where reasonably normal members were exposed to reasonably natural environments. Appendix B contains a brief bibliography of some of the other work conducted in the last 30 years in the area of corrosion of steel reinforcement. Again, Appendix B is not intended to be a complete listing. It is only intended to provide some of the key references to work in this area.

A.1 Field Tests on Large-Scale Specimens

Duffaut, Duhoux and Heuze [A.1] exposed 108 specimens between high and low tide in the Rance estuary (France) for a period of 12 years. At the end of this time the specimens were broken open and the corrosion assessed visually. A large number of variables were considered but a very subjective numerical scale, ranging from 0 which would indicate no corrosion to 4 for very severe corrosion, was used. Unfortunately, crack widths were not measured and it is simply reported that the crack widths were in the range 0.5 to 1 mm. This is wider than is allowed by normal practice. The presence of cracks had a major influence on the degree of corrosion but the influence of cover was only significant when combined with low concrete strength.

Roshore [A.2] reported on tests of 158 beams exposed on the shores of Treat Island, Maine. The exposure site was such that all the specimens were immersed twice a day in seawater and the specimens were exposed to between 70 and 160 freeze -thaw cycles per year. A great many variables were studied including crack widths, which were measured yearly. Statistical analysis of the results up to 1963 showed only two variables to be significant. These were (1) air entrainment; no beams without air entrainment survived for more than four winters, and (2) steel type; beams reinforced with modern deformed bars were significantly more durable than those using 'old style' bars. Cracking and crack width did not appear to have a significant influence on durability. It should be noted, however, that the prime cause of deterioration of these beams was likely to have been frost damage rather than corrosion.

Carpantier and Soretz [A.3] carried out tests on 12 nominally identical beams which were loaded in the laboratory and were sprayed with water for four hours twice a week for 2 years. The beams were divided into three groups of four which were subjected to different loading regimes. All beams were initially loaded to a level which produced cracks of 0.2 - 0.3 mm average width. Four of the beams were then unloaded and left unloaded for the full two years; four were unloaded and loaded on alternate days and four were maintained under

load. At the end of the exposure period, the beams were unloaded and the corroded length measured. The corrosion on the unloaded beams was minimal. Corrosion, sometimes heavy, was observed on the other two sets of beams. However, for crack widths greater than 0.2mm, no reasonable relationship between crack width and corroded length could be postulated from the data obtained. Accidental changes in cover indicated that there is an influence of cover; higher covers giving shorter corroded lengths.

Houston and Atimtay [A.4] report tests on 82 slabs and beams subjected to daily spraying with 3% salt solution for up to 2 years. The variables considered were cover, steel stress and cracking, mix proportions, bar diameter and the position of steel in the mold during casting. At the end of the test, the beams were broken open and the percentage of the bar surface which had been corroded was measured. It was found that the dominant variables influencing corrosion were the water/cement ratio and the ratio of cover, c, to bar diameter, d_b. Cracking was found to have only a minimal influence. Low values of c/d_b led to extensive corrosion and the development of longitudinal splitting and spalling of the cover. Serious deterioration did not occur where c/d_b was 3 or more.

Two extensive series of exposure tests were carried out by the Institut fur Massivbau of the Technical University, Munich [A.5-6]. Series of beams were loaded to produce crack widths in the general range of 0.1 to 0.4mm. The specimens were then exposed in three different environments: normal urban atmosphere, heavily polluted industrial atmosphere and marine. A number of the specimens were broken open after 1, 2, 4 and 10 years exposure and the average depth of corrosion at each crack was measured. Results have been reported at intervals by various authors from 1964 when Rehm and Moll [A.5] reported on results obtained after 1 and 2 years exposure to 1976 when Schiessl [A.6] produced the final results. Rehm and Moll found that, at two years, the frequency, amount and local extension of corrosion at cracks increased with increasing surface width. However, after 10 years exposure, Schiessl was able to show that there was no significant relationship between crack width and the amount of corrosion.

A.2 Concrete Specimen Tests

There are several experimental series which effectively monitored the corrosion of reinforcing steel in actual concrete samples and are often cited in the literature. Two of them, however, stand out. Pfeifer's study [A.7] is impressive in size, scope and clarity of presentation. K.C. Clear, et al., have completed time-to-corrosion studies on concrete slabs for the Federal Highway Administration (FHWA) that address a wide range of corrosion factors. The five volumes of "Time-To-Corrosion of Reinforcing Steel in Concrete Slabs" that present their

findings span nine years of work (1973-1982), and are frequently referenced in papers discussing corrosion of reinforcing steel in concrete. Both the Pfiefer and Clear studies used test procedures based on the assumption that a primary cause of reinforcement corrosion is the presence of macroscopic galvanic cells in the concrete.

In 1972, the FWHA began a sponsored study performed by Clear, et. al. [A.8], in which 124 reinforced concrete slabs (4 ft. by 5 ft. by 6 in.) were subjected to daily salt applications over an extended period of time in outdoor conditions. Volume One of this study concerns the effects of mix design and construction parameters on the corrosion resistance of reinforced concrete. Volume Two reports the electrical potential and chloride intrusion data of the concrete specimens after 330 daily salt applications. In Volume Three of this study, the performance results after 830 daily salt applications are summarized. The performance of the slabs was determined using results of electrical half-cell potential monitoring (copper-copper sulfate, CSE), visual inspections, and chloride analysis.

As a result of their initial work, Clear et al. obtained values for an average threshold concentration of chloride at which corrosion was initiated in concrete reinforcement. The threshold values can be expressed as parts per million based on concrete weight or as parts per million based on weight of cement. Expressed in this latter convention, their results indicate a mean threshold value of 2000 ppm Cl^- by weight of cement.

Extensive tests (over 1200 samples) on the chloride content versus slab depth gave Clear et al. not only the ability to relate chloride concentration with time-to-corrosion of reinforcing steel, but the results of these studies also found that both concrete w/c ratio and depth of clear cover have a major influence on the time to corrosion.

Volume Three of the FHWA study by Clear also addresses the relationship between daily salting of test slabs to the frequency of field salting of actual structures. A quantitative relationship between simulated test and actual field performance is necessary if one is to extend information gained from simulated tests to expected performance of existing and proposed structures.

In order to relate the effects of daily salting on specimens with real-time seasonal saltings, twenty-eight - 2 ft. x 2.5 ft. x 6 inch concrete slabs were fabricated using the same mix design and fabrication procedures as the standard time-to-corrosion test slabs. After 330 daily saltings, these slabs were found to exhibit similar chloride profiles as the larger standard slabs, so results could be translated to the larger slabs. The small slabs were introduced to different three types of chloride exposure: a) standard test daily ponding with 3% NaCl solution; b) salting with rock salt (NaCl) only when snow or ice was on the slab with no

dams to retain melted solution on the slabs (8 saltings in 1974-75 winter season); c) ponding with 3% NaCl solution twice per week from December 1, 1974, to February 28, 1975, i.e., 26 saltings per season.

The results of this correlation experiment show that based on average corrosion threshold depths, one time-to-corrosion salting for this study was equivalent to roughly between 0.70 and 0.82 field saltings. If one estimates a typical number of saltings per season in a northern climate (Minneapolis, Minnesota) to be 25, then 830 time-to-corrosion salt applications would be equivalent to approximately 23 service years. This assumes all other exposure conditions to be the same for both sample and service structure, and neglects the effects of cyclic loading and cracking on the actual structure. Cyclic loading and the typical service cracks which would be present on an actual structure would accelerate the migration of chlorides to the level of the reinforcing steel at concentrated locations.

Virmani and Clear monitored the corrosion performance of epoxy-coated reinforcing steel, and a calcium nitrite admixture to protect black reinforcing steel in concrete in an experimental study for the Federal Highway Administration [A.9]. Both systems were compared to uncoated steel in concrete without admixtures. Results of this test series were based on thirty-one relatively large slabs monitored over a two year test period (1980-82). Test specimens were cast in 2 ft. x 5 ft. x 6 in. slabs containing two mats of steel reinforcement. The top mat consisted of four 51 inch long bars with two 18 inch long cross bars directly below. The bottom mat of steel consisted of seven 51 inch long bars with four 18 inch long cross bars beneath them. All epoxy-coated bars were #6 bars, while uncoated #4, #5, and #6 steel bars were also used. A clear cover of 3/4 inch over the top mat of steel was provided in all specimens. The distance between the longer bars in the top and bottom mats was 2-3/8 inches. Test slabs were cast with the following reinforcing steel configurations: a) epoxy-coated bars in the top mat, uncoated bars in the bottom mat; b) epoxy-coated bars in both mats; c) uncoated bars in both mats. The concrete for all specimens had a w/c ratio of 0.53. The concrete was mixed and placed in two lifts. The lower lift in each specimen was chloride free. The upper lifts of all samples contained a specified amount of sodium chloride dissolved in the concrete mix water. After consistent curing procedures were complete, the slabs were mounted on 3 ft. posts at the FWHA outdoor exposure site and monitoring began. The combination of relatively permeable concrete (w/c = 0.53), high chloride concentrations at the top steel level, a large bottom (cathodic) steel to top (anodic) steel area ratio, and a small separation distance between the steel layers contributed to an accelerated corrosion environment.

The large difference in chloride concentrations between the top and bottom steel levels creates a potential difference between the two steel levels, which drives the corrosion cell. A large

cathode connected to a small anode creates an "area" effect which accelerates the corrosion process. Because the overall reaction of corroding reinforcing steel is usually controlled, or limited, by the reduction reaction occurring at the cathode, a larger cathodic area is able to increase the limiting reaction and therefore accelerate the total reaction rate. The small separation distance between the steel layers reduces the internal resistance of the corrosion cell, and therefore aids the corrosion reaction.

The results of the Virmani and Clear study [A.9] indicated that epoxy-coated reinforcing steel provided a very effective corrosion prevention system, by increasing the electrical resistance between the macrocell anode and cathode (i.e. top and bottom mat of reinforcing steel). It was concluded in the report that if an uncoated reinforcing steel bar is assigned an arbitrary life of one year in chloride contaminated concrete, epoxy-coated reinforcing steel bars would require 46 years exposure in the same environment for the corrosion cell to consume an equivalent amount of iron.

Clear and Virmani also concluded that the use of calcium nitrite admixtures were effective in reducing the corrosion of uncoated reinforcing steel in chloride contaminated concrete. If uncoated reinforcing steel in nitrite-free concrete is assigned an arbitrary life of one year, "it would require between 5 and 29 years for the same rebar in concrete containing 2.75 percent calcium nitrite solids by weight of cement and chlorides in the range of 22.6 to 8.4 lbs Cl^- /yd^3 to undergo equal iron consumption".

The study by Pfeifer et al. [A.7] was intended to monitor and compare the effectiveness of several currently available corrosion protection systems for reinforced and prestressed concrete. The initial portion of this study consisted of testing 124 prisms in a pilot program. After the 44 week pilot study, systems showing the most promising corrosion protection were incorporated into 19 full-size specimens, tested over a period of 370 days.

The pilot prisms were 12 inches square with variable depths of 7, 8 and 9 inches, corresponding to top mat clear covers of 1, 2, and 3 inches respectively. The steel reinforcement in each prism was distributed into a top mat of 2-#4 reinforcing bars and a bottom mat of 4-#4 bars. The bottom mat of reinforcement was placed with one inch of clear cover in all test configurations, in order to provide equal access of oxygen to the bottom steel. A 4 inch thickness of concrete was maintained between the steel mats in all specimens. In addition to variable depth of clear cover, Pfeifer et al. configured systems with variable water/cement ratios of 0.32, 0.40 and 0.50, variable cement factors (94 lb. bags/cu. yd.) of 4.60, 6.08, and 7.47, the use of coated, uncoated and galvanized reinforcing steels, the addition of calcium nitrite admixture, and the application of penetrating silane and methacrylate coating systems, into 58 total combinations.

The specimen design and test details used in this study allowed for accelerated corrosion to take place due to the following specifics. The test prisms were subjected to moisture and chloride by ponding with a 15 percent sodium chloride solution (roughly 5 times the chloride level of seawater). The ponding cycle used in this study was 100 hours with ponded solution at 60 to 80 °F, followed by a fresh water rinse and 68 hours of drying at 100 °F. The alternating wetting and drying periods accelerated the migration of chlorides through the concrete. Elevated temperatures are known to accelerate corrosion reactions. The experimental procedure introduced an electrochemical potential difference between the two mats of reinforcing steel as a result of differing chloride concentrations between the two levels of reinforcing steel. The concrete at the bottom layer of steel remained in a considerably lower chloride ion concentration environment relative to the top mat, due to the greater distance required for the ions to permeate. In addition, this experiment took advantage of the previously described "area effect" for a macroscopic corrosion cell, by having twice the amount of cathodic steel (bottom mat) to anodic steel (top mat) area.

The corrosion monitoring variables and techniques used in the Pfeifer et al. [A.7] and the Clear et al. [A.8] studies were essentially the same. The variables measured were as follows:

1. Corrosion current.
2. Instant-off potential (driving voltage).
3. Electrical resistance between the top and bottom mats.
4. Half-cell electrical potentials between the top and bottom mats (vs. copper-copper sulfate electrode).

In both of these studies, galvanic current was assumed to occur when the top steel became "anodic" and the bottom steel became "cathodic" due to a change in the electrochemical potentials of the surroundings of the two layers of steel. This difference in electrochemical potentials could be traced to differences in oxygen content, pH, and moisture content, but was primarily due to the differential concentration of chloride ions surrounding the two layers of steel. By electrically connecting the top and bottom mats of reinforcing steel with an external circuit and monitoring the current flow, the authors were able to determine the rate of corrosion by applying Faraday's law:

$$M = \frac{I_{corr,T}\ t\ W}{F\ V}$$

where,

M = corrosion loss (g/cm^2)
$I_{corr,T}$ = total current involved in the process (amp.-hour)
t = time (hours)
W = molecular weight (grams)

V = valence
F = 96500 coulombs

The corrosion current could be related to the amount of metal lost to corrosion by the fact that each 1.0 amp-hour of current consumes 1.04 grams of iron.

The "instant-off" potential was taken to determine the electromotive force driving the corrosion cell. Both the Pfeifer et al. and the Virmani et al. investigations defined this reading as the voltage difference between the two mats of steel taken immediately after opening the circuit between the two. The instantaneous reading is necessary due to the fact that the individual layers of steel will begin to polarize away from each other after the electrical connection between the two layers is opened.

The impedance (resistance), in ohms, of the electrical path between the two mats of steel was determined in both studies using an AC electrical resistance monitor. This measurement, together with the current and the driving voltage readings were related by the Ohm's law equation:

$$V = I R$$

where:

V = Instantaneous driving voltage (volts)
I = Corrosion current (amperes)
R = Resistance (ohms)

Both studies also included the measurement of the electrical potential between the top mats of reinforcing steel and copper-copper sulfate ($Cu\text{-}CuSO_4$) half-cells placed at various locations on the top surface of the concrete specimens. Half-cell measurements allow for benchmark comparisons as to the relative potential difference between any given electrode (anode or cathode), and a standardized electrode (the half-cell). Based on work done by Stratfull and others at Caltrans [A.10] this nondestructive test is now recognized as a method to indicate probable zones of corrosion activity, and is described by ASTM C 876 [A.11].

The Pfeifer study [A.7] used a linear regression analysis to determine a relationship between their experimentally determined corrosion current and potential readings. Based on 209 half-cell potential readings from 52 concrete specimens, the following relationship was derived:

$$I = -774.2P - 184.2$$

where:

I = corrosion current (microamperes)
P = Cu-$CuSO_4$ half-cell potential (volts)

Based on this analysis, the Pfeifer, et al., study determined that corrosion could occur at half-cell potential readings between -0.20 and -0.25 volts. The ASTM C 876 test specifications [A.11] list that readings between -0.20 and -0.35 volts are in the "uncertain" range, while readings < -0.35 volts have a 90% probability of corrosion activity occurring. After 44 weeks of testing, the Pfeifer study had 22 specimens that developed significant corrosion activity, while 102 specimens did not. The results clearly indicated that the depth of clear cover over the reinforcement was a significant corrosion inhibitor. In no cases, did any specimen with a clear cover greater than 2 inches exhibit any corrosion activity. Within the specimen groups having 1 inch of clear cover, there was no consistent effect of variable w/c ratio.

A 1986 corrosion study was undertaken by Hope and Ip at Queen's University, Kingston, Ontario, Canada, on concrete slabs exposed to both laboratory and outdoor conditions [A.12]. The purpose of this test was to address the effects of chloride in concrete containing admixed chloride and chloride-bearing aggregates. The authors were primarily interested in the measurement of microcell corrosion of the steel. Hope and Ip cast sixty 2.5 x 12 x 16 in. (64 x 300 x 400 mm) slabs, in ten sets of six. The slabs were cast with three 0.51 in. (13 mm) diameter mild steel electrodes for corrosion monitoring - two working electrodes and one reference electrode. Differential levels of calcium chloride dihydrate, from 0 to 2 percent by mass of cement, were admixed into eight of the sets. Two sets of slabs contained chloride-bearing aggregates, 0.136 and 0.197 percent chloride-ion content respectively, in bound form. CSA, Type 10, normal portland cement was used in all slabs. The water/cement ratio was 0.45, aggregate/cement ratio 4.45, air content of 6 percent, and slump 3 $\pm$ 1 in. (75 $\pm$ 25 mm).

Half of the slabs were stored outdoors, the remainder in the laboratory. The laboratory slabs were subjected to alternate wet and dry cycles of 3 and 11 days. The wet cycle was accomplished by soaking in aerated water; the dry cycle was completed in laboratory air. After 310 days, two slabs from each set were cycled with a 14 day oven drying period at 100 °F, a 14 day wet soaking period, and a 14 day air drying period. Corrosion measurements were typically made every 3 and 14 days on the indoor slabs, and every month on the outdoor slabs.

The primary corrosion monitoring system used by Hope and Ip was the linear polarization technique. Based on the results of their experimental program, Hope and Ip concluded that the chloride threshold limit to initiate corrosion of reinforcing steel in concrete was between

2000 and 4000 ppm calcium chloride dihydrate by mass of cement, depending on the test method. These results correlated well with the work discussed earlier, performed by Clear et al. [A.8], which indicated a mean threshold value of 2000 ppm Cl^- for corrosion initiation.

Coggins and French studied the chloride ion concentrations found in three prestressed girders and the deck of a twenty year old bridge removed from service over Interstate 694 in Minneapolis, Minnesota [33]. Samples were taken at various depths from 20 locations on each of two girders, 7 locations on another girder, and 5 locations on the original bridge deck. The samples were analyzed by the "Berman method" for determining total chloride content. Their findings indicated that chloride ion concentrations present in prestressed bridge girders at depths of less than 1-1/2 inches varied greatly due to the degree of exposure associated with the location of the samples. The total chloride concentration values at depths of 1-1/2 inches or less ranged from 1180 to 40 ppm by weight of concrete.

The actual maximum chloride ion values recorded at depths of 1-1/2 inches or greater were not found to be significantly higher than 250 ppm by weight of concrete. Coggins and French found no evidence of corrosion of the prestressing strands in the bridge girders, except for the end faces where the epoxy coating had been chipped. Rust stains on the concrete were present at this location, however no spalling was evident. Samples taken from the original bridge deck contained a much greater concentration of chloride ion. This result is expected due to the direct application and ponding of deicing salts upon the deck. The top steel layer in the deck was located at a depth of 1-1/2 inches. At this depth, the reported chloride ion concentrations ranged from 1110 to 1940 ppm by weight of concrete. Coggins and French estimated a 20% cement factor, which translates into chloride concentrations present at the level of steel from 5550 to 9700 ppm by weight of cement. Despite the fact that average chloride concentration values at this depth were found to be twice the FHWA replacement level of 3000 ppm by weight of cement, the deck investigated showed no significant deterioration due to corrosion effects.

It is significant, that even with the gross simplifications described in the first studies by Clear and Hays dating from 1972 [A.8], the results from that investigation show a loose correlation with actual samples from structures that were in-service. The 20-year old bridge deck analyzed by Coggins and French contained an average value of 1900 ppm chloride by weight of concrete at the one inch depth [A.13]. Based on typical concrete construction practices in the late 1960's, one could estimate the w/c ratio of the bridge deck to be between 0.40 and 0.50. The chloride concentration at a one inch depth of a concrete slab from the Clear and Hay study after 830 saltings (roughly 23 service years) for w/c ratio of 0.50 was 2912 ppm, and for w/c ratio of 0.40 was 404 ppm, chlorides by weight of concrete. This comparison, while not conclusive, tends to confirm that the time-to-corrosion values used to relate the

experimental method used in the FHWA studies to actual field saltings were not unrealistic.

Jang and Iwasaki examined the corrosion of reinforcing steel in concrete from a metallurgic viewpoint, i.e. how the composition of the rebars affects the corrosion process, and the impact of the corrosion phenomenon on the microstructure of reinforcing steel [A.14]. Reinforcing steel was tested in both a simulated pore solutions and actual concrete blocks. The goal of their study was to develop a simple galvanic current measurement method of corrosion monitoring, and to study the effect of chloride concentration, welding and bending on the corrosion or reinforcing steel in concrete. Corroded rebar samples taken from an in-situ bridge deck and tunnel pavement in St. Paul and Minneapolis, Minnesota were also analyzed. The concrete containing the reinforcing steel samples had been subjected to years of applied road salts based on common service conditions for a northern snow belt state. The concrete surrounding the field samples was reported to contain 1100 ppm Cl^-. Assuming a 4000 lb./cu. yd. unit weight for the concrete, and a cement factor of 6, the result is equivalent to approximately 7800 ppm Cl^- by weight of cement. This value is roughly 2 to 3 times the value needed to initiate corrosion determined by Hope, Ip and Clear, as discussed earlier.

Jang and Iwasaki monitored the reactions of two electrically connected samples of reinforcing steel placed in environments having differing chloride concentrations and found that the behavior of the rebars was galvanic. The measurements were made with a Princeton EG&G Model 350-A corrosion measurement console. The rebar containing the higher salt concentration became the anode, while rebar in the chloride-free environment became the cathode. The measurements taken between reinforcing steels in a simulated concrete solution corresponded well to those taken between field specimens of rebar embedded in concrete. The results from the Jang and Iwasaki investigation support the macrocell model of reinforcing steel corrosion in concrete. From the simulated corrosion cell experiments, Jang and Iwasaki found that the galvanic currents between rebar specimens increased with increasing chloride concentration. A very significant result reported from this study was that the galvanic current measurements of welded and bent reinforcing steels were approximately two orders of magnitude higher than those of ordinary rebars.

Jang and Iwasaki explain that welding can lead to significant differences in the electrochemical properties between weld metal, heat-affected zone, and base metal. As a result, "the weld metal was more active than the base metal, and acted as an anode" [A.14]. The bent reinforcing steel experienced plastic deformations which formed areas of dislocations of the metal. Areas with a high density of dislocations are described as unstable thermodynamically and in a high energy state compared to areas without dislocations. The plastic deformation of the reinforcing steel leads to adjacent areas with significant differences

electrochemical properties, thus resulting in higher corrosion rates than unbent reinforcing steel.

From microscopic study of corroded reinforcing steel, Jang and Iwasaki found that in addition to sites of plastic deformation and weld locations, severe corrosion occurred near grid-intersections and material defects in the microstructure of the reinforcing steel. They also found that the corrosion of rebars initiated and propagated along rebar material grain boundaries. In short, impurities in the form of inclusions (e.g. sulfur), and dissimilar constituents (e.g. ferrite and pearlite) commonly found in the mild steel usually used as reinforcing steel can have a significant effect on the corrosion rate of steel in an aggressive environment. The Jang and Iwasaki results lead to important considerations from the structural design perspective. The designer of RC structures should be cognizant of the fact that welded reinforcing steel has a much higher potential to suffer corrosion than non-welded reinforcement. For the structures that are considered particularly susceptible to the threat of reinforcing steel corrosion, the designer may wish to consider options other than welding for reinforcing steel. Additionally important, although not always considered in RC design, is the quality of the reinforcing steel itself. Jang and Iwasaki have shown that reinforcing steel having a high percentage of impurities is susceptible to corrosion.

A great number of other excellent research projects have been done on the corrosion of reinforcing steel in concrete. The body of knowledge on reinforcing steel corrosion has grown dramatically in the past 20 years. And even though the phenomenon of corrosion of steel in concrete is extremely complex, advances in corrosion protection have been made. Corrosion research has resulted in the improvement of materials (e.g. epoxy coated rebars, non-chloride based admixtures), corrosion prevention systems such as cathodic protection systems, and corrosion measurement methods. As a result of corrosion research on reinforcing steel in concrete, new and more effective methods of field measurement studies have been developed. Current work in corrosion systems monitoring equipment has developed linear polarization (L.P.) test equipment suitable for field studies of structures. These systems have several advantages over the previous standard field corrosion monitoring technique of half-cell potential mapping (ASTM C 876 - 87). The L.P. procedure is relatively rapid, the corrosion rate is actually calculated (rather than the probability of corrosion), and there is a growing world-wide database that can be used in interpreting the results.

REFERENCES

[A.1] Duffaut, P., Duhoux, L., and Heuze, B., "Corrosion des Aciers dans le Beton Arme - Essais Realises dans le Estuaire de la Rance de 1959 a 1971," Annales de l'Institute Technique de Batiment et Travaux Publiques, Paris, May 1973.

[A.2] Roshore, E.C., "Tensile Crack Exposure Tests: Results of Tests of Reinforced Concrete Beams 1955-1963," US Army Engineer Waterways Experiment Station Technical Memorandum 6-124, Vicksburg, November 1964.

[A.3] Carpantier, L., and Sorentz, S., "Contribution a l'Etude de la Corrosion des Aramatures de Beton Arme," Annales de l'Institute Technique de Batiment et Travaux Publiques, Paris, July-August 1966.

[A.4] Houston, J.T., and Atimtay, E., "Corrosion of Reinforcing Steel Embedded in Structural Concrete," Research Report 112-1F, Center For Highway Research, The University of Texas at Austin, March 1972.

[A.5] Rehm, G., and Moll, H., "Versuche zum Studium des Einfluss der Reissbreite auf die Rostbilding an der Bewehrung von Stahlbeton-Bauteilen," Deuscher Ausschuss fur Stahlbeton -Heft 169, Berlin, 1964

[A.6] Schiessl, P., "Admissible Crack Widths in R.C. Structures," Inter-Association Colloquium on the Behavior in Service of Concrete Structures, Preliminary Reports, Vol. II, N. 3-17, Liege, Belgium, 1975.

[A.7] Pfeifer, D.W., "Protective Systems for New Prestressed and Substructure Concrete," FHWA-RD: 86/193, Federal Highway Administration, Washington, D.C., 1986.

[A.8] Clear, K.C., et al., "Time to Corrosion of Reinforcing Steel in Concrete Slabs," Volumes I-V, FHWA-RD: 73/32, 73/33, 76/70, 82/028, 83/012, Federal Highway Administration, Washington, D.C., 1973-1979.

[A.9] Clear, K.C., and Virmani, Y.P., "Solving Rebar Corrosion Problems in Concrete - Methods and Materials," in Solving Rebar Corrosion Problems in Concrete, National Association of Corrosion Engineers, Houston, 1982.

[A.10] Stratfull, R., "Half-Cell Potentials and the Corrosion of Steel in Concretes," Highway Research Record, No. 433, Transportation Research Board, Washington,

1973 pp. 12-21

[A.11] American Society for Testing and Materials, Standard Test Method for Half Cell Potentials of Reinforcing Steel in Concrete, ASTM C-876, Philadelphia, 1980.

[A.12] Hope, b.B., and Ip, A.K., "Chloride Corrosion Threshold in Concrete," ACI Journal, Vol. 84, No. 4, 1987.

[A.13] Coggins, F., and French, C.W., "Material Properties of a Twenty-Year-Old Prestressed Concrete Bridge Girder Obtained by NDT," Structural Engineering Report 89-03, Dept. of Civil and Mineral Eng., University of Minnesota, Twin Cities.

[A.14] Jang, J.W., and Iwasaki, I., "Rebar Corrosion Under Simulated Concrete Conditions Using Galvanic Current Measurements," paper submitted to TRB, 1991.

APPENDIX B

BIBLIOGRAPHY

[1] ACI Committee 201 , "Guide to Durable Concrete (ACI 201.2 R-77)," ACI Journal, Vol. 74, No. 12, Dec 1977.

[2] ACI Committee 546, "Guide for Repair of Concrete Bridge Superstructures," Concrete International, Vol. 2, No. 9., Sept. 1980, pp. 69-88.

[3] ACI Committee 345, "Standard Practice for Concrete Highway Bridge Deck Construction," Concrete International, Vol.3, No. 2, Sept. 1981, pp. 19-53.

[4] Alonso, C., Andrade, C., González, J.A., "Relation Between Resistivity and Corrosion Rate of Reinforcements in Carbonated Mortar Made With Several Cement Types," Cement and Concrete Research, Volume 8, pp. 687-698, 1988.

[5] American Society for Testing and Materials, Standard Test Method for Half Cell Potentials of Reinforcing Steel in Concrete, ASTM C-876, Philadelphia, 1980.

[6] Andrade, C., et. al, "The Determination of the Corrosion Rate of Steel Embedded in Concrete by the Polarization Resistance and AC Impedance Methods," Corrosion Effect of Stray Currents and the Techniques for Evaluating Corrosion of Rebars in Concrete, ASTM STP 906, V. Chaker, Ed., American Society for Testing and Materials, Philadelphia, 1986.

[7] Apostolos, John A., "Cathodic Protection of Reinforced Concrete by Using Metallized Coatings and Conductive Paints," Bridge Maintenance, Management, Corrosion Control, Heating and Deicing Chemical, Transportation Research Record 962, Transportation Research Board, Washington, 1984, pp. 22-28

[8] ASTM D 3963M-87, "Standard Specification for Epoxy-Coated Reinforcing Steel," ASTM Book of Annual Standards 1990.

[9] ASTM C 876-87, "Standard Test Method for Half-Cell Potentials of Uncoated Reinforcing Steel in Concrete," ASTM Book of Annual Standards 1990.

[10] Beeby, A.W., "Corrosion of Reinforcing Steel in Concrete and its Relation to Cracking," The Structural Engineer, Vol. 56A, No. 3, March 1978, pp. 77-81.

[11] Beeby, W. A., "Cracking and Design Against Corrosion," in Corrosion of Steel Reinforcements in Concrete Construction, Society of Chemical Industry, London, 1979, pp. 15-30.

[12] Beeby, A.W., "Corrosion of Reinforcing Steel in Concrete and its Relation to Cracking," The Structural Engineer, Vol. 56A, No. 3, 1978, pp. 78-81 .

[13] Beeby, A.W., "Cracking, Cover, and Corrosion of Reinforcement," Concrete International, Vol. 5, No. 2, Feb. 1983, pp. 35-40.

[14] Berkeley, K.G.L., and Pathmanaben, S., Cathodic Protection of Reinforcement Steel in Concrete, Butterworth & Co., London, 1990.

[15] Bickley, J.A., "Potential for Carbonation of Concrete in Canada" Paul Klieger Symposium on Performance of Concrete, ACI SP-122, David Whiting, ed., American Concrete Institute, Detroit, MI, 1990.

[16] Building Code Requirements for Reinforced Concrete, ACI 318-89, American Concrete Institute, Detroit, MI, 1989.

[17] Bukovatz, J.E., and Crumpton, C.F., "Kansas' Experience with Interlayer Membranes on Salt-Contaminated Bridge Decks," Bridge Maintenance, Management, Corrosion Control, Heating and Deicing Chemical, Transportation Research Record 962, Transportation Research Board, Washington, 1984, pp. 66-69.

[18] Carpantier, L., and Sorentz, S., "Contribution a l'Etude de la Corrosion des Aramatures de Beton Arme," Annales de l'Institute Technique de Batiment et Travaux Publiques, Paris, July-August 1966.

[19] Chin, D., "A Calcium Nitrite-Based, Non-Corrosive, Non-Chloride Accelerator," Corrosion, Concrete and Chlorides, Steel Corrosion in Concrete: Causes and Restraints, ACI SP-102, Frances W. Gibson, ed., American Concrete Institute, Detroit, MI, 1987.

[20] Clear, K.C., "Time to Corrosion of Reinforcing Steel in Concrete Slabs," Transportation Research Record No. 500, Transportation Research Board, Washington, D.C., 1974, pp. 16-24.

[21] Clear, K.C., et. al., Time-to-Corrosion of Reinforcing Steel in Concrete Slabs,

Vol.I. FHWA-RD: 73/32., Federal Highway Administration, Washington D.C., 1973.

[22] Clear, K.C., et. al., Time-to-Corrosion of Reinforcing Steel in Concrete Slabs, Vol. II. FHWA-RD: 73/33., Federal Highway Administration, Washington D.C., 1973.

[23] Clear, K.C., et. al., Time-to-Corrosion of Reinforcing Steel in Concrete Slabs, Vol. V. FHWA-RD: 83/012., Federal Highway Administration, Washington D.C., 1979.

[24] Clear, K.C., et. al., Time-to-Corrosion of Reinforcing Steel in Concrete Slabs, Vol. IV. FHWA-RD: 82/028., Federal Highway Administration, Washington D.C., 1978.

[25] Clear, K.C., et. al., Time-to-Corrosion of Reinforcing Steel in Concrete Slabs, Vol. III. FHWA-RD: 76/70., Federal Highway Administration, Washington D.C., 1976.

[26] Clear, K.C., and Virmani, Y.P., "Solving Rebar Corrosion Problems in Concrete - Methods and Materials," in Solving Rebar Corrosion Problems in Concrete, National Association of Corrosion Engineers, Houston, 1983.

[27] Clear, K.C., "Measuring the Rate of Corrosion of Steel in Field Concrete Structures," paper prepared by Kenneth C. Clear, Inc., Sterling, VA, January 1989.

[28] Clear, K., Virmani, Y., "Solving Rebar Corrosion Problems in Concrete, Research Update: Methods and Materials," Solving Rebar Corrosion Problems in Concrete, National Association of Corrosion Engineers, Houston, 1982.

[29] Clifton, J., Beeghly, H., Mathey, R., Nonmetallic Coatings for Concrete Reinforcing Bars, FHWA-RD-74-18, National Bureau of Standards, Washington, D.C., 1974.

[30] Clifton, J.R., Knab, L.I., "Service Life of Concrete," NISTIR 89-4086, United States Department of Commerce National Institute of Standards and Technology, Gaithersburg, MD, 1989.

[31] Coggins, F., French, K., "Material Properties of a Twenty-Year-Old Prestressed Bridge Girder Obtained By Nondestructive Testing," Structural Engineering Report No. 89-03., Department of Civil and Mineral Engineering, University of Minnesota, July 1989.

[32] Cohen, M.D., Olek, J., "Silica Fume in PCC: The Effects of Form on Engineering

Performance," Concrete International, Volume 11, No. 11, 1989.

[33] Cornet, I., Bresler, B., "Critique of Testing Procedures Related to the Performance of Galvanized Steel Reinforcement in Concrete," Corrosion of Reinforcing Steel in Concrete, ASTM STP 713 D, E. Tonini & J.M. Gaidis, Eds., American Society for Testing and Materials, Philadelphia, 1980.

[34] Corrosion of Steel in Concrete, Report of the Technical Committee 60-CSC, The International Union of Testing and Research Laboratories for Materials and Structures (RILEM), P. Schiessl, editor, Chapman and Hall, London, 1988.

[35] Crane, A.P., (editor) Corrosion of Reinforcement in Concrete Construction, Ellis Horwood Ltd., Chichester, England, 1983, (25 articles).

[36] Crumpton, C.F. and Bukovatz, J.E. "Corrosion and Kansas Bridges," Trans portation Research Record No. 500, Transportation Research Board, Washington, D.C., 1974, pp 25-31.

[37] Crumpton, C.F., McCollom, B.F., and Stratton, F.W. "Epoxy Injection Repairs Delaminated Bridge Decks," Civil Engineering, ASCE, Vol. 44, No.11, Nov. 1974, pp. 55-57.

[38] Dana, J.S. and Peters, R.J., "Corrosion of Highway Structures," Transportation Research Record No. 539, Transportation Research Board, Washington, D.C., 1975, pp. 27-37.

[39] Dehghanian C., Locke C., "Electrochemical Behavior of Steel in Concrete as a Result of Chloride Diffusion into Concrete: Part 2," Corrosion - NACE, Volume 38, No. 9, September, 1982.

[40] Denda, D., "Parking Garage Repair and Retrofit: How Big is the Underlying Problem?," Concrete Technology Today, Volume 12, Number 2, July 1991, pp. 4-5.

[41] Duffaut, P., Duhoux, L., and Heuze, B., "Corrosion des Aciers dans le Beton Arme - Essais Realises dans le Estuaire de la Rance de 1959 a 1971," Annales de l'Institute Technique de Batiment et Travaux Publiques, Paris, May 1973.

[42] Escalante, E., Ito, S., "Measuring the Rate of Corrosion of Steel in Concrete," A Compilation of Papers on Rebar Corrosion - 1976-1982, National Association of

Corrosion Engineers, Houston, 1984.

[43] Federal Highway Administration Memorandum, "Bridge Deck Deterioration, A 1981 Perspective," Office of Research, FHA, Dec. 1981.

[44] Fédération International de la Précontrainte, Condensed Silica Fume in Concrete, Thomas Telford Ltd., London, 1988.

[45] Feldman, R.F., Huang Cheng-yi, "Resistance of Mortars Containing Silica Fume to Attack by a Solution Containing Chlorides," Cement and Concrete Research, Volume 15, pp. 411-420, 1985.

[46] Feliu, S., Gonzãlez, J.A., Feliu, S., Jr., Andrade, C., "Relationship Between Conductivity of Concrete and Corrosion of Reinforcing Bars," British Corrosion Journal, Vol. 24, No. 3, 1989, pp. 195-198.

[47] FIP, "Tentative Recommendations for the Corrosion Protection of Unbonded Tendons," PCI Journal, Vol.28, No. 1, Jan/Feb 1983, pp. 40-49.

[48] Flick, L.D., Lloyd, J.P., "Corrosion of Steel in Internally Sealed Concrete Beams Under Load," Corrosion of Reinforcing Steel in Concrete, ASTM STP 713 D, E. Tonini & J.M. Gaidis, Eds., American Society for Testing and Materials, Philadelphia, 1980.

[49] Fontana, M.G., Corrosion Engineering, McGraw-Hill, Inc., New York, NY, 1986.

[50] Fraczek, J., "A Review of Electrochemical Principles as Applied to Corrosion of Steel in a Concrete or Grout Environment," Corrosion, Concrete and Chlorides, Steel Corrosion in Concrete: Causes and Restraints, ACI SP-102, Frances W. Gibson, ed., American Concrete Institute, Detroit, MI, 1987.

[51] Frascoia, R.I., "Field Performance of Experimental Bridge Deck Membranes in Vermont," Bridge Maintenance, Management, Corrosion Control, Heating and Deicing Chemical, Transportation Research Record 962, Transportatation Research Board, Washington, 1984, pp. 57-65.

[52] Fromm, H.J., "Cathodic Protection of Rebar in Concrete Bridge Decks," Materials Protection, Vol. 11, 1977, pp. 21-29.

[53] Gautefall, O., Vennesland, O, "Effects of Cracks on the Corrosion of Embedded Steel in Silica-Concrete Compared to Ordinary Concrete," Nordic Concrete Research, Publication No. 2, Oslo, December, 1983.

[54] Gaynor, R., "Understanding Chloride Percentages," Corrosion, Concrete and Chlorides, Steel Corrosion in Concrete: Causes and Restraints, ACI SP-102, Frances W.Gibson, ed., American Concrete Institute, Detroit, MI, 1987.

[55] Gjorv, O., "Steel Corrosion in Reinforced and Prestressed Concrete Structures," Nordisk Betong, Vol. 2, No. 4, 1982, pp. 147-151.

[56] Gouda, V.K., Mourad, H.M., "Galvanic Cells Encountered in The Corrosion of Steel Reinforcement -III. Differential Surface Condition Cells," Corrosion Science, Volume 15, 1975, pp. 317-328.

[57] Gouda, V.K., Mourad, H.M., "Galvanic Cells Encountered in The Corrosion of Steel Reinforcement -I. Differential pH Cells," **Corrosion Science**, Volume 14, 1974, pp. 681-690.

[58] Gouda, V.K., Mourad, H.M., "Galvanic Cells Encountered in The Corrosion of Steel Reinforcement -IV. Differential Aeration Cells," **Corrosion Science**, Volume 15, 1975, pp. 329-336.

[59] Gouda, V.K., Mourad, H.M., "Galvanic Cells Encountered in The Corrosion of Steel Reinforcement -II. Differential Salt Concentration Cells," **Corrosion Science**, Volume 15, 1975, pp. 307-315.

[60] Hausmann, D.A. "Steel Corrosion in Concrete, How Does it Occur?," Materials Protection, Vol. 6, No. 11, Nov. 1967, pp 19-23.

[61] **Highway Statistics, 1989**, United States Department of Transporation, Federal Highway Administration, Washington D.C., p. 135.

[62] Hime, W., Erlin, B., "Some Chemical and Physical Aspects of Phenomena Associated with Chloride-Induced Corrosion," **Corrosion, Concrete and Chlorides, Steel Corrosion in Concrete: Causes and Restraints**, ACI SP-102, Frances W. Gibson, ed., American Concrete Institute, Detroit, MI, 1987.

[63] Hinatsu, J.T., Graydon, W.F., Foulkes, F.R., "Voltammetric Behavior of Iron in

Cement. I. Development of a Standard Procedure for Measuring Voltammograms," **Journal of Applied Electrochemistry**, Volume 19, 1989, pp. 868-876.

[64] Holm, J., "Comparison of the Corrosion Potential of Calcium Chloride and a Calcium Nitrate Based Non-Chloride Accelerator - a Macro-Cell Corrosion Approach," **Corrosion, Concrete and Chlorides, Steel Corrosion in Concrete: Causes and Restraints**, ACI SP-102, Frances W.Gibson, ed., American Concrete Institute, Detroit, MI, 1987.

[65] Hope, B.B., Ip, A.K., "Chloride Corrosion Threshold in Concrete," **ACI Materials Journal**, Volume 84, No. 4, 1987.

[66] Houston, J.T., and Atimtay, E., "Corrosion of Reinforcing Steel Embedded in Structural Concrete," Research Report 112-1F, Center For Highway Research, The University of Texas at Austin, March 1972.

[67] Husock, B., and Wilson, R.M., "Overview of the Rebar Corrosion Problem," in Solving Rebar Corrosion Problems in Concrete, National Association of Corrosion Engineers, Houston, 1983.

[68] Isecke, B., "Failure Analysis of the Collapse of the Berlin Congress Hall," in Crane, A.P. (ed.), Corrosion of Reinforcement in Concrete Construction, Ellis Horwood Lt., Chichester, U.K. 1983, pp. 79-90 (2 refs.).

[69] Jabar, T., Braun Engineering Company, Minneapolis, MN, personal conversation.

[70] Jang, J.W., Iwasaki, I., "Rebar Corrosion Under Simulated Concrete Conditions Using Galvanic Current Measurements," A paper submitted to: Transportation Research Board, 2101 Constitution Avenue, N.W., Washington, D.C., 1991.

[71] Litvan, G.G., "Deterioration of Parking Structures," **Durability of Concrete, Vol I**, ACI SP-126, V.M. Malhotra, ed., American Concrete Institute, Detroit, MI, 1991.

[72] Locke, C.E., "Mechanism of Corrosion of Steel in Concrete," in Solving Rebar Corrosion Problems in Concrete, National Association of Corrosion Engineers, Houston, 1983 (15 refs.).

[73] Locke, C.E., "Corrosion of Steel in Portland Cement Concrete: Fundamental Studies," **Corrosion Effect of Stray Currents and the Techniques for Evaluating**

Corrosion of Rebars in Concrete, ASTM STP 906, V. Chaker, Ed., American Society for Testing and Materials, Philadelphia, 1986.

[74] Malhotra, V.M. (editor) Performance of Concrete in Marine Environment, ACI SP-65, American Concrete Institute, Detroit, 1980.

[75] Manning, D.G., "Detecting Defects and Deterioration in Highway Structures," NCHRP Synthesis of Highway Practice 118, Transportation Research Board, Washington, D.C., July 1985.

[76] Manning, D.G., Clear, K.C., and Schell, H.C., "Cathodic Protection of Bridge SubStructures: Burlington Bay Skyway Test Site - Design and Construction Phases (Part I) ; Initial Performance of Systems 1 to 4 (Part II) Bridge Maintenance, Management, Corrosion Control, Heating and Deicing Chemical, Transportation Research Record 962, Transportation Research Board, Washington, 1984, pp. 29-50.

[77] Manning, D.G. and Holt, F.B., "Detecting Delamination in Concrete Bridge Decks," Concrete International, Vol.2, No. 11, Nov. 1980, pp. 34-41.

[78] Marusin, S.L., "Influence of Superplasticizers, Polymer Admixtures, and Silica Fume in Concrete on Chloride Ion Permeability," **Permeability of Concrete**, ACI SP-108, D. Whiting, A. Walitt, Ed., American Concrete Institute, Detroit, 1988.

[79] McBee, W.C., Sullivan, T.A., and Jong, B.W., "Corrosion-Resistant Sulfur Concretes," Report of Investigation No. 8758, U.S. Bureau of Mines, 1983.

[80] Mindess, S., Young, J.F., **Concrete**, Prentice-Hall, Englewood Cliffs, New Jersey, 1981.

[81] Monteiro, P.J.M., Gjorv, O.E., Mehta, P.K., "Microstructure of the Steel-Cement Interface in the Presence of Chloride," **Cement and Concrete Research**, Volume 15, pp. 781-784, 1985.

[82] Moore, D.G., Klodt, D.T., Hensen, R.J., "Protection of Steel in Prestressed Concrete Bridges," NCHRP Report 90, Highway Research Board, Washington, D.C., 1970, (103 refs.).

[83] NCHRP, "Long-Term Rehabilitation of Salt-Contaminated Bridge Decks," National Cooperative Highway Research Program Report 257, Transportation Research Board,

Washington, D.C., April 1983.

[84] NCHRP, "Durability of Concrete Bridge Decks," National Cooperative Highway Research Program Synthesis 57, May 1979.

[85] Ozyildirim, C., Halstead, W., "Resistance to Chloride Ion Penetration of Concretes Containing Fly Ash, Silica Fume, or Slag," **Permeability of Concrete**, ACI SP-108, D. Whiting, A. Walitt, Ed., American Concrete Institute, Detroit, 1988.

[86] Parker, D.G., "Microsilica Concrete. Part 1: The Material." **Concrete**, Volume 19-H10, 1985, pp 21-22.

[87] Pepper, L., Pike, R.G., and Willet, J.A., (eds.), Corrosion of Metals in Concrete, ACI SP-49, American Concrete Institute, Detroit, 1975, (10 articles).

[88] Perraton, D., et. al., "Permeabilities of Silica Fume Concrete," **Permeability of Concrete**, ACI SP-108, D. Whiting, A. Walitt, Ed., American Concrete Institute, Detroit, 1988.

[89] Peterson, C.A., "Survey of Parking Structure Deterioration and Distress," Concrete International, Vol. 2, No. 3, Mar. 1980, pp. 53-61.

[90] Pfeifer, D.W., **Protective Systems for New Prestressed and Substructure Concrete**, FHWA-RD: 86/193., Federal Highway Administration, Washington D.C., 1980.

[91] Pike, R.G., Hay, R.E., Clifton, J.R., Beeghly, H.F., and Mathey, R.G., "Nonmetalic Protective Coatings of Concrete Reinforcing Steel," Transportation Research Record No. 500, Transportation Research Board, 1974, pp. 36-44.

[92] Pinjarkar, S.G., Osborn, A.E.N., Koob, M.J., and Pfeifer, D.W., "Rehabilitation of Parking Decks With Superplasticized Concrete Overlay," Concrete International, Vol. 2, No. 3, Mar. 1980, pp. 62-67.

[93] Portland Cement Association, "Bridge Deck Renewal with Thin-Bonded Concrete Resurfacing,' Concrete Information, PCA, Skokie, 1980.

[94] Poston, R. W., **Improving Durability of Bridge Decks by Transverse Prestressing**, unpublished Doctorial Thesis, The University of Texas at Austin,

December, 1984.

[95] Poston, R., "Improving Durability of Bridge Decks by Transverse Prestressing," Ph.D. Dissertation, The University of Texas at Austin, December 1984, 639 pp. 167 refs.

[96] Pourbaix, M., **Lectures On Electrochemical Corrosion**, Plenum Press, New York, N.Y., 1973.

[97] Rasheeduzzafar, et. al., "Influence of Cement Composition on the Corrosion of Reinforcement and Sulfate Resistance of Concrete," **ACI Materials Journal**, Volume 87, No. 2., 1990.

[98] Ray, R., "The Bridge Deck Problem - An Analysis of Potential Solutions," Public Roads, Vol. 39, No. 4, March 1976, pp. 142-147.

[99] Rehm, G., and Moll, H., "Versuche zum Studium des Einfluss der Reissbreite auf die Rostbilding an der Bewehrung von Stahlbeton-Bauteilen," Deuscher Ausschuss fur Stahlbeton - Heft 169, Berlin, 1964.

[100] RILEM 12-CRC Committee "Corrosion of Reinforcement and Prestressed Tendons--A 'State of the Art' Report" Materiaux et Constuctions. vol 9 no 51, May-June 1976, pp. 187-206, in English, sponsored by RILEM.

[101] Roshore, E.C., "Tensile Crack Exposure Tests: Results of Tests of Reinforced Concrete Beams 1955-1963," US Army Engineer Waterways Experiment Station Technical Memorandum 6-124, Vicksburg, November 1964.

[102] Schiessl, P., Admissible Crack Widths in R.C. Structures, Inter-Association Colloquium on the Behavior in Service of Concrete Structures, Preliminary Reports, Vol. II, N. 3-17, Liege, Belgium, 1975.

[103] Sereda, P.J. and Litvan, G.G., (eds.), Durability of Building Materials and Components, ASTM SP 691, Philadelphia, 1980.

[104] Shanafelt, G.O., "Bridge Designs to Reduce and Facilitate Maintenance and Repair," NCHRP Synthesis of Highway Practice 123, Transportation Research Board, Washington, D.C., December 1985, (29 refs.).

[105] Slater, J.E., **Corrosion of Metals in Association with Concrete**, ASTM STP 818, American Society for Testing and Materials, Philadelphia, 1983.

[106] Smith, P., "Effects of Two Non-Chloride Accelerating Agents on Setting Characteristics of Portland Cement Mortars," **Corrosion, Concrete and Chlorides, Steel Corrosion in Concrete: Causes and Restraints**, ACI SP-102, Frances W. Gibson, ed., American Concrete Institute, Detroit, MI, 1987.

[107] Somayaji, S., Keeling, D., Heidersbach, R., "Corrosion of Reinforcing Steel in Concrete Exposed to Marine and Freshwater Environments," **Paul Klieger Symposium on Performance of Concrete**, ACI SP-122, David Whiting, ed., American Concrete Institute, Detroit, MI, 1990.

[108] Stratfull, R.F., "Criteria for the Cathodic Protection of Bridge Decks," in Corrosion of Reinforcement in Concrete Construction, Crane (ed.) Ellis Horwood Ltd., Chichester, England, 1983, pp. 287-331.

[109] Stratfull, R., "Half-Cell Potentials and the Corrosion of Steel in Concretes," Highway Research Record, No. 433, Transportation Research Board, Washington, 1973, pp. 12-21.

[110] Stratfull, R.F., Jurkovich, W.J., and Spellman, D.L. "Corrosion Testing of Bridge Decks" Transportation Research Record no 539. TRB. 1975, pp. 50-59, 20 ref.

[111] Takagi, N., Miyagawa, T., Amasaki, S., Kojima, T., "Chloride Corrosion of Reinforcing Steel in Silica Fume Concrete Exposed to Marine Environment," **Durability of Concrete, Vol. I**, ACI SP-126, V.M. Malhotra, ed., American Concrete Institute, Detroit, MI, 1991.

[112] Todd, P.L. "Initial Corrosion Survey of the Bay Area Rapid Transit System" Transportation Research Record no 500, TRB, 1974, pp. 45-59.

[113] Tonini, D.E. and Gaidas, W.R. (editors) Corrosion of Reinforcing Steel in Concrete, ASTM STP 713. American Society for Testing and Materials, Philadelphia, 1980.

[114] Treadaway, K.W.J., "Durability of Steel in Concrete," in Corrosion of Steel Reinforcements in Concrete Construction, Society of Chemical Industry, London, 1979, pp. 1-14.

[115] Vassie, P.R., "Non-destructive Evaluation of the Corrosion of Concrete Reinforcements by Chlorides," in Corrosion of Steel Reinforcements in Concrete Construction, Society of Chemical Industry, London, 1979, pp. 57-78.

[116] Watson, S.C. (editor) Joint Sealing and Bearing Systems for Concrete Structures, ACI SP-70. American Concrete Institute. Detroit, 1981, 36 articles, Vol 1.

[117] Webster, T.E., "ACI Forum: Influence of Chlorides in Reinforced Concrete," **Corrosion, Concrete and Chlorides, Steel Corrosion in Concrete: Causes and Restraints**, ACI SP-102, Frances W. Gibson, ed., American Concrete Institute, Detroit, MI, 1987.

[118] Weed, R.M. "Recommended Depth of Cover for Bridge Deck Steel" Transportation Research Record no 500, TRB, 1974, pp. 32-35, 3 ref.

[119] Weyers, R.E., and Cady, P.D., "Deep Grooving - A Method for Impregnating Concrete Bridge Decks - Development (Part I) and Application (Part II)," Bridge Maintenance, Management, Corrosion Control, Heating and Deicing Chemical, Transportation Research Record 962, Transportation Research Board, Washington, 1984, pp. 10-19.

[120] Wheat, H.G., Eliezer, Z., "Comments on the Identification of a Chloride Threshold in the Corrosion of Steel in Concrete," **Corrosion**, February 1987, pp. 126-128.

[121] Whiting, D., "Concrete Materials, Mix Design, Construction Practices and Their Effects on the Corrosion of Reinforcing Steel," **A Compilation of Papers on Rebar Corrosion - 1976-1982,** National Association of Corrosion Engineers, Houston, 1984.

[122] Whiting, D. "Influence of Concrete Materials, Mix, and Construction Practices on the Corrosion of Reinforcing Steel" Materials Performanc, Vol. 17 No. 12, Dec 1978, pp. 9-15.

[123] Wranglén, G., **An Introduction to Corrosion and Protection of Metals**, Chapman and Hall, New York, N.Y., 1985.

[124] Yau, S.S. and Hartt, W.H. "Influence of Selected Chelating Admixtures upon Concrete Cracking due to Embedded Metal Corrosion" Corrosion of Reinforcing Steel in Concrete ASTM STP 713, 1980, pp. 51-63, 7 ref.

[125] Young, J.F., "A Review of the Pore Structure of Cement Paste and Concrete and its Influence on Permeability," **Permeability of Concrete**, ACI SP-108, D. Whiting, A. Walitt, Ed., American Concrete Institute, Detroit, 1988.